The Measure Problem in Eternal Inflation

by

Andrea De Simone

Submitted to the Department of Physics
in partial fulfillment of the requirements for the degree of

Doctor of Philosophy

at the

MASSACHUSETTS INSTITUTE OF TECHNOLOGY

June 2010

Author .....
Department of Physics
May 4, 2010

Certified by ....
Alan H. Guth
Victor F. Weisskopf Professor of Physics
Thesis Supervisor

Accepted by .....
Krishna Rajagopal
Professor of Physics
Associate Department Head for Education

The Measure Problem in Eternal Inflation

by

Andrea De Simone

Submitted to the Department of Physics
on May 4, 2010, in partial fulfillment of the
requirements for the degree of
Doctor of Philosophy

Abstract

Inflation is a paradigm for the physics of the early universe, and it has received a great deal of experimental support. Essentially all inflationary models lead to a regime called eternal inflation, a situation where inflation never ends globally, but it only ends locally. If the model is correct, the resulting picture is that of an infinite number of "bubbles", each of them containing an infinite universe, and we would be living deep inside one of these bubbles. This is the multiverse. Extracting meaningful predictions on what physics we should expect to observe within our bubble encounters severe ambiguities, like ratios of infinities. It is therefore necessary to adopt a prescription to regulate the diverging spacetime volume of the multiverse. The problem of defining such a prescription is the *measure problem*, which is a major challenge of theoretical cosmology.

In this thesis, I shall describe the measure problem and propose a promising candidate solution: the *scale-factor cutoff measure*. I shall study this measure in detail and show that it is free of the pathologies many other measures suffer from. In particular, I shall discuss in some detail the "Boltzmann brain" problem in this measure and show that it can be avoided, provided that some plausible requirements about the landscape of vacua are satisfied.

Two interesting applications of the scale-factor cutoff measure are investigated: the probability distributions for the cosmological constant and for the curvature parameter. The former turns out to be such that the observed value of the cosmological constant is quite plausible. As for the curvature parameter, its distribution using the scale-factor measure predicts some chance to detect a nonzero curvature in the future.

Thesis Supervisor: Alan H. Guth
Title: Victor F. Weisskopf Professor of Physics

Acknowledgments

This thesis is the result of years of studies and it would have never been possible without the presence and the help of several people I have been fortunate to be in contact with.

I would like to express my deep gratitude to my advisor, Prof. Alan Guth, for his wise guidance, tireless patience and constant support. Then I wish to thank my family who has always been a firm point of reference and a safe harbor. Many thanks go to my friends for their reliable company and the joyful moments spent together. Finally, I am indebted to Elisa, to whom this thesis is dedicated, for incessantly injecting enthusiasm and happiness into my life.

A Elisa

Contents

List of Figures

Chapter 1

Introduction

This Chapter is devoted to introduce the problem which is the subject of the present thesis. After briefly recalling some basic material of standard cosmology (see e.g. Ref. [1] for a comprehensive account), we shall introduce inflation and review its successes in Section 1.1, and then we shall turn to discuss a generic feature of inflationary models known as "eternal inflation" (Section 1.2). Finally, in Section 1.3 we shall describe how the rest of the thesis is organized.

1.1 Inflation

Inflation [2, 3, 4] is one of the basic ideas of modern cosmology and has become a paradigm for the physics of the early universe. In addition to solving the shortcomings of the standard Big Bang theory, inflation has received a great deal of experimental support, for example it provided successful predictions for observables like the mass density of the Universe and the fluctuations of the cosmic microwave background radiation. Before discussing inflation in more detail, let us first review some background material about standard cosmology, which serves also to introduce the notation, and outline its major shortcomings.

1.1.1 Standard cosmology and its shortcomings

The standard cosmology is based upon the spatially homogeneuos and isotropic Universe described by the Friedmann-Robertson-Walker (FRW) metric:

$$ds^2 = dt^2 - a(t)^2 \left[\frac{dr^2}{1-kr^2} + r^2(d\theta^2 + \sin^2\theta^2 d\phi^2) \right] , \tag{1.1}$$

where $a(t)$ is the cosmic scale factor and the curvature signature is $k = -1, 0, 1$ for spaces of constant negative, zero, positive spatial curvature, respectively. The evolution of the scale factor is governed by the Einstein equations, where the energy-momentum tensor is assumed to be that of a perfect fluid with total energy density $\rho_{\rm tot}$ and pressure p. One of the Einstein equations takes the simple form (known as

the Friedmann equation):

$$H^2 \equiv \left(\frac{\dot{a}}{a}\right)^2 = \frac{8\pi G}{3}\rho_{\rm tot} - \frac{k}{a^2}\,, \tag{1.2}$$

where H is the Hubble parameter and G is the Newton's constant. Another of the Einstein equations provides the equation for the acceleration of the scale factor:

$$\frac{\ddot{a}}{a} = -\frac{4\pi G}{3}(\rho + 3p)\,. \tag{1.3}$$

Let us define the parameter

$$\Omega \equiv \frac{\rho_{\rm tot}}{\rho_c}\,, \tag{1.4}$$

where $\rho_c \equiv 3H^2/(8\pi G)$ is the critical density. The situation where $\Omega = 1$ corresponds to a spatially flat Universe. In fact, using the Friedmann equation (1.2) the above definition can be re-written as

$$\Omega - 1 = \frac{k}{a^2 H^2}\,. \tag{1.5}$$

The parameter $|\Omega - 1|$ grows with time during radiation- and matter-dominated eras, and since we observe today that the density is very close to the critical density [5] $\Omega_0 = 1.0195 \pm 0.0325$, Ω must have been equal to unity to an extremely high accuracy (of about one part in 10^{60} if we start the radiation-dominated era at the Planck time, 10^{-43} s). Therefore, an extreme degree of fine tuning is necessary to arrange such a precise initial value of the density parameter of the Universe. This is the *flatness (or fine-tuning) problem.*

The flatness problem is also connected to the *entropy problem*, which is understanding why the total entropy of the visible Universe is incredibly large: $S_U \sim 10^{90}$. In fact, the entropy in a comoving volume of radius a and temperature T is $S \simeq (aT)^3$ whereas during radiation domination the Hubble parameter is $H \sim T^2/M_P$, where the Planck mass is $M_P \equiv G^{-1/2} = 1.22 \times 10^{19}$ GeV. So, Eq. (1.5) becomes

$$\Omega - 1 \simeq \frac{M_P^2}{T^2}\frac{k}{S^{2/3}}\,. \tag{1.6}$$

This relation tells us that Ω at early times is so close to 1 because the total entropy of the universe is enormous. For example, at the Planck scale, the entropy of 10^{90} corresponds to $\Omega - 1 \sim 10^{-60}$.

The high degree of homogeneity of the Cosmic Microwave Background (CMB), one part in 10^5, is amazing. But this poses a serious problem for cosmology. The photons received today are emitted from regions that were causally disconnected in the past on the last scattering surface, because they were out of the particle horizon. Our present horizon corresponds to an angle of 1° on the last scattering surface, while we observe isotropic and uniform CMB temperature across the whole sky. Understanding why different microphysical processes occurring in causally disconnected regions turn out

to give the same physical properties to such a great precision is the *horizon problem.*

1.1.2 The inflationary Universe

Inflation elegantly solves at once the problems associated with the standard Big Bang cosmology. The inflationary era is defined as the epoch in the early history of the Universe when it underwent a period of accelerated expansion, $\ddot{a} > 0$. According to Eq. (1.3), this condition is equivalent to $\rho + 3p < 0$. For the sake of simplicity, we shall only consider here a more stringent condition for inflation, $p = -\rho$. A period of the Universe satisfying this condition is called the de Sitter stage. During this stage the energy density and the Hubble parameter are constant, and thus the scale factor grows exponentially in time.

Inflation provides an explanation for the initial condition that Ω is close to 1 to a high precision. In fact, during inflation, the Hubble rate is nearly constant and the curvature parameter $\Omega - 1$ is proportional to $1/a^2$ (see Eq. (1.5)), thus its final value at the end of inflation is related to the primordial initial value by

$$\frac{|\Omega - 1|_{\rm final}}{|\Omega - 1|_{\rm initial}} = \left(\frac{a_{\rm final}}{a_{\rm initial}}\right)^{-2} \equiv e^{-2N_e}\,, \tag{1.7}$$

where N_e is the number of e-foldings. As long as the inflatioary period is long enough, Ω will be exponentially driven to unity. Therefore, the Universe coming out of inflation is spatially flat to a very high accuracy. To match the observations, it is necessary to have $N_e \sim 60$ and this is sufficient to dilute away almost any value the curvature parameter may start with. Furthermore, the large amount of entropy produced during the non-adiabatic phase transition from the end of inflation and the beginning of the radiation-dominated era also accounts for the origin of the huge entropy of the Universe. Therefore, inflation reduces the problem of explaining very large numbers like 10^{90} to explaining about 60 e-foldings of inflation.

If the Universe underwent a period when the physical scales evolve faster than the horizon scale, it is possible to make the CMB photons in causal contact at some primordial time before the last-scattering surface. The physical size of a perturbation grows as the scale factor: $\lambda \sim a$, while the horizon scale is $H^{-1} = a/\dot{a}$. If a period exists in the early history of the Universe when

$$\frac{d}{dt}\frac{\lambda}{H^{-1}} = \ddot{a} > 0\,, \tag{1.8}$$

the CMB photons may have been in causal contact at that time, thus explaining the homogeneity and isotropy observed today. Such an epoch of accelerated expansion is precisely what we call the inflationary stage.

Inflation can also be responsible for the physical processes giving rise to the structures we observe in the Universe today. In fact, primordial small quantum fluctuations of the energy density get stretched during inflation, exit the horizon and get frozen; when they re-enter the horizon at some matter- or radiation-dominated epoch, these fluctuations will start growing giving rise to the formation of all the structures we

observe.

The mechanism of inflation can be realized by means of a simple scalar field ϕ, called the inflaton, whose energy is dominant in the Universe and with a kinetic energy much smaller than the potential energy $V(\phi)$. The energy density and the pressure of the scalar field are given by

$$\rho_\phi = \frac{\dot{\phi}^2}{2} + V(\phi)\,, \tag{1.9}$$

$$p_\phi = \frac{\dot{\phi}^2}{2} - V(\phi)\,. \tag{1.10}$$

If the kinetic energy is negligible with respect to the potential energy $\dot{\phi}^2 \ll V(\phi)$, and if the energy density of the inflaton dominates over other forms of energy density (such as matter or radiation) we would have a de Sitter stage $p_\phi = -\rho_\phi$ and the Friedmann equation would read

$$H^2 \simeq \frac{8\pi G}{3} V(\phi)\,. \tag{1.11}$$

Thus, inflation gets driven by the vacuum energy of the inflaton field.

When $\dot{\phi}^2 \ll V(\phi)$ and $\ddot{\phi} \ll 3H\dot{\phi}$, the scalar field "slowly rolls" down its potential. Therefore, the equation of motion of the field

$$\ddot{\phi} + 3H\dot{\phi} + V'(\phi) = 0\,, \tag{1.12}$$

where the prime refers to the derivative with respect to ϕ, reduces in this "slow-roll" regime to

$$3H\dot{\phi} \simeq -V'(\phi)\,. \tag{1.13}$$

1.2 Eternal Inflation and the Measure Problem

It has turned out that essentially all inflationary models lead to a regime called *eternal inflation*; it is a situation where inflation never ends globally, but it only ends locally. The inflating region grows exponentially without limit, while pieces of it break off to form "bubble" (or "pocket") universes ad infinitum.

Essentially two distinct mechanisms make eternal inflation possible: false-vacuum eternal inflation (for the so-called "small field" inflationary models) and slow-roll eternal inflation (for the so-called "large field", or chaotic, inflationary models).

Consider a potential of the form depicted in Figure 1-1. The plateau of the potential at $\phi = 0$ corresponds to a false vacuum and the scalar field will decay to the true vacuum $\phi = \phi_0$ at a lower potential. This process can be described as the nucleation of a bubble of true vacuum, where the field value is $\phi = \phi_0$, in an environment of false vacuum where $\phi = 0$; such a bubble will then expand at the speed of light and will eventually fill out the whole space [6]. Adding inflation to this picture leads to dramatic consequences: besides decaying into regions of true vacuum,

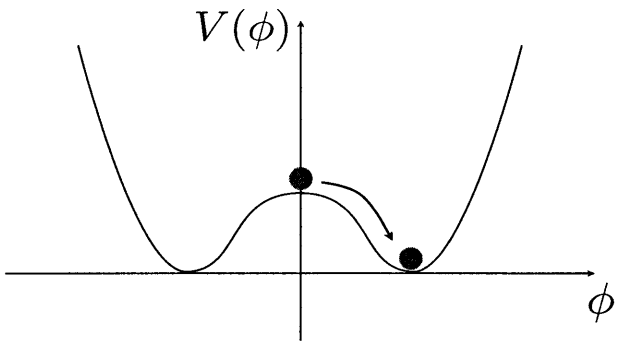

Figure 1-1: Schematic form of a potential giving rise to false-vacuum eternal inflation.

the false vacuum region also expands exponentially. At a given time t, the physical inflating volume of the false vacuum expands by a factor $e^{3H(t-t_0)}$ with respect to the volume $V(t_0)$ present at time t_0, but there is also a nonzero probability to decay into true vacuum:

$$V_{\rm infl}(t) = V(t_0)\, e^{3H(t-t_0)} e^{-\lambda V_4(t,t_0)}\,, \tag{1.14}$$

where λ is the decay rate per unit 4-volume and $V_4(t,t_0)$ is the 4-volume of the past light-cone of a point at time t.

In the limit where the reference time is very early in the past, $t_0 \ll H^{-1}$, one has $V_4(t,t_0) \simeq (4\pi/3)(t-t_0)/H^3$ and we can write Eq. (1.14) as

$$V_{\rm infl}(t) \simeq V(t_0)\, e^{\left(3H - \frac{4\pi}{3}\frac{\lambda}{H^3}\right)(t-t_0)}\,, \tag{1.15}$$

and it is apparent that, as long as the decay rate is sufficiently small ($\lambda < (9/4\pi)H^4$), the volume continues to increase exponentially with time. In other words, bubbles of true vacuum do not grow fast enough to catch up with the exponential expansion of the false vacuum, which never disappears and thus inflation never ends.

Now consider the case of slow-roll eternal inflation, with a potential energy function of the form shown in Figure 1-2. Consider a region of one Hubble volume (H^{-3}). In a time interval of one Hubble time, $\Delta t = H^{-1}$, a reference length scale expands by a factor of $e^{H\Delta t} = e$. So, a volume will expand by a factor of $e^3 \simeq 20$. The field correlators in a de Sitter background are such that

$$\langle \phi^2(t+\Delta t)\rangle - \langle \phi^2(t)\rangle = \frac{H^3}{4\pi^2}\Delta t\,. \tag{1.16}$$

This means that regions separated by more than about a Hubble length are not correlated. Thus the initial volume breaks up into 20 independent causally disconnected regions. During such a time interval, in any of the independent regions the change in

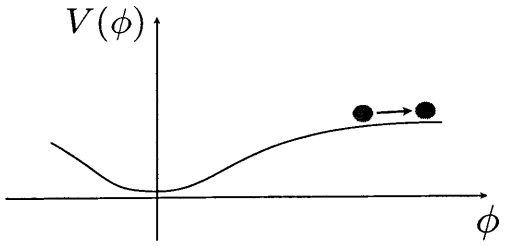

Figure 1-2: Schematic form of a potential giving rise to slow-roll eternal inflation.

the field is given by the sum of a classical motion and a quantum fluctuation:

$$\Delta\phi = \Delta\phi_{\rm cl} + \Delta\phi_{\rm qu}\,. \tag{1.17}$$

Now, the classical term is simply $\Delta\phi_{\rm cl} = |\dot{\phi}_{\rm cl}|H^{-1}$. While the quantum fluctuation in a de Sitter background is $\Delta\phi_{\rm qu} \approx H/2\pi$. There is always a probability that $\Delta\phi > 0$, i.e. that the field climbs up the potential, as suggested pictorially in Figure 1-2. If this probabiliy is bigger than approximately 1/20, the number of inflating regions with $\phi > \phi_0$ is greater at $t_0 + \Delta t$ than it was at t_0, and inflation never ends. For gaussian fluctuations, this condition is equivalent to have $\Delta\phi_{\rm qu} \gtrsim 0.61|\Delta\phi_{\rm cl}|$, or

$$\frac{H}{2\pi} \gtrsim 0.61|\dot{\phi}_{\rm cl}|H^{-1}\,. \tag{1.18}$$

The Friedmann equation during inflation (1.11) and the equation of motion in the slow-roll regime (1.13) imply that $\dot{\phi}_{\rm cl} \simeq -V'/(3H) \simeq H'/(4\pi)$. Thus, the condition (1.18) for eternal inflation reads:

$$\frac{H^2}{H'} \gtrsim 0.3\,. \tag{1.19}$$

If the model is correct, the resulting picture is that of an infinite number of bubbles, each of them containing an infinite universe, and we would be living deep inside one of these pockets. This is the "multiverse". Extracting meaningful predictions on what physics we should expect to observe within our pocket encounters severe ambiguities, like ratios of infinities. It is therefore necessary to adopt a prescription to regulate the diverging spacetime volume of the multiverse. The problem of defining such a prescription is the so-called *measure problem* which is a major challenge of theoretical cosmology. Solving this problem means defining a consistent way to

regularize the infinities of the multiverse, making possible to compare quantities and obtain probabilistic predictions.

1.3 Structure of the thesis

In Chapter 2, we shall describe the measure problem, some proposals for measures of the multiverse and propose a promising candidate solution: the scale-factor cutoff measure. We shall discuss this measure in detail, both in its local formulation and in its possible nonlocal modications which capture the same physics at large scales, but which would in some way average over the local effects of galaxies. We show that the scale-factor cutoff measure is free of the pathologies mentioned above. In particular, we discuss in some detail the Boltzmann brain problem in this measure and show that it can be avoided, provided that some plausible requirements about the landscape of vacua are satisfied.

We shall then turn to two interesting applications of the scale-factor cutoff measure: the probability distributions for the cosmological constant Λ (Chapter 3) and for the curvature parameter Ω_k (Chapter 4). The cosmological constant is an example of an important cosmological variable that is determined probabilistically in a multiverse picture. Its probability distribution in the scale-factor cutoff measure turns out to be such that the observed value of Λ is quite plausible. As for the curvature parameter, its distribution using the scale-factor measure predicts non-negligible chances to detect $\Omega_k \geq 10^{-4}$ in the future. Then, in Chapter 5, we shall turn to the theoretical question of the Boltzmann brains in the scale-factor cutoff measure. Finally, Chapter 6 contains the concluding remarks.

Three appendices supply complementary material to the discussions of the main text. In Appendix A the issue of independence of the initial state is discussed. Appendix B is devoted to a careful analysis of the collapse density threshold and contains review material as well as some new results. In Appendix C, we analyze the nucleation of Boltzmann Brains in Schwarzschild-de Sitter space.

The material presented in this thesis is based on three papers, each of which presents the joint work of my collaborators and myself. The implications of the scale-factor cutoff measure for the cosmological constant were discussed in Ref. [32], with Alan Guth, Michael Salem and Alexander Vilenkin; the implications for Boltzmann brains were discussed in Ref. [34], with Alan Guth, Andrei Linde, Mahdiyar Noorbala, Michael Salem and Alexander Vilenkin; and the implications for Ω_k were discussed in Ref. [51] with Michael Salem.

Chapter 2

The Scale-factor Cutoff Measure

In this Chapter, we describe some of the measures proposed in the literature. We then turn to introduce and define our candidate solution of the measure problem, the *scale-factor cutoff measure*, which is the subject of this thesis, and analyze some of its consequences. In particular, we show that the scale-factor cutoff measure is not afflicted with some of the serious problems arising in other approaches.

2.1 Some proposed measures

The measure problem has been addressed in several different ways so far [7, 8, 9, 10, 11, 12, 13, 14, 15, 16, 17, 18, 19, 20, 21, 22, 23, 24]. Different approaches in general make different observational predictions, and some of these apparently conflict with observation. For example, approaches that define probabilities with respect to a global proper-time foliation [7, 8, 9, 18, 10] suffer a "youngness paradox," predicting that we should have evolved at a very early cosmic time, when the conditions for life were very hostile [25, 26]. Volume-weighting measures, like the so-called "gauge invariant" or "stationary" measures [11, 19, 23] and the pocket-based measures [12, 13, 14, 15], have a "runaway inflation" problem (also known as "Q catastrophe"). These measures predict that we should observe severely large or small values of the primordial density contrast [27, 28] and the gravitational constant [29], while these parameters appear to sit comfortably near the middle of their respective anthropic ranges [30, 29]. (Some suggestions to possibly get around this issue have been described in Refs. [28, 31].)

The causal patch measure [16, 17] and the scale-factor cutoff measure [32, 33] survive these hazards. Furthermore, under reasonable assumptions about the landscape [16, 34], these measures do not suffer a "Boltzmann brain" paradox [35, 36, 37, 38, 39, 40, 41], a situation in which the spacetime volume is overwhelmingly dominated by empty de Sitter space, in which observers who form randomly from thermal fluctuations vastly outnumber observers who evolve normally through evolutionary processes beginning with a big bang. There is also encouraging evidence that these measures coincide with probability measures stemming from independent theoretical considerations [22, 24]. Thus we consider these measures to be promising proposals to regulate the diverging spacetime volume of the multiverse.

Of the several measure proposed in the literature, we are going to spend a few more words only about the three most studied examples, which are also representatives of the different classes of measures.

Proper Time Cutoff Measure. Perhaps the simplest way to regulate the infinities of eternal inflation is to impose a cutoff on a hypersurface of constant global time [7, 8, 9, 10, 11]. To introduce a global time cutoff, we start with a patch of a spacelike hypersurface Σ somewhere in the inflating part of spacetime, and follow its evolution along the congruence of geodesics orthogonal to Σ. The spacetime region covered by this congruence will typically have infinite spacetime volume, and will include an infinite number of pockets (if the patch does not grow without limit, one chooses another initial patch Σ and starts again). In the global-time cutoff approach we introduce a time coordinate t, and restrict our attention to the finite spacetime region $\Gamma(\Sigma, t_c)$ swept out by the geodesics prior to $t = t_c$, where t_c is a cutoff which is taken to infinity at the end of the calculation. The relative probability of any two types of events A and B is then defined to be

$$\frac{p(A)}{p(B)} \equiv \lim_{t_c \to \infty} \frac{n(A, \Gamma(\Sigma, t_c))}{n(B, \Gamma(\Sigma, t_c))} , \tag{2.1}$$

where $n(A, \Gamma)$ and $n(B, \Gamma)$ are the number of events of types A and B respectively in the spacetime region Γ. In particular, the probability P_j of measuring parameter values corresponding to a pocket of type j is proportional to the number of independent measurements made in that type of pocket, within the spacetime region $\Gamma(\Sigma, t_c)$, in the limit $t_c \to \infty$.

The time coordinate t is "global" in the sense that constant-time surfaces cross many different pockets. Note however that it does not have to be global for the entire spacetime, so the initial surface Σ does not have to be a Cauchy surface for the multiverse. It need not be monotonic, either, where for nonmonotonic t we limit $\Gamma(\Sigma, t_c)$ to points along the geodesics prior to the first occurrence of $t = t_c$.

As we shall discuss in more detail in appendix A, probability distributions obtained from this kind of measure are independent of the choice of the hypersurface Σ.[1] They do depend, however, on how one defines the time parameter t. To understand this sensitivity to the choice of cutoff, note that the eternally inflating universe is rapidly expanding, such that at any time most of the volume is in pockets that have just formed. These pockets are therefore very near the cutoff surface at $t = t_c$, which explains why distributions depend on exactly how that surface is drawn.

The proper time cutoff measure corresponds to the choice $t = \tau$, where τ is the proper time along the congruence of geodesics. As we shall discuss in the Section 2.2.3, this measure suffers from a severe "youngness problem", a situation in which

[1]Here, and in most of the paper, we assume an irreducible landscape, where any metastable inflating vacuum is accessible from any other such vacuum through a sequence of transitions. Alternatively, if the landscape splits into several disconnected sectors, each sector will be characterized by an independent probability distribution and our discussion will still be applicable to any of these sectors. The distribution in case of a reducible landscape is discussed in appendix A.

the spacetime volume is overwhelmingly dominated by pocket universes that have just formed. Observers who take a little less time to evolve are hugely more numerous than their slower-evolving counterparts, suggesting that we should most likely have evolved at a very early cosmic time, when the conditions for life were rather hostile.

Pocket-based Measure. The novelty of this approach [14, 15] is to compare the numbers of different types of bubbles instead of comparing the volumes occupied by different vacua. The probability of observing vacuum of type j is then proportional to the abundance p_j of bubbles of type j, which is given by the ratio

$$p_j = \lim_{\epsilon \to 0} \frac{N_j(> \epsilon)}{N(> \epsilon)}\,, \tag{2.2}$$

where $N(> \epsilon)$ is the total number of bubbles with comoving size bigger than ϵ and $N_j(> \epsilon)$ is the number of j-bubbles with comoving size bigger than ϵ. The comoving size of a bubble is defined by projecting back each bubble onto an initial hypersurface Σ_0, through a congruence of geodesics, and then measuring the volume of the "image" on Σ_0. This measure is plagued by the "Q catastrophe", in which the pocket universes typically have a level of inhomogeneity that is either huge or negligibly small. This issue will be studied in Sect. 2.2.4.

Causal Patch Measure. Motivated by holography and the quantum properties of black holes, the attention is shifted from the global to the local point of view, i.e. to what a single observer can see within her horizon (the "causal patch") [16]. The prescription is that of following an ensemble of probe worldlines as they pass through the multiverse of vacua, and counting only the volume which is in causal contact with the points of these worldlines. In this approach most of the landscape volume is excluded from consideration. As already mentioned, this measure, together with the scale-factor cutoff measure does not suffer from the pathologies, like the youngness problem or the Q catastrophe. On the other hand, unlike the scale-factor cutoff measure we shall introduce in the next section, the causal patch measure is highly sensitive to the initial conditions, i.e. which vacuum the probe worldline starts from.

2.2 The Scale-factor cutoff measure

2.2.1 Definitions

The scale-factor cutoff measure belongs to the class of global time cutoff measures intruduced in the previous section. The choice of the time coordinate, the *scale-factor time*, is defined by

$$t = \ln a\,, \tag{2.3}$$

where a is the expansion factor along the geodesics. The scale-factor time is related to the proper time τ by

$$dt = H\, d\tau\,, \tag{2.4}$$

where H is the Hubble expansion rate of the congruence. The term "scale factor" is often used in the context of homogeneous and isotropic geometries; yet on very large and on very small scales the multiverse may be very inhomogeneous. A simple way to deal with this is to take the factor H in Eq. (2.4) to be the local divergence of the four-velocity vector field along the congruence of geodesics orthogonal to Σ,

$$H(x) \equiv \frac{1}{3}\, u^{\mu}{}_{;\mu}\,. \tag{2.5}$$

When more than one geodesic passes through a point, the scale-factor time at that point may be taken to be the smallest value among the set of geodesics. In collapsing regions $H(x)$ is negative, in which case the corresponding geodesics are continued unless or until they hit a singularity.

This "local" definition of scale-factor time has a simple geometric meaning. The congruence of geodesics can be thought of as representing a "dust" of test particles scattered uniformly on the initial hypersurface Σ. As one moves along the geodesics, the density of the dust in the orthogonal plane decreases. The expansion factor a in Eq. (2.3) can then defined as $a \propto \rho^{-1/3}$, where ρ is the density of the dust, and the cutoff is triggered when ρ drops below some specified level.

Although the local scale-factor time closely follows the FRW scale factor in expanding spacetimes — such as inflating regions and thermalized regions not long after reheating — it differs dramatically from the FRW scale factor as small-scale inhomogeneities develop during matter domination in universes like ours. In particular, the local scale-factor time nearly grinds to a halt in regions that have decoupled from the Hubble flow. It is not clear whether we should impose this particular cutoff, which would essentially include the entire lifetime of any nonlinear structure that forms before the cutoff, or impose a cutoff on some nonlocal time variable that more closely tracks the FRW scale factor.

There are a number of nonlocal modifications of scale factor time that both approximate our intuitive notion of FRW averaging and also extend into more complicated geometries. One drawback of the nonlocal approach is that no single choice looks more plausible than the others. For instance, one nonlocal method is to define the factor H in Eq. (2.4) by spatial averaging of the quantity $H(x)$ in Eq. (2.5). A complete implementation of this approach, however, involves many seemingly arbitrary choices regarding how to define the hypersurfaces over which $H(x)$ should be averaged, so we here set this possibility aside. A second, simpler method is to use the local scale-factor time defined above, but to generate a new cutoff hypersurface by excluding the future lightcones of all points on the original cutoff hypersurface. In regions with nonlinear inhomogeneities, the underdense regions will be the first to reach the scale-factor cutoff, after which they quickly trigger the cutoff elsewhere. The resulting cutoff hypersurface will not be a surface of constant FRW scale factor, but the fluctuations of the FRW scale factor on this surface should be insignificant.

As a third and final example of a nonlocal modification of scale factor time, we recall the description of the local scale-factor cutoff in terms the density ρ of a dust of test particles. Instead of such a dust, consider a set of massless test particles, emanating uniformly in all directions from each point on the initial hypersurface Σ. We can then construct the conserved number density current J^μ for the gas of test particles, and we can define ρ as the rest frame number density, i.e. the value of J^0 in the local Lorentz frame in which $J^i = 0$, or equivalently $\rho = \sqrt{J^2}$. Defining $a \propto \rho^{-1/3}$, as we did for the dust of test particles, we apply the cutoff when the number density ρ drops below some specified level. Since null geodesics are barely perturbed by structure formation, the strong perturbations inherent in the local definition of scale factor time are avoided. Nonetheless, we have not studied the properties of this definition of scale factor time, and they may lead to complications. Large-scale anisotropic flows in the gas of test particles can be generated as the particles stream into expanding bubbles from outside. Since the null geodesics do not interact with matter except gravitationally, these anisotropies will not be damped in the same way as they would be for photons. The large-scale flow of the gas will not redshift in the normal way, either; for example, if the test particles in some region of an FRW universe have a nonzero mean velocity relative to the comoving frame, the expansion of the universe will merely reduce the energies of all the test particles by the same factor, but will not cause the mean velocity to decrease. Thus, the detailed predictions for this definition of scale-factor cutoff measure remain a matter for future study.

The local scale-factor cutoff and each of the three nonlocal definitions correspond to different global-time parameterizations and thus to different spacetime measures. In general they make different predictions for physical observables; however with regard to the quantities we shall be interested in (probability distributions for cosmological constant and curvature parameter, and relative number of normal observers and Boltzmann brains) their predictions are essentially the same. For the remainder of this thesis we refer to the generic nonlocal definition of scale factor time, for which we take the FRW time as a suitable approximation.

2.2.2 General features of the multiverse

To facilitate later discussion, let us now describe some general properties of eternally inflating spacetimes. The volume fraction f_i occupied by vacuum i on constant scale-factor time slices can be found from the rate equation [42],

$$\frac{df_i}{dt} = \sum_j M_{ij} f_j \,, \tag{2.6}$$

where the transition matrix M_{ij} is given by

$$M_{ij} = \kappa_{ij} - \delta_{ij} \sum_r \kappa_{ri} \,, \tag{2.7}$$

and κ_{ij} is the transition rate from vacuum j to vacuum i per Hubble volume per Hubble time. This rate can also be written

$$\kappa_{ij} = (4\pi/3) H_j^{-4} \Gamma_{ij} \,, \tag{2.8}$$

where Γ_{ij} is the bubble nucleation rate per unit spacetime volume and H_j is the Hubble expansion rate in vacuum j.

The solution of Eq. (2.6) can be written in terms of the eigenvectors and eigenvalues of the transition matrix M_{ij}.

It is easily verified that each terminal vacuum is an eigenvector with eigenvalue zero. We here define "terminal vacua" as those vacua j for which $\kappa_{ij} = 0$ for all i. Thus the terminal vacua include both negative-energy vacua, which collapse in a big crunch, and stable zero-energy vacua. It was shown in Ref. [14] that all of the other eigenvalues of M_{ij} have negative real parts. Moreover, the eigenvalue with the smallest (by magnitude) real part is pure real; we call it the "dominant eigenvalue" and denote it by $-q$ (with $q > 0$). Assuming that the landscape is irreducible, the dominant eigenvalue is nondegenerate. In that case the probabilities defined by the scale-factor cutoff measure are independent of the initial state of the multiverse, since they are determined by the dominant eigenvector.[2]

For an irreducible landscape, the late-time asymptotic solution of Eq. (2.6) can be written in the form[3]

$$f_j(t) = f_j^{(0)} + s_j e^{-qt} + \dots \,, \tag{2.9}$$

where the constant term $f_j^{(0)}$ is nonzero only in terminal vacua and s_j is proportional to the eigenvector of M_{ij} corresponding to the dominant eigenvalue $-q$, with the constant of proportionality determined by the initial distribution of vacua on Σ. It was shown in Ref. [14] that $s_j \leq 0$ for terminal vacua, and $s_j > 0$ for nonterminal vacua, as is needed for Eq. (2.9) to describe a nonnegative volume fraction, with a nondecreasing fraction assigned to any terminal vacuum.

By inserting the asymptotic expansion (2.9) into the differential equation (2.6) and extracting the leading asymptotic behavior for a nonterminal vacuum i, one can

[2]In this work we assume that the multiverse is irreducible; that is, any metastable inflating vacuum is accessible from any other such vacuum via a sequence of tunneling transitions. Our results, however, can still be applied when this condition fails. In that case the dominant eigenvalue can be degenerate, in which case the asymptotic future is dominated by a linear combination of dominant eigenvectors that is determined by the initial state. If transitions that increase the vacuum energy density are included, then the landscape can be reducible only if it splits into several disconnected sectors. That situation was discussed in Appendix A, where two alternative prescriptions were described. The first prescription (preferred by the authors) leads to initial-state dependence only if two or more sectors have the same dominant eigenvalue q, while the second prescription always leads to initial-state dependence.

[3]M_{ij} is not necessarily diagonalizable, but Eq. (2.9) applies in any case. It is always possible to form a complete basis from eigenvectors and generalized eigenvectors, where generalized eigenvectors satisfy $(M - \lambda I)^k s = 0$, for $k > 1$. The generalized eigenvectors appear in the solution with a time dependence given by $e^{\lambda t}$ times a polynomial in t. These terms are associated with the nonleading eigenvalues omitted from Eq. (2.9), and the polynomials in t will not change the fact that they are nonleading.

show that

$$(\kappa_i - q)s_i = \sum_j \kappa_{ij}\, s_j\,, \tag{2.10}$$

where κ_j is the total transition rate out of vacuum j,

$$\kappa_j \equiv \sum_i \kappa_{ij}\,. \tag{2.11}$$

The positivity of s_i for nonterminal vacua then implies rigorously that q is less than the decay rate of the slowest-decaying vacuum in the landscape:

$$q \leq \kappa_{\rm min} \equiv \min\{\kappa_j\}\,. \tag{2.12}$$

Since "upward" transitions (those that increase the energy density) are generally suppressed, we can gain some intuition by first considering the case in which all upward transition rates are set to zero. (Such a landscape is reducible, so the dominant eigenvector can be degenerate.) In this case M_{ij} is triangular, and the eigenvalues are precisely the decay rates κ_i of the individual states. The dominant eigenvalue q is then exactly equal to $\kappa_{\rm min}$.

If upward transitions are included but assumed to have a very low rate, then the dominant eigenvalue q is approximately equal to the decay rate of the slowest-decaying vacuum [43],

$$q \approx \kappa_{\rm min}\,. \tag{2.13}$$

The slowest-decaying vacuum (assuming it is unique) is the one that dominates the asymptotic late-time volume of the multiverse, so we call it the dominant vacuum and denote it by D. Hence,

$$q \approx \kappa_D\,. \tag{2.14}$$

The vacuum decay rate is typically exponentially suppressed, so for the slowest-decaying vacuum we expect it to be extremely small,

$$q \ll 1\,. \tag{2.15}$$

Note that the corrections to Eq. (2.14) are comparable to the upward transition rate from D to higher-energy vacua, but for large energy differences this transition rate is suppressed by the factor $\exp(-8\pi^2/H_D^2)$ [44]. Here and throughout the remainder of this paper we use reduced Planck units, where $8\pi G = c = k_B = 1$. We shall argue in Section 5.3 that the dominant vacuum is likely to have a very low energy density, so the correction to Eq. (2.14) is very small even compared to q.

A possible variant of this picture, with similar consequences, could arise if one assumes that the landscape includes states with nearby energy densities for which the upward transition rate is not strongly suppressed. In that case there could be a group of vacuum states that undergo rapid transitions into each other, but very slow transitions to states outside the group. The role of the dominant vacuum could then be played by this group of states, and q would be approximately equal to some appropriately averaged rate for the decay of these states to states outside the group.

Under these circumstances q could be much less than $\kappa_{\rm min}$. An example of such a situation is described in Subsection 5.2.5.

In the asymptotic limit of late time t, the physical volume that thermalizes into nonterminal vacua of type j between times t and $t + dt$ has the form

$$dV_{*j} = C_j e^{\gamma t} dt\,, \tag{2.16}$$

where C_j is a constant that depends on the type of pocket. (This was derived in Ref. [45] for models with quantum diffusion and in Refs. [46] and [47] for models with bubble nucleation.) The value of γ in Eq. (2.16) is the same for all pockets, but it depends on the choice of time variable t. With a proper-time slicing, it is given by

$$\gamma \sim 3H_{\rm max} \qquad (t = \tau)\,, \tag{2.17}$$

where $H_{\rm max}$ is the expansion rate of the highest-energy vacuum in the landscape, and corrections associated with decay rates and upward tunneling rates have been ignored. In this case the overall expansion of the multiverse is driven by this fastest-expanding vacuum, which then "trickles down" to all of the other vacua. With scale-factor slicing, all regions would expand as $a^3 = e^{3t}$ if it were not for the continuous loss of volume to terminal vacua with negative or zero Λ. Because of this loss, the value of γ is slightly smaller than 3, and the difference is determined mostly by the rate of decay of the slowest-decaying (dominant) vacuum in the landscape [43],

$$\gamma = 3 - q \approx 3 - \kappa_D \qquad (t = \ln a)\,. \tag{2.18}$$

2.2.3 The youngness bias

As we have already mentioned, the proper-time cutoff measure leads to rather bizarre predictions, collectively known as the youngness paradox [48, 49, 47]. With proper time slicing, Eqs. (2.16) and (2.17) tell us that the growth of volume in regions of all types is extremely fast, so at any time the thermalized volume is exponentially dominated by regions that have just thermalized. With this super-fast expansion, observers who take a little less time to evolve are rewarded by a huge volume factor. This means most observers form closer to the cutoff, when there is much more volume available. Assuming that $H_{\rm max}$ is comparable to Planck scale, as one might expect in the string theory landscape, then observers who evolved faster than us by $\Delta\tau = 10^9$ years would have an available thermalized volume which is larger than the volume available to us by a factor of

$$e^{\gamma\,\Delta\tau} \sim e^{3H_{\rm max}\,\Delta\tau} \sim \exp(10^{60})\,. \tag{2.19}$$

Unless the probability of life evolving so fast is suppressed by a factor greater than $\exp(10^{60})$, then these rapidly evolving observers would outnumber us by a huge factor. Since these observers would measure the cosmic microwave background (CMB) temperature to be $T = 2.9$ K, it would be hard to explain why we measure it to be $T = 2.73$ K. Note that because $H_{\rm max}\Delta\tau$ appears in the exponent, the situation is

qualitatively unchanged by considering much smaller values of $H_{\max}$ or $\Delta\tau$.

The situation with a scale-factor cutoff is very different. To illustrate methods used throughout this paper, let us be more precise. Let Δt denote the interval in scale-factor time between the time of thermalization, t_*, and the time when some class of observers measures the CMB temperature. A time cutoff excludes the counting of observers who measure the CMB temperature at times later than t_c, so the number of counted observers is proportional to the volume that thermalizes at time $t_* < t_c - \Delta t$. (For simplicity we focus on pockets that have the same low-energy physics as ours.) The volume of regions thermalized per unit time is given by Eq. (2.16). During the time interval Δt, some of this volume may decay by tunneling transitions to other vacua. This effect is negligible, and we henceforth ignore it. For a given Δt, the thermalized volume available for observers to evolve, as counted by the scale-factor cutoff measure, is

$$\mathcal{V}(\Delta t) \propto \int_{-\infty}^{t_c-\Delta t} e^{\gamma t_*}\, dt_* \propto e^{-\gamma \Delta t}. \tag{2.20}$$

To compare with the results above, consider the relative amounts of volume available for the evolution of two different civilizations, which form at two different time intervals since thermalization, Δt_1 and Δt_2:

$$\frac{\mathcal{V}(\Delta t_1)}{\mathcal{V}(\Delta t_2)} = e^{\gamma(\Delta t_2 - \Delta t_1)} = (a_2/a_1)^{\gamma}\,, \tag{2.21}$$

where a_i is the scale factor at time $t_* + \Delta t_i$. Thus, taking $\gamma \approx 3$, the relative volumes available for observers who measure the CMB at the present value ($T = 2.73$ K), compared to observers who measure it at the value of 10^9 years ago ($T = 2.9$ K), is given by

$$\frac{\mathcal{V}(2.73\text{ K})}{\mathcal{V}(2.9\text{ K})} \approx \left(\frac{2.73\text{ K}}{2.9\text{ K}}\right)^3 \approx 0.8\,. \tag{2.22}$$

Thus, the youngness bias is very mild in the scale-factor cutoff measure. Yet, as we shall see, it can have interesting observational implications.

2.2.4 Expectations for the density contrast Q and the curvature parameter Ω

Pocket-based measures, as well as "gauge-invariant" measures, suffer from a "Q catastrophe" where one expects to measure extreme values of the primordial density contrast Q. To see this, note that these measures exponentially prefer parameter values that generate a large number of e-folds of inflation. This by itself does not appear to be a problem, but Q is related to parameters that determine the number of e-folds. The result of this is a selection effect that exponentially prefers the observation of either very large or very small values of Q, depending on the model of inflation and on which inflationary parameters scan (i.e., which parameters vary significantly across

the landscape) [27, 28]. On the other hand, we observe Q to lie comfortably in the middle of the anthropic range [30], indicating that no such strong selection effect is at work.[4] Note that a similar story applies to the magnitude of the gravitational constant G [29].

With the scale-factor cutoff, on the other hand, this is not a problem. To see this, consider a landscape in which the only parameter that scans is the number of e-folds of inflation; all low-energy physics is exactly as in our universe. Consider first the portions of the hypersurfaces Σ_q that begin slow-roll inflation at time t_q in the interval dt_q. These regions begin with a physical volume proportional to $e^{\gamma t_q}\, dt_q$, and those that do not decay grow by a factor of e^{3N_e} before they thermalize at time $t_* = t_q + N_e$. If κ_I is the transition rate out of the slow-roll inflationary phase (as defined in Eq. (2.8)), then the fraction of volume that does not undergo decay is $e^{-\kappa_I N_e}$.

After thermalization at time t_*, the evolution is the same in all thermalized regions. Therefore we ignore this common evolution and consider the number of observers measuring a given value of N_e to be proportional to the volume of thermalization hypersurfaces that appear at times earlier than the cutoff at scale-factor time t_c. This cutoff requires $t_* = t_q + N_e < t_c$. Summing over all times t_q gives

$$P(N_e) \propto e^{(3-\kappa_I)N_e} \int_{-\infty}^{t_c - N_e} e^{\gamma t_q}\, dt_q \propto e^{(3-\gamma-\kappa_I)N_e}\,. \tag{2.23}$$

Even though the dependence on N_e is exponential, the factor

$$3 - \gamma - \kappa_I \approx \kappa_D - \kappa_I \tag{2.24}$$

is exponentially suppressed. Thus we find $P(N_e)$ is a very weak function of N_e, and there is not a strong selection effect for a large number of e-folds of slow-roll inflation. In fact, since the dominant vacuum D is by definition the slowest-decaying vacuum, we have $\kappa_I > \kappa_D$. Thus the scale-factor cutoff introduces a very weak selection for smaller values of N_e.

Because of the very mild dependence on N_e, we do not expect the scale-factor measure to impose significant cosmological selection on the scanning of any inflationary parameters. Thus, there is no Q catastrophe — nor is there the related problem for G — and the distribution of Q is essentially its distribution over the states in the landscape, modulated by inflationary dynamics and any anthropic selection effects.

The distribution $P(N_e)$ is also important for the expected value of the curvature parameter Ω. This is because the deviation of Ω from unity decreases during an inflationary era,

$$|\Omega - 1| \propto e^{-2N_e}\,. \tag{2.25}$$

Hence pocket-based and "gauge-invariant" measures, which exponentially favor large values of N_e, predict a universe with Ω extremely close to unity. The distributions

[4] Possible resolutions to this problem have been proposed in Refs. [27, 28, 31, 7].

of Ω from a variety of models have been calculated using a pocket-based measure in Refs. [12] and [46].

On the other hand, as we have just described, the scale-factor cutoff measure does not significantly select for any value of N_e. There will still be some prior distribution of N_e, related to the distributions of inflationary parameters over the states in the landscape, but it is not necessary that N_e be driven strongly toward large values (in fact, it has been argued that small values should be preferred in the string landscape, see e.g. Ref. [50]). Thus, it appears that the scale-factor cutoff allows for the possibility of a detectable negative curvature. The probability distribution of Ω in this type of measure has been studied in Ref. [51] and it will be discussed in detail in Chapter 4.

2.3 Conclusions

In this Chapter, we have introduced and defined the scale-factor cutoff measure and shown that it does not suffer from some of the problems afflicting other proposed measures. The most severe of these is the "youngness paradox" — the prediction of an extremely youth-dominated distribution of observers — which follows from the proper-time cutoff measure. The scale-factor cutoff measure, on the other hand, predicts only a very mild youngness bias, which is consistent with observation. Another problem, which arises in pocket-based and "gauge-invariant" measures, is the Q catastrophe, where one expects to measure the amplitude of the primordial density contrast Q to have an unfavorably large or small value. This problem ultimately stems from an exponential preference for a large number of e-folds of slow-roll inflation in these measures. The scale-factor cutoff does not strongly select for more inflation, and thus does not suffer from a Q catastrophe. An unattractive feature of causal patch and comoving-volume measures is that their predictions are sensitive to the assumptions one makes about the initial conditions for the multiverse. Meanwhile, the scale-factor cutoff measure is essentially independent of the initial state. This property reflects the attractor character of eternal inflation: the asymptotic late-time evolution of an eternally inflating universe is independent of the starting point.

In the following Chapters we shall analyze the scale-factor cutoff measure more quantitatively by studying the probability distributions of the cosmological constant and of the cuvature parameter, as well as the issue of Boltzmann brain domination.

Chapter 3

The Distribution of the Cosmological Constant

The subject of this Chapter is the prediction of the cosmological constant Λ [52, 53, 54, 55, 56, 57], which is arguably a major success of the multiverse picture. Most calculations of the distribution of Λ in the literature [56, 57, 58, 59, 60, 61] do not explicitly specify the measure, but in fact correspond to using the pocket-based measure. The distribution of positive Λ in a causal-patch measure has also been considered [62]. The authors of Ref. [62] emphasize that the causal-patch measure gives a strong suppression for values of Λ more than about ten times the observed value, while anthropic constraints alone might easily allow values 1000 times larger than observed, depending on assumptions. Here, we calculate the distribution for Λ in the scale-factor cutoff measure, considering both positive and negative values of Λ, and compare our results with those of other approaches. We find that our distribution is in a good agreement with the observed value of Λ, and that the scale-factor cutoff gives a suppression for large positive values of Λ that is very similar to that of the causal-patch measure.

This Chapter is organized as follows. After stating our model assumptions in section 3.1, we compute the probability distribution of Λ for the pocket-based measure in section 3.2, reproducing previous results. Then we calculate the distribution for the scale-factor cutoff, both for the nonlocal "FRW" measure discussed in section 2.2.1 (section 3.3) and the "local" measure (section 3.4). In all cases we study positive and negative values of Λ. Our main results are summarized in section 3.5. Appendix B at the end of the thesis refers particularly to this Chapter. In fact, it contains an analysis of the evolution of the collapse density threshold, along with a description of the linear growth function of density perturbations.

3.1 Model assumptions

We now consider a landscape of vacua with the same low-energy physics as we observe, except for an essentially continuous distribution of possible values of Λ. According to Eq. (2.16), the volume that thermalizes between times t_* and $t_* + dt_*$ with values

of cosmological constant between Λ and $\Lambda + d\Lambda$ is given by

$$dV_*(\Lambda) = C(\Lambda) d\Lambda \, e^{\gamma t_*} dt_* \,. \tag{3.1}$$

The factor of $C(\Lambda)$ plays the role of the "prior" distribution of Λ; it depends on the spectrum of possible values of Λ in the landscape and on the dynamics of eternal inflation. The standard argument [52, 56] suggests that $C(\Lambda)$ is well approximated by

$$C(\Lambda) \approx \text{const}\,, \tag{3.2}$$

because anthropic selection restricts Λ to values that are very small compared to its expected range of variation in the landscape. The conditions of validity of this heuristic argument have been studied in simple landscape models [43, 63, 64], with the conclusion that it does in fact apply to a wide class of models. Here, we shall assume that Eq. (3.2) is valid.

Anthropic selection effects are usually characterized by the fraction of matter that has clustered in galaxies. The idea here is that a certain average number of stars is formed per unit galactic mass and a certain number of observers per star, and that these numbers are not strongly affected by the value of Λ. Furthermore, the standard approach is to assume that some minimum halo mass M_G is necessary to drive efficient star formation and heavy element retention. Since we regulate the volume of the multiverse using a time cutoff, it is important for us to also track at what time observers arise. We assume that after halo collapse, some fixed proper time lapse $\Delta\tau$ is required to allow for stellar, planetary, and biological evolution before an observer can measure Λ. Then the number of observers measuring Λ before some time τ in a thermalized volume of size V_* is roughly

$$\mathcal{N} \propto F(M_G, \tau - \Delta\tau) V_* \,, \tag{3.3}$$

where F is the collapse fraction, measuring the fraction of matter that clusters into objects of mass greater than or equal to M_G, at time $\tau - \Delta\tau$.

Anthropic selection for structure formation ensures that within each relevant pocket matter dominates the energy density before Λ does. Thus, all thermalized regions evolve in the same way until well into the era of matter domination. To draw upon this common evolution, within each pocket we define proper time τ with respect to a fixed time of thermalization, τ_*. It is convenient to also define a reference time τ_m such that τ_m is much larger than the time of matter-radiation equality and much less than the time of matter-Λ equality. Then evolution before time τ_m is the same in every pocket, while after τ_m the scale factor evolves as

$$\tilde{a}(\tau) = \begin{cases} H_\Lambda^{-2/3} \sinh^{2/3}(\frac{3}{2} H_\Lambda \tau) & \text{for } \Lambda > 0 \\ H_\Lambda^{-2/3} \sin^{2/3}(\frac{3}{2} H_\Lambda \tau) & \text{for } \Lambda < 0\,. \end{cases} \tag{3.4}$$

Here we have defined

$$H_\Lambda \equiv \sqrt{|\Lambda|/3}\,, \tag{3.5}$$

and use units with $G = c = 1$. The prefactors $H_\Lambda^{-2/3}$ ensure that early evolution is identical in all thermalized regions. This means the global scale factor a is related to $\tilde{a}$ by some factor that depends on the scale-factor time t_* at which the region of interest thermalized.

In the case $\Lambda > 0$, the rate at which halos accrete matter decreases with time and halos may settle into galaxies that permit quiescent stellar systems such as ours. The situation with $\Lambda < 0$ is quite different. At early times, the evolution of overdensities is the same; but when the proper time reaches $\tau_{\rm turn} = \pi/3H_\Lambda$, the scale factor begins to decrease and halos begin to accrete matter at a rate that increases with time. Such rapid accretion may prevent galaxies from settling into stable configurations, which in turn would cause planetary systems to undergo more frequent close encounters with passing stars. This effect might become significant even before turnaround, since our present environment benefits from positive Λ slowing the collision rate of the Milky Way with other systems.

For this reason, we use Eq. (3.3) to estimate the number of observers if $\Lambda > 0$, but for $\Lambda < 0$ we consider two alternative anthropic hypotheses:

A. we use Eq. (3.3), but of course taking account of the fact that the proper time τ cannot exceed $\tau_{\rm crunch} = 2\pi/3H_\Lambda$; or

B. we use Eq. (3.3), but with the hypothesis that the proper time τ is capped at $\tau_{\rm turn} = \pi/3H_\Lambda$.

Here $\tau_{\rm crunch}$ refers to the proper time at which a thermalized region in a collapsing pocket reaches its future singularity, which we refer to as its "crunch." Anthropic hypothesis A corresponds to the assumption that life can form in any sufficiently massive collapsed halo, while anthropic hypothesis B reflects the assumption that the probability for the formation of life becomes negligible in the tumultuous environment following turnaround. Similar hypotheses for $\Lambda < 0$ were previously used in Ref. [61]. It seems reasonable to believe that the truth lies somewhere between these two hypotheses, perhaps somewhat closer to hypothesis B.

3.2 Distribution of Λ using a pocket-based measure

Before calculating the distribution of Λ using a scale-factor cutoff, we review the standard calculation [56, 57, 58, 59, 60, 61]. This approach assumes an ensemble of equal-size regions with a flat prior distribution of Λ. The regions are allowed to evolve indefinitely, without any time cutoff, so in the case of $\Lambda > 0$ the selection factor is given by the asymptotic collapse fraction at $\tau \to \infty$. For $\Lambda < 0$ we shall consider anthropic hypotheses A and B. This prescription corresponds to using the

pocket-based measure, in which the ensemble includes spherical regions belonging to different pockets and observations are counted in the entire comoving history of these regions. The corresponding distribution function is given by

$$P(\Lambda) \propto \begin{cases} F(M_G, \tau \to \infty) & \text{for } \Lambda > 0 \\ F(M_G, \tau_{\rm crunch} - \Delta\tau) & \text{for } \Lambda < 0 \ \ (A) \\ F(M_G, \tau_{\rm turn} - \Delta\tau) & \text{for } \Lambda < 0 \ \ (B)\,, \end{cases} \tag{3.6}$$

where, again, $\tau_{\rm crunch} = 2\pi/3H_\Lambda$ is the proper time of the crunch in pockets with $\Lambda < 0$, while $\tau_{\rm turn} = \pi/3H_\Lambda$.

We approximate the collapse fraction F using the Press-Schechter (PS) formalism [65], which gives

$$F(M_G, \tau) = \mathrm{erfc}\left[\frac{\delta_c(\tau)}{\sqrt{2}\,\sigma(M_G, \tau)}\right], \tag{3.7}$$

where $\sigma(M_G, \tau)$ is the root-mean-square fractional density contrast $\delta M/M$ averaged over a comoving scale enclosing mass M_G and evaluated at proper time τ, while δ_c is the collapse density threshold. As is further explained in appendix B, $\delta_c(\tau)$ is determined by considering a "top-hat" density perturbation in a flat universe, with an arbitrary initial amplitude. $\delta_c(\tau)$ is then defined as the amplitude reached by the linear evolution of an overdensity of nonrelativistic matter $\delta\rho_m/\rho_m$ that has the same initial amplitude as a top-hat density perturbation that collapses to a singularity in proper time τ. $\delta_c(\tau)$ has the constant value of 1.686 in an Einstein-de Sitter universe (i.e., flat, matter-dominated universe), but it evolves with time when $\Lambda \neq 0$ [66, 67]. We simulate this evolution using the fitting functions (B.23), which are accurate to better than 0.2%. Note, however, that the results are not significantly different if one simply uses the constant value $\delta_c = 1.686$.

Aside from providing the collapse fraction, the PS formalism describes the "mass function," i.e. the distribution of halo masses as a function of time. N-body simulations indicate that PS model overestimates the abundance of halos near the peak of the mass function, while underestimating that of more massive structures [68]. Consequently, other models have been developed (see e.g. Refs. [69]), while others have studied numerical fits to N-body results [70, 61]. From each of these approaches, the collapse fraction can be obtained by integrating the mass function. We have checked that our results are not significantly different if we use the fitting formula of Ref. [61] instead of Eq. (3.7). Meanwhile, we prefer Eq. (3.7) to the fit of Ref. [61] because the latter was performed using only numerical simulations with $\Lambda > 0$.

The evolution of the density contrast σ is treated linearly, to be consistent with the definition of the collapse density threshold δ_c. Thus we can factorize the behavior of $\sigma(M_G, \tau)$, writing

$$\sigma(M_G, \tau) = \bar{\sigma}(M_G)\, G_\Lambda(\tau)\,, \tag{3.8}$$

where $G_\Lambda(\tau)$ is the linear growth function, which is normalized so that the behavior for small τ is given by $G_\Lambda(\tau) \sim (3H_\Lambda\tau/2)^{2/3}$. In appendix B we shall give exact integral

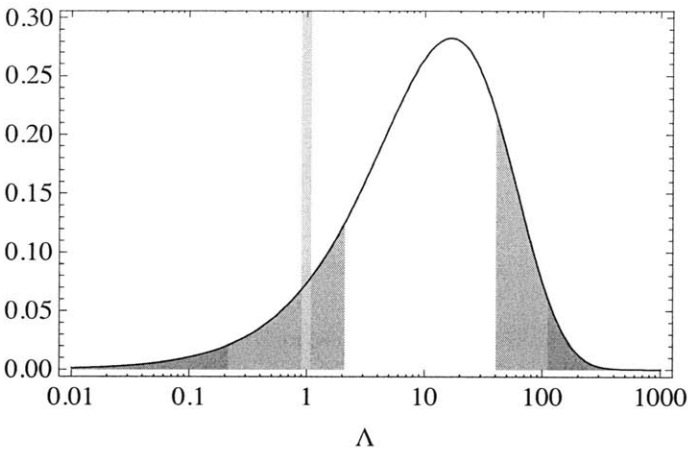

Figure 3-1: The normalized distribution of Λ for $\Lambda > 0$, with Λ in units of the observed value, for the pocket-based measure. The vertical bar highlights the value we measure, while the shaded regions correspond to points more than one and two standard deviations from the mean.

expressions for $G_\Lambda(\tau)$, and also the fitting formulae (B.12) and (B.13), taken from Ref. [61], that we actually used in our calculations. Note that for $\Lambda \geq 0$ the growth rate $\dot{G}_\Lambda(\tau)$ always decreases with time ($\ddot{G}_\Lambda(\tau) < 0$), while for $\Lambda < 0$ the growth rate reaches a minimum at $\tau \approx 0.24\tau_{\rm crunch}$ and then starts to accelerate. This accelerating rate of growth is related to the increasing rate of matter accretion in collapsed halos after turnaround, which we mentioned above in motivating the anthropic hypothesis B.

The prefactor $\bar{\sigma}(M_G)$ in Eq. (3.8) depends on the scale M_G at which the density contrast is evaluated. According to our anthropic model, M_G should correspond to the minimum halo mass for which star formation and heavy element retention is efficient. Indeed, the efficiency of star formation is seen to show a sharp transition: it falls abruptly for halo masses smaller than $M_G \sim 2 \times 10^{11} M_\odot$, where $M_\odot$ is the solar mass [71]. Peacock [61] showed that the existing data on the evolving stellar density can be well described by a Press-Schechter calculation of the collapsed density for a single mass scale, with a best fit corresponding to $\sigma(M_G, \tau_{1000}) \approx 6.74 \times 10^{-3}$, where τ_{1000} is the proper time corresponding to a temperature $T = 1000$ K. Using cosmological parameters current at the time, Peacock found that this perturbation amplitude corresponds to an effective galaxy mass of $1.9 \times 10^{12}\, M_\odot$. Using the more recent WMAP-5 parameters [5], as is done throughout this thesis,[1] we find (using Ref. [72] and the CMBFAST program) that the corresponding effective galaxy mass is $1.8 \times 10^{12}\, M_\odot$.

Unless otherwise noted, in this Chapter we set the prefactor $\bar{\sigma}(M_G)$ in Eq. (3.8) by choosing $M_G = 10^{12}\, M_\odot$. Using the WMAP-5 parameters and the CMBFAST pro-

[1]The relevant values are $\Omega_\Lambda = 0.742$, $\Omega_m = 0.258$, $\Omega_b = 0.044$, $n_s = 0.96$, $h = 0.719$, and $\Delta^2_{\mathcal{R}}(k = 0.02\,{\rm Mpc}^{-1}) = 2.21 \times 10^{-9}$.

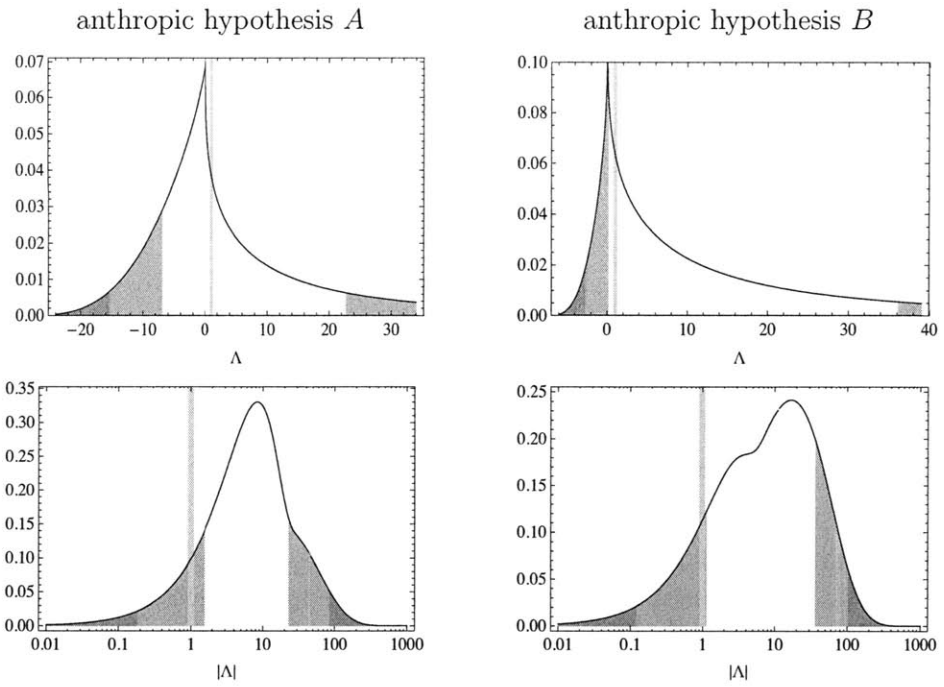

Figure 3-2: The normalized distribution of Λ, with Λ in units of the observed value, for the pocket-based measure. The left column corresponds to anthropic hypothesis A while the right column corresponds to anthropic hypothesis B. Meanwhile, the top row shows $P(\Lambda)$ while the bottom row shows $P(|\Lambda|)$. The vertical bars highlight the value we measure, while the shaded regions correspond to points more than one and two standard deviations from the mean.

gram, we find that at the present cosmic time $\sigma(10^{12}\, M_\odot) \approx 2.03$. This corresponds to $\sigma(10^{12}\, M_\odot, \tau_{1000}) \approx 7.35 \times 10^{-3}$.

We are now prepared to display the results, plotting $P(\Lambda)$ as determined by Eq. (3.6). We first reproduce the standard distribution of Λ, which corresponds to the case when $\Lambda > 0$. This is shown in Fig. 3-1. We see that the value of Λ that we measure is between one and two standard deviations from the mean. Throughout the Chapter, the vertical bars in the plots merely highlight the observed value of Λ and do not indicate its experimental uncertainty. The quality of the fit depends on the choice of scale M_G; in particular, choosing smaller values of M_G weakens the fit [73, 60]. Note however that the value of M_G that we use is already less than that recommended by Ref. [61].

Fig. 3-2 shows the distribution of Λ for positive and negative values of Λ. We use $\Delta\tau = 5 \times 10^9$ years, corresponding roughly to the age of our solar system. The left column corresponds to choosing anthropic hypothesis A while the right column corresponds to anthropic hypothesis B. To address the question of whether the observed value of $|\Lambda|$ lies improbably close to the special point $\Lambda = 0$, in the second row we plot the distributions for $P(|\Lambda|)$. We see that the observed value of Λ lies

only a little more than one standard deviation from the mean, which is certainly acceptable. (Another measure of the "typicality" of our value of Λ has been studied in Ref. [60]).

3.3 Distribution of Λ using the scale-factor cutoff measure

We now turn to the calculation of $P(\Lambda)$ using a scale-factor cutoff to regulate the diverging volume of the multiverse. When we restrict attention to the evolution of a small thermalized patch, a cutoff at scale-factor time t_c corresponds to a proper time cutoff τ_c, which depends on t_c and the time at which the patch thermalized, t_*. Here we take the thermalized patch to be small enough that scale-factor time t is essentially constant over hypersurfaces of constant τ. Then the various proper and scale-factor times are related by

$$t_c - t_* = \int_{\tau_*}^{\tau_c} H(\tau)\, d\tau = \ln\left[\tilde{a}(\tau_c)/\tilde{a}(\tau_*)\right]. \tag{3.9}$$

Recall that all of the thermalized regions of interest share a common evolution up to the proper time τ_m, after which they follow Eqs. (3.4). Solving for the proper time cutoff τ_c gives

$$\tau_c = \frac{2}{3} H_\Lambda^{-1} \mathrm{arcsinh}\left[\tfrac{3}{2} H_\Lambda \tau_m\, e^{\frac{3}{2}(t_c - t_* - C)}\right], \tag{3.10}$$

for the case $\Lambda > 0$, and

$$\tau_c = \frac{2}{3} H_\Lambda^{-1} \arcsin\left[\tfrac{3}{2} H_\Lambda \tau_m\, e^{\frac{3}{2}(t_c - t_* - C)}\right], \tag{3.11}$$

for $\Lambda < 0$. The term C is a constant that accounts for evolution from time τ_* to time τ_m. Note that as $t_c - t_*$ is increased in Eq. (3.11), τ_c grows until it reaches the time of scale-factor turnaround in the pocket, $\tau_{\rm turn} = \pi/3H_\Lambda$, after which the expression is ill-defined. Physically, the failure of Eq. (3.11) corresponds to when a thermalized region reaches turnaround before the scale-factor time reaches its cutoff at t_c. After turnaround, the scale factor decreases; therefore these regions evolve without a cutoff all the way up to the time of crunch, $\tau_{\rm crunch} = 2\pi/3H_\Lambda$.

When counting the number of observers in the various pockets using a scale-factor cutoff, one must keep in mind the dependence on the thermalized volume V_* in Eq. (3.3), since in this case V_* depends on the cutoff. As stated earlier, we assume the rate of thermalization for pockets containing universes like ours is independent of Λ. Thus, the total physical volume of all regions that thermalized between times t_* and $t_* + dt_*$ is given by Eq. (2.16), and is independent of Λ. Using Eq. (3.3) to count the number of observers in each thermalized patch, and summing over all times

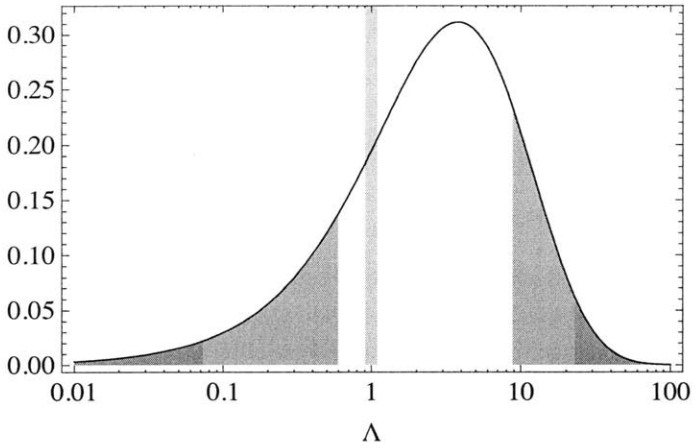

Figure 3-3: The normalized distribution of Λ for $\Lambda > 0$, with Λ in units of the observed value, for the scale-factor cutoff. The vertical bar highlights the value we measure, while the shaded regions correspond to points more than one and two standard deviations from the mean.

below the cutoff, we find

$$P(\Lambda) \propto \int_{-\infty}^{t_c} F[M_G, \tau_c(t_c, t_*) - \Delta\tau]\, e^{\gamma t_*} dt_* \,. \tag{3.12}$$

Note that regions thermalizing at a later time t_* have a greater weight $\propto e^{\gamma t_*}$. This is an expression of the youngness bias in the scale-factor measure. The Λ dependence of this distribution is implicit in F, which depends on $\delta_c(\Lambda, \tau_c - \Delta\tau)/\sigma_{\rm rms}(\Lambda, \tau_c - \Delta\tau)$, and in turn on $\tau_c(\Lambda)$, which is described below.

For pockets with $\Lambda > 0$, the cutoff on proper time τ_c is given by Eq. (3.10). Meanwhile, when $\Lambda < 0$, τ_c is given by Eq. (3.11), when that expression is well-defined. In practice, the constant C of Eqs. (3.10) and (3.11) is unimportant, since a negligible fraction of structures form before the proper time τ_m. Furthermore, for a reference time τ_m chosen deep in the era of matter domination, the normalized distribution is independent of τ_m. As mentioned above, for sufficiently large $t_c - t_*$ Eq. (3.11) becomes ill-defined, corresponding to the thermalized region reaching its crunch before the scale-factor cutoff. In this case we set $\tau_c = \tau_{\rm crunch}$ or $\tau_c = \tau_{\rm turn}$, corresponding to the anthropic hypothesis A or B described above.

To compare with previous work, we first display the distribution of positive Λ in Fig. 3-3. We have set $\gamma = 3$ and use $\Delta\tau = 5 \times 10^9$ years. Clearly, the scale-factor cutoff provides an excellent fit to observation, when attention is limited to $\Lambda > 0$. Note that the scale-factor-cutoff distribution exhibits a much faster fall off at large Λ than the pocket-based distribution in Fig. 3-1. The reason is not difficult to understand. For larger values of Λ, the vacuum energy dominates earlier. The universe then begins expanding exponentially, and this quickly triggers the scale-factor cutoff. Thus,

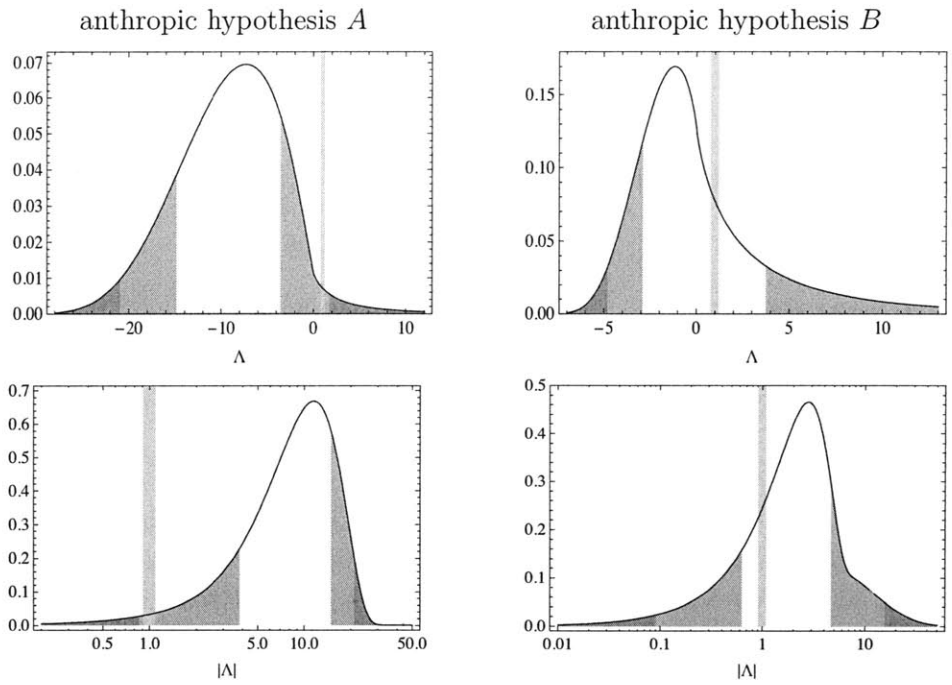

Figure 3-4: The normalized distribution of Λ, with Λ in units of the observed value, for the scale-factor cutoff. The left column corresponds to anthropic hypothesis A while the right column corresponds to anthropic hypothesis B. Meanwhile, the top row shows $P(\Lambda)$ while the bottom row shows $P(|\Lambda|)$. The vertical bars highlight the value we measure, while the shaded regions correspond to points more than one and two standard deviations from the mean.

pockets with larger values of Λ have an earlier cutoff (in terms of the proper time) and have less time to evolve observers. This tendency for the cutoff to kick in soon after Λ-domination may help to sharpen the anthropic explanation [58, 74] of the otherwise mysterious fact that we live so close to this very special epoch (matter-Λ equality) in the history of the universe.

The distribution of Λ for positive and negative values of Λ is displayed in Fig. 3-4, using the same parameter values as before. We see that the distribution with anthropic hypothesis A provides a reasonable fit to observation, with the measured value of Λ appearing just within two standard deviations of the mean. Note that the weight of this distribution is dominated by negative values of Λ, yet anthropic hypothesis A may not give the most accurate accounting of observers in pockets with $\Lambda < 0$. Anthropic hypothesis B provides an alternative count of the number of observers in regions that crunch before the cutoff, and we see that the corresponding distributions provide a very good fit to observation.

The above distributions all use $\Delta\tau = 5 \times 10^9$ years and $M_G = 10^{12} M_\odot$. These values are motivated respectively by the age of our solar system and by the mass of our galactic halo, the latter being a good match to an empirical fit determining

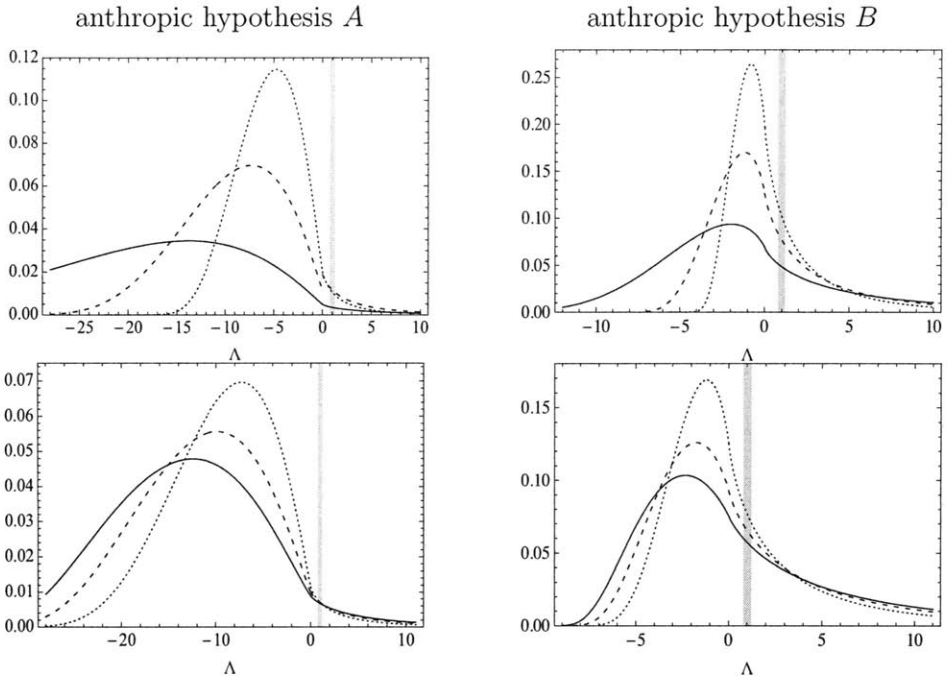

Figure 3-5: The normalized distribution of Λ, with Λ in units of the observed value in the scale-factor cutoff. The left column corresponds to anthropic hypothesis A while the right column corresponds to anthropic hypothesis B. The top row displays curves for $\Delta\tau = 3$ (solid), 5 (dashed), and 7 (dotted) $\times 10^9$ years, with $M_G = 10^{12}\, M_\odot$, while the bottom row displays curves for $M_G = 10^{10}\, M_\odot$ (solid), $10^{11}\, M_\odot$ (dashed), and $10^{12}\, M_\odot$ (dotted), with $\Delta\tau = 5 \times 10^9$ years. The vertical bars highlight the value of Λ that we measure.

the halo mass scale characterizing efficient star formation [61]. Yet, to illustrate the dependence of our main result on $\Delta\tau$ and M_G, in Fig. 3-5 we display curves for both anthropic hypotheses A and B, using $\Delta\tau = 3$, 5, and 7×10^9 years and using $M_G = 10^{10}$, 10^{11}, and $10^{12} M_\odot$. The distribution varies significantly as a result of these changes, but the fit to the observed value of Λ remains good.

3.4 Distribution of Λ using the "local" scale-factor cutoff measure

Let us now repeat the analysis for the case when we treat the scale-factor time t' as a purely local quantity, defined by Eqs. (2.4)-(2.5), where we use the prime to help distinguish the results here from those of the "FRW" scale-factor time t. We freeze the value of scale-factor time when H becomes negative. The strategy of the previous section was to divide the congruence of geodesics into small "patches", such that on any hypersurface orthogonal to the congruence of a given patch, the scale-factor time

and proper time were essentially constant. Then, we counted the number of observers in an arbitrary such patch that featured reheating at scale-factor time t'_*, and then summed over all t'_* . Let us take up this strategy again. Only, we are careful to note that aside from the curvature from bubble wall geometry, there is curvature due to quantum fluctuations of the inflaton and subsequent big bang evolution. Thus, the above patches should be made small enough that this smaller-scale curvature is constant over any patch.

The distribution of observed values of Λ can then be written

$$P(\Lambda) \propto \int_{-\infty}^{t'_c} \mathcal{A}(\Lambda; t'_c, t'_*) e^{\gamma t'_*} dt'_* \,, \tag{3.13}$$

where $\mathcal{A}(\Lambda; t'_c, t'_*)$ is the typical number of observers seeing cosmological constant Λ in a patch that thermalizes at scale-factor time t'_*, before scale-factor time t'_c , and we shall set $\gamma = 3$. As before, we restrict our attention to observers in galaxies with mass M_G and model the evolution of these galaxies as that of a spherical top-hat overdensity. A given patch can be characterized by its curvature κ at the time of reheating. Since our reference class of observers is equivalent to galaxies with mass M_G, and because we use the top-hat approximation for the curvature, we can bundle patches so that they enclose a comoving mass M_G. Note that the probability that Λ is measured before scale-factor time t_c in such a patch is a step function with respect to the curvature κ of such a patch: either κ is so large that the patch turns around or collapses before t_c, or not. We restrict attention to regions that feature inflation as in our universe, so that κ has an approximately Gaussian distribution, with root- mean-square so as to reflect the primordial curvature perturbation on scales enclosing mass M_G in our universe. Thus the distribution of values of κ is proportional to $e^{-\kappa^2/2\kappa^2_{\rm rms}}$, and inserting the step-function behaviour noted above we find

$$\mathcal{A}(\Lambda; t'_c, t'_*) \propto \mathrm{erfc}\left[\frac{\kappa_{\rm min}(\Lambda; t'_c, t'_*)}{\sqrt{2}\kappa_{\rm rms}}\right] \,, \tag{3.14}$$

where $\kappa_{\rm min}(\Lambda; t'_c, t'_*)$ is the smallest curvature κ for which a spherical overdensity turns around or collapses, between reheating scale-factor time t'_* and the cutoff t'_c.

In the idealization of spherical top-hat overdensities, each patch can be described by an FRW metric, with scale factor A. Patches that contain observers expand from scale factor A_* at t'_* to some maximum scale factor $A_{\rm turn}(\Lambda, \kappa, A_*)$, and then turn around and collapse. The scale-factor time between reheating and turnaround is $t'_{\rm turn} - t'_* = \ln(A_{\rm turn}/A_*)$. In terms of scale-factor time t', if a patch turns around before the cutoff t_c, then it contains observers. In other words, if

$$t'_c - t'_* \geq \ln(A_{\rm turn}/A_*) \tag{3.15}$$

the patch contains observers. We can use Birkhoff's theorem to map the evolution of a spherical overdensity to that of a closed FRW universe. Hence we write the

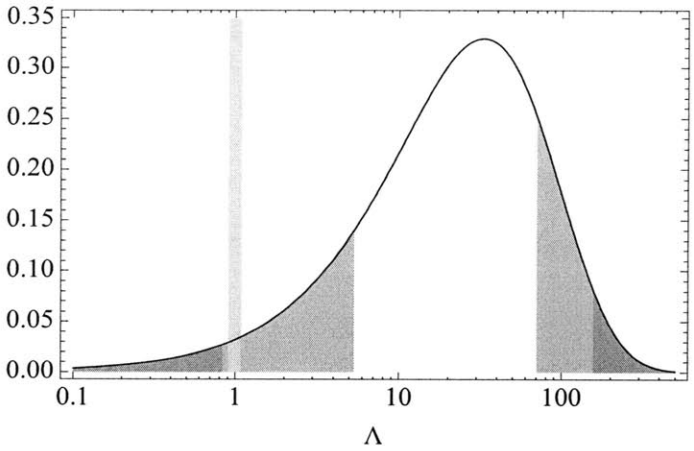

Figure 3-6: The normalized distribution of Λ for $\Lambda > 0$, with Λ in units of the observed value, for the "local" scale-factor cutoff. The vertical bar highlights the value we measure, while the shaded regions correspond to points more than one and two standard deviations from the mean.

Friedmann equation,

$$H^2 = \frac{8\pi G}{3}\left[\rho_\Lambda + \frac{\rho_0}{A^3} - \frac{\kappa}{A^2}\right], \tag{3.16}$$

where we have normalized the scale factor A such that $A = 1$ when the matter density equals ρ_0. The local scale factor A turns around when the local Hubble rate $H = 0$, i.e. when

$$\rho_\Lambda A^3 - \kappa A + \rho_0 = 0\,. \tag{3.17}$$

Let us call the solution of this cubic equation $A_{\rm turn}(\kappa)$; it can in principle be written in closed form. Furthermore, the expression can be inverted, to give the curvature as a function of $A_{\rm turn}$: $\kappa(A_{\rm turn})$. In fact, we can find this function directly from Eq. (3.17). Thus,

$$\kappa(A_{\rm turn}) = \frac{1}{A_{\rm turn}}\left[\rho_0 + \rho_\Lambda A_{\rm turn}^3\right]. \tag{3.18}$$

Now, $\kappa_{\rm min}$ is simply the value of κ for which $t_c' - t_*' = \ln(A_{\rm turn}/A_*)$, so

$$\kappa_{\rm min}(\Lambda; t_c', t_*') = \frac{1}{A_*}e^{t_*'-t_c'}\left[\rho_0 + \rho_\Lambda A_*^3 e^{3(t_c'-t_*')}\right]. \tag{3.19}$$

We can trade the variable t_*' from the variable $A_{\rm turn}$ using Eq. (3.15) and then express the probability distribution Eq. (3.13) as

$$P(\Lambda) \propto \int_{-\infty}^{t_c'} {\rm erfc}\left[\frac{\rho_0 + \rho_\Lambda A_{\rm turn}^3}{\sqrt{2}\kappa_{\rm rms} A_{\rm turn}}\right]\frac{A_*^3}{A_{\rm turn}^4} dA_{\rm turn}\,, \tag{3.20}$$

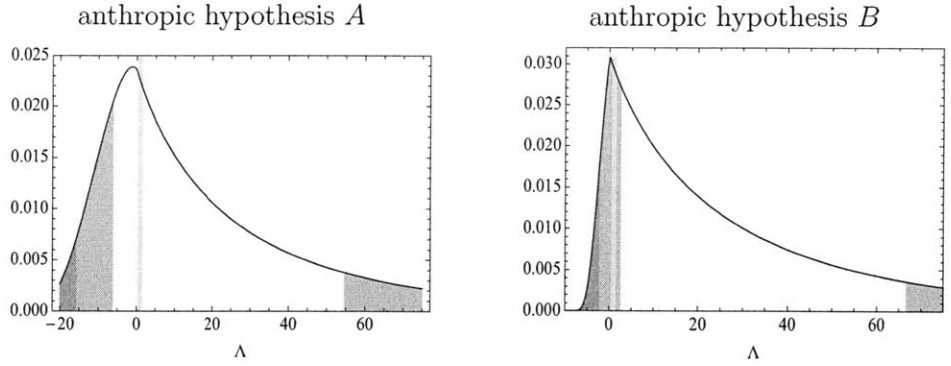

Figure 3-7: The normalized distribution of Λ, with Λ in units of the observed value, for the "local" scale-factor cutoff. The left column corresponds to anthropic hypothesis A while the right column corresponds to anthropic hypothesis B. The vertical bars highlight the value we measure, while the shaded regions correspond to points more than one and two standard deviations from the mean.

We can write $\kappa_{\rm rms} = (5/3)\rho_0\sigma_0$, where σ_0 is the density constrast evaluated on a comoving scale enclosing mass M_G, when $A = 1$. Taking ρ_0 to be evaluated at a time deep in matter domination, the early universe behaviour of each patch is the same. Thus, A_* is independent of Λ. Furthermore, we may take $A_* \to 0$ in the lower limit of integration, since the erfc gives negligible contribution there. Now, $A_{\rm turn}$ is a dummy variable of integration, so we can replace $A_{\rm turn} \to z$ and re-write Eq. (3.20) as

$$P(\Lambda) \propto \int_0^\infty {\rm erfc}\left[\frac{1+(\rho_\Lambda/\rho_0)z^3}{\sqrt{2}\kappa_{\rm rms}(5/3)\sigma_0 z}\right]\frac{1}{z^4}dz\,. \tag{3.21}$$

The result is surprisingly simple in form. The result should be independent of at what time we set $A = 1$, so long as it is deep into matter domination. To see this, note that deep in matter domination $\sigma \propto A$. So, let us write $\rho_\Lambda/\rho_0 = \hat{\Lambda}x_0$, where $\hat{\Lambda}$ is the cosmological constant measure in units of the value measured in our Universe. Then $\sigma \propto x_0^{1/3}$, and x_0 is independent of Λ. Clearly, we can perform a variable redefinition on Eq. (3.21), and x_0 cancels out. We choose ρ_0 to be the matter density when the radiation temperature is $T = 1000$ K. This gives $\rho_\Lambda/\rho_0 = 5.82\times10^{-8}\hat{\Lambda}$, and $\sigma_0 = 7.35\times10^{-3}$. The resulting probability distribution for positive Λ is plotted in Figure 3-6.

So far, we never assumed a particular sign for ρ_Λ, so the result of Eq. (3.21) should essentially apply both positive and negative Λ. The exception concerns our assumption that observers arise whenever the scale factor reaches $A_{\rm turn}$ before t_c'. In negative Λ universes, we must ensure there is sufficient time between turnaround (collapse) and the nal FRW singularity, for observers to arise. Let us formulate this constraint as follows. Denote the FRW scale factor within a collapsing universe using

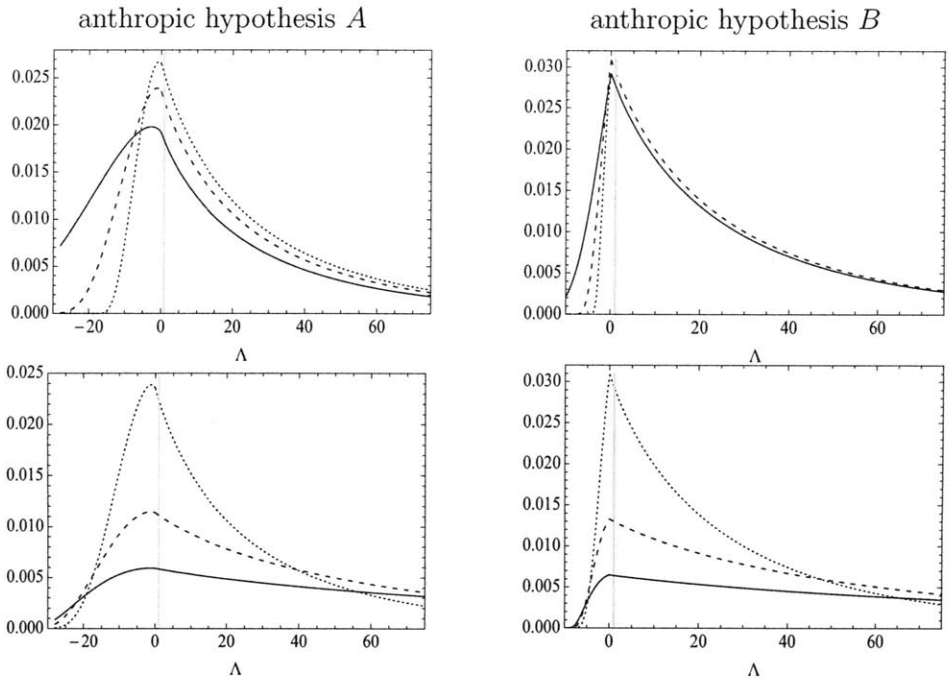

Figure 3-8: The normalized distribution of Λ, with Λ in units of the observed value in the "local" scale-factor cutoff. The left column corresponds to anthropic hypothesis A while the right column corresponds to anthropic hypothesis B. The top row displays curves for $\Delta\tau = 3$ (solid), 5 (dashed), and 7 (dotted) $\times 10^9$ years, with $M_G = 10^{12}\, M_\odot$, while the bottom row displays curves for $M_G = 10^{10}\, M_\odot$ (solid), $10^{11}\, M_\odot$ (dashed), and $10^{12}\, M_\odot$ (dotted), with $\Delta\tau = 5 \times 10^9$ years. The vertical bars highlight the value of Λ that we measure.

$a(\tau)$, where τ is the FRW proper time. Then we may demand,

$$\ln\left[\frac{A_{\rm turn}}{A_*}\right] \leq \ln\left[\frac{a(\tau_{\rm turn} - \Delta\tau)}{a(\tau_*)}\right] . \tag{3.22}$$

for $\Lambda < 0$. Here, $\tau_{\rm turn} = \pi/3H_\Lambda$ is the proper time of turnaround, $\Delta\tau$ is the time lapse we require between the turnaround of the local scale factor A and the turnaround of the FRW scale factor a, and τ_* is the proper time of reheating. Using Eq. (3.4), we can solve (3.22) for $A_{\rm turn}$ and get the upper limit

$$A_{\rm turn} \leq \left(\frac{\rho_0}{\rho_\Lambda}\right)^{1/3} \sin^{2/3}\left[\frac{\pi}{2} - \frac{3}{2}H_\Lambda \Delta\tau\right] , \tag{3.23}$$

for $\Lambda < 0$.

The distribution of Λ for positive and negative values of Λ is displayed in Fig. 3-7, using $\Delta\tau = 5 \times 10^9$ years and $M_G = 10^{12} M_\odot$. We see that both distributions provide reasonably good fits to observation, with the measured value of Λ appearing just

within one or two standard deviations of the mean. In Fig. 3-8 we display curves for both anthropic hypotheses A and B, using $\Delta\tau = 3$, 5, and 7×10^9 years and using $M_G = 10^{10}$, 10^{11}, and $10^{12} M_\odot$. The distribution varies significantly as a result of these changes, but the fit to the observed value of Λ remains good.

3.5 Conclusions

The main focus of this Chapter has been on the probability distribution for the cosmological constant Λ. Although the statistical distribution of Λ among states in the landscape is assumed to be flat, imposing a scale-factor cutoff modulates this distribution to prefer smaller values of Λ. Combined with appropriate anthropic selection effects, this gives a distribution of Λ that is in a good fit with observation. We have calculated the distribution for positive and negative values of Λ, as well as for the absolute value $|\Lambda|$. For $\Lambda > 0$, we adopted the standard assumption that the number of observers is proportional to the fraction of matter clustered in halos of mass greater than $10^{12} M_\odot$, and allowed a fixed proper time interval $\Delta\tau = 5 \times 10^9$ years for the evolution of observers in such halos. For $\Lambda < 0$, we considered two possible scenarios, which probably bracket the range of reasonable possibilities. The first (scenario A) assumes that observations can be made all the way to the big crunch, so we count all halos formed prior to time $\Delta\tau$ before the crunch. The second (scenario B) assumes that the contracting negative-Λ phase is hazardous to life, so we count only halos that formed at time $\Delta\tau$ or earlier before the turnaround.

Our results show that the observed value of Λ is within two standard deviations from the mean for scenario A, and within one standard deviation for scenario B. In the latter case, the fit is better than that obtained in the "standard" calculations [56, 57, 58, 59, 60, 61], which assume no time cutoff (this is equivalent to choosing a pocket-based measure on the multiverse). The causal patch measure also selects for smaller values of Λ providing, in the case of positive Λ, a fit to observation similar to that of the scale-factor cutoff [62]. Note, however, that the approach of Ref. [62] used an entropy-based anthropic weighting (as opposed to the structure-formation-based approach used here) and that the distribution of negative Λ has not been studied in this measure.

We have verified that our results are robust with respect to changing the parameters M_G and $\Delta\tau$. The agreement with the data remains good for M_G varying between 10^{10} and $10^{12} M_\odot$ and for $\Delta\tau$ varying between 3×10^9 and 7×10^9 years.

Chapter 4

The Distribution of the Curvature Parameter

An interesting feature of the scale-factor cutoff measure is that it does not reward regions of the multiverse for having longer periods of slow-roll inflation. Thus, one might hope that in our bubble slow-roll inflation did not last long enough to wash away all of the relics of the bubble nucleation event. One such relic is the large geometric curvature of the bubble at the time of its nucleation. (Note that the large-curvature initial bubble is still homogeneous and isotropic, due to the symmetries of the eternally-inflating vacuum in which it nucleates [75, 76].) In this Chapter, we study the probability distribution of the curvature parameter Ω_k,

$$\Omega_k = 1 - \frac{8\pi G}{3H^2}\rho_{\rm total}\,, \tag{4.1}$$

where H is the Hubble parameter and $\rho_{\rm total}$ is the total energy density of our universe.

For simplicity, we only focus on the scale-factor cutoff measure. The joint probability distribution for Ω_k and the cosmological constant, using the causal entropic principle [77], has been already investigated in Ref. [78]. The case of the causal patch measure was explored in Ref. [79]. The predictions of all these approaches turn out to be very similar.

We first study the effect of anthropic selection in favor of small Ω_k, which derives from the tendency of large curvature to inhibit structure formation. Anthropic distributions for the curvature parameter have previously been estimated by Vilenkin and Winitzki [46] and by Garriga, Tanaka, and Vilenkin [12]; however that work did not include a non-zero cosmological constant. The cosmological constant was included in a more recent calculation by Freivogel, Kleban, Rodriguez Martinez, and Susskind [50]; however that work did not take into account the Gaussian distribution of primordial density perturbations, which allows for structure formation even when the curvature is large enough to prevent the collapse of a typical-amplitude density fluctuation. We provide a complete treatment of the problem, using updated cosmological data. Although anthropic selection strongly suppresses the probability to measure $\Omega_k > 0.6$ or so, by itself it does not strongly select for values of Ω_k as small as the present observational bound.

The curvature parameter today Ω_k^0 depends exponentially on the number of e-folds of slow-roll inflation N_e. The authors of Ref. [50] proposed a simple toy model of inflation in the landscape, for which they find N_e to follow the distribution $dP_0(N_e) \propto N_e^{-4} dN_e$. We adopt this model and use the scale-factor cutoff measure to predict the distribution of Ω_k among bubbles like ours in the multiverse. The result is essentially what one might guess by ignoring volume weighting, anthropic selection, and the effects of the measure. The predicted distribution of Ω_k prefers values below that expected from cosmic variance [80, 81], but it gives reasonable hope for Ω_k to be significantly larger. Specifically, there is about a 6% chance to observe $\Omega_k^0 \geq 10^{-3}$ and about an 11% chance to observe $\Omega_k^0 \geq 10^{-4}$, the latter corresponding roughly to b to which Ω_k can in principle be determined [81]. These predictions rely on some simple assumptions about inflation, including a reheating temperature of $T_* \approx 10^{15}$ GeV. (All else being equal, lowering the reheating temperature increases the likelihoods for these observations.)

To make the above predictions as precise as possible, we have assumed that Ω_k^0 is measured at the present cosmic time, and input the observational constraint $\Omega_k^0 \leq 0.013$ [5] (for simplicity we treat this 95% confidence level as a hard bound). Yet, related to the question of what we (observers living at the present cosmic time) expect to measure, there is the question of what typical observers (i.e. those living at arbitrary times) in bubbles like ours measure. To address this question it is convenient to work with a time-invariant measure of curvature; for this we choose

$$k = \left(\frac{\Omega_k^3}{\Omega_\Lambda \Omega_m^2} \right)^{1/3}, \tag{4.2}$$

which in effect expresses the inverse curvature radius squared, $r_{\rm curv}^{-2} = H^2 \Omega_k$, in units related to the late-time matter density and cosmological constant (here Ω_Λ is the density parameter of the cosmological constant, Ω_m is that of non-relativistic matter). As before we restrict attention to bubbles just like ours, including the value of the cosmological constant, and times after non-relativistic matter domination, when presumably all of the observers arise. One can then ask how typical is our measurement, $k \leq 0.035$. Using the scale-factor cutoff, we find that observers typically observe k to satisfy this bound.

Because anthropic selection is rather weak in the vicinity of the bound $k \leq 0.035$, we can rule out certain distributions of N_e, because they predict that we should measure k to be much larger than we do. The assumptions referred to above relate $k = 0.035$ to $N_e = 63.7$ e-folds of inflation. Although anthropic selection is weak for N_e near to and greater than this number, it becomes strong at $N_e \approx 61$. Thus, a landscape distribution of N_e can be ruled out if its weight over the interval $63.7 \leq N_e$ is much less than its weight over the interval $61 \lesssim N_e < 63.7$. Different assumptions about inflation (for example higher or lower reheating temperature) merely shift the numbers in these inequalities.

The remainder of this Chapter is organized as follows. In Section 4.1, we review some background material that is relevant to our main calculation, a description of how one can model bubble geometry before and after slow-roll inflation (Section 4.1.1),

and some background on structure formation in an open FRW universe (Section 4.1.2). The distribution of Ω_k is calculated in Section 4.2. In Section 4.3 we discuss anthropic considerations and describe how our results can be used to rule out hypothetical models of inflation in the landscape. The analysis of Sections 4.2 and 4.3 is discussed in the context of the local definition of the scale-factor cutoff measure in Section 4.4, where it is shown the predictions are qualitatively unchanged. We draw our conclusions in Section 4.5.

4.1 Background

4.1.1 The Geometry of pocket nucleation

We here provide some background on the geometry of bubble nucleation; this section is largely based on Ref. [46] (a similar analysis can be found in Ref. [33]). To begin, consider a bubble of our vacuum that nucleates at scale-factor time $t_{\rm nuc}$. The parent vacuum in which our bubble nucleates can be described by flat de Sitter coordinates with metric

$$ds^2 = -dt^2 + e^{2t}\left(dr^2 + r^2 d\Omega_2^2\right) , \tag{4.3}$$

where t is the flat de Sitter time, defined so as to coincide with the scale-factor time in the parent vacuum, and $d\Omega_2^2 = d\theta^2 + \sin^2\theta d\phi^2$. We assume the parent vacuum has larger vacuum energy than ours. The nucleation process is then as described in Ref. [75]: the bubble starts as a small three-sphere and expands at a rate that rapidly approaches the speed of light.

Inside the bubble, we take interest in the open FRW coordinates (τ, ξ), which are described by the metric

$$ds^2 = -d\tau^2 + \tilde{a}^2(\tau)\left(d\xi^2 + \sinh^2\xi\, d\Omega_2^2\right) . \tag{4.4}$$

Here $\tilde{a}(\tau)$ is the scale factor within the bubble, which should not be confused with that outside the bubble. We define proper time τ such that $\tau = 0$ at the bubble wall. The coordinates (τ, ξ) are natural to an observer inside the bubble — surfaces of constant proper time τ have constant energy density and a constant curvature term $1/\tilde{a}^2$, i.e. the Einstein field equation gives

$$H^2 - \frac{1}{\tilde{a}^2} = \frac{8\pi G}{3}\rho_{\rm total} . \tag{4.5}$$

Note that curves of constant ξ, θ, and ϕ define a congruence of comoving geodesics inside the bubble.

In order to obtain a simple relationship between the global geodesic congruence and that defined inside the bubble, we consider a simple model of bubble nucleation [46]. Specifically, we model the false-vacuum inflation of the parent vacuum, the tunneling event, and the subsequent evolution in the bubble (up to reheating) using a single scalar field φ, with potential $V(\varphi)$ (as illustrated in Fig. 4-1). Fur-

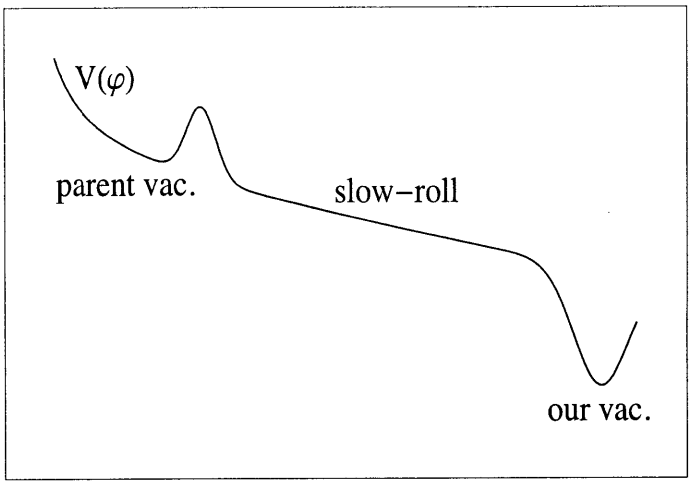

Figure 4-1: The potential $V(\varphi)$ describing the parent vacuum, slow-roll inflation potential, and our vacuum.

thermore, we assume the tunneling barrier of V is such that $V(\varphi)$ is nearly the same before and after tunneling, and that gravitational effects of the bubble wall are negligible. Due to the symmetries of the tunneling instanton, the field φ emerges after tunneling with zero 'velocity', $d\varphi/d\tau = 0$ [75]. Therefore, at very early times τ the geometry inside the bubble is approximately de Sitter.

Because the vacuum energy is nearly the same outside and just inside the bubble, and the geometry in both regions is de Sitter, constant r geodesics pass unaffected through the bubble wall. Thus, in this de Sitter region the global geodesic congruence and that inside the bubble are related by the usual relationship between flat and open de Sitter coordinates:

$$\begin{aligned} H_i t(\tau,\xi) &= \ln\left[\cosh(H_i\tau) + \sinh(H_i\tau)\cosh\xi\right] \\ H_i r(\tau,\xi) &= \frac{\sinh(H_i\tau)\sinh\xi}{\cosh(H_i\tau) + \sinh(H_i\tau)\cosh\xi}\,, \end{aligned} \tag{4.6}$$

where H_i is the Hubble rate of the parent vacuum. Note that H_i is not the Hubble rate at early times in the bubble, even though the energy density V is nearly the same in both regions. This is because of the curvature term in Eq. (4.5). Solving Eq. (4.5) in the limit $V(\varphi) \approx V(\varphi_i) = 3H_i^2/8\pi G$, one finds

$$\tilde{a}(\tau) = H_i^{-1}\sinh(H_i\tau)\,, \tag{4.7}$$

(the singularity $a \to 0$ as $\tau \to 0$ is only a coordinate singularity). This solution holds as long as $V(\varphi)$ does not change significantly, i.e. as long as $H_i\tau \ll \sqrt{16\pi G}\,V/V'$, where the prime denotes φ-differentiation [46].

After entering the de Sitter region just inside the bubble wall, geodesics of constant r (which are comoving in the parent vacuum) asymptote to the geodesics of constant

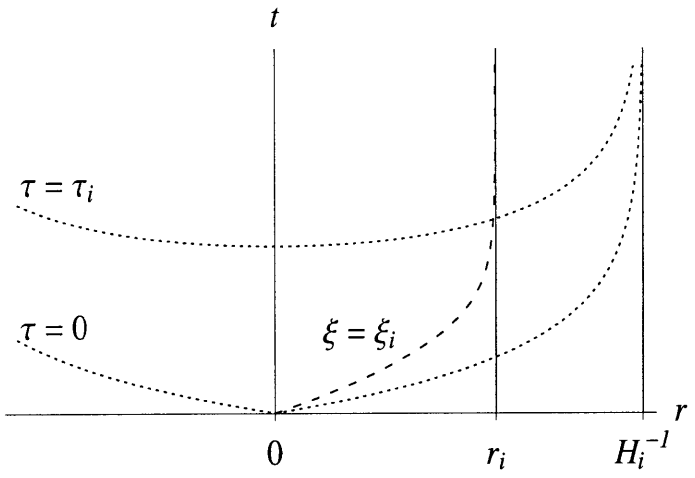

Figure 4-2: The geometry near the bubble boundary.

ξ (which are comoving in the bubble), up to corrections of order $e^{-H_i\tau}$. See Fig. 4-2 for an illustration. We assume that we can map these geodesics onto each other with reasonable accuracy during the early de Sitter expansion, i.e. we assume there exists a time τ_i satisfying $1 \ll H_i\tau_i \ll \sqrt{16\pi G}\, V/V'$. The scale-factor time at τ_i is then given by

$$t_i = t_{\rm nuc} + H_i\tau_i + 2\ln\cosh\left(\xi/2\right) , \tag{4.8}$$

which is obtained by taking the limit $H_i\tau_i \gg 1$ of Eqs. (4.6).

After the proper time τ_i, the bubble expands through N_e e-folds of slow-roll inflation, reheats, and then undergoes big bang evolution. We shall take interest in a reference class of observers who measure Ω_k^0 at the same FRW proper time, τ_0. We denote the number of e-folds of expansion along a constant-ξ geodesic from reheating to this time N_0. Then the scale-factor time at which these observers measure Ω_k^0 can be written

$$t_0 = t_{\rm nuc} + H_i\tau_i + 2\ln\cosh\left(\xi/2\right) + N_e + N_0 \, . \tag{4.9}$$

Note that t_0 is a function of ξ. Thus, the scale-factor cutoff, which requires $t_0 \leq t_c$, implies a cutoff on the FRW coordinate ξ, $\xi \leq \xi_c$, with

$$\xi_c = 2\cosh^{-1}\exp\left[\frac{1}{2}\left(t_c - t_{\rm nuc} - H_i\tau_i - N_e - N_0\right)\right] . \tag{4.10}$$

The cutoff ξ_c in turn implies that the constant $\tau = \tau_0$ hypersurface on which Ω_k^0 is measured, Σ_0, is finite.

The number of observers that arise in the bubble before the cutoff t_c is proportional to the physical volume of Σ_0. More precisely, the number of observers is proportional to the matter density on Σ_0 times its physical volume. After inflation the matter

density dilutes with cosmic expansion, so the number of observers can be taken to be proportional to comoving volume of Σ_0 at reheating

$$V_* = 4\pi\tilde{a}^3(\tau_*)\int_0^{\xi_c}\sinh^2\xi\, d\xi\,, \tag{4.11}$$

where τ_* is the proper time of reheating. Note that the bubble scale factor at proper time τ_i is $\tilde{a}(\tau_i) \approx \frac{1}{2}H_i^{-1}e^{H_i\tau_i}$ — this is Eq. (4.7) in the limit $H_i\tau \gg 1$. Thus Eq. (4.11) can be written

$$V_* = \frac{\pi}{2}\,H_i^{-3}e^{3(H_i\tau_i+N_e)}\int_0^{\xi_c}\sinh^2\xi\, d\xi\,. \tag{4.12}$$

In Section 4.2 we take interest in the volume at thermalization, V_*, as well as the curvature parameter Ω_k^0, evaluated on the hypersurface Σ_0, as a function of N_e. The curvature parameter at τ_0 can be related to its value at any previous (proper) time using

$$\Omega_k^0 = \Omega_k^q\,(\tilde{a}_q H_q/\tilde{a}_0 H_0)^2\,, \tag{4.13}$$

where the subscript 0 denotes quantities evaluated at τ_0, and q denotes quantities evaluated at some previous time. We set the previous time to be that of bubble nucleation, $\tau = 0$ in open FRW coordinates. From Eqs. (4.5) and (4.7), we see $\tilde{a}(\tau)H(\tau) \to 1$ and $\Omega_k(\tau) \to 1$ as $\tau \to 0$. During inflation the scale factor expands exponentially with time, while after inflation it is convenient to write the scale factor as a function of the temperature T, as opposed to the proper time τ. Assuming instantaneous reheating and conserving entropy in comoving volumes, the scale factor at temperature T can be written

$$\tilde{a}(T) = \frac{1}{2}H_i^{-1}e^{H_i\tau_i+N_e}\left(\frac{g_*T_*^3}{gT^3}\right)^{1/3}\,, \tag{4.14}$$

where T_* is the reheating temperature and g counts the effective number of degrees of freedom in thermal equilibrium (g_* being the corresponding quantity at the reheating temperature). We neglect $H_i\tau_i$ next to N_e in the exponent of Eq. (4.14), which allows us to write

$$\Omega_k^0 = \left(\frac{2H_i\, g_0^{1/3}T_0}{H_0\, g_*^{1/3}T_*}\right)^2 e^{-2N_e}\,. \tag{4.15}$$

The error introduced by ignoring $H_i\tau_i$ can be offset by a small shift in the value of N_e; however, we treat N_e as an unknown, scanning parameter, and such a shift is not important to our results. To proceed, we make educated guesses at the unknown parameters in Eq. (4.15). First, note that according to our assumption of instantaneous reheating, the Hubble rate and temperature at reheating are related by $H_*^2 = (8\pi^3G/90)\,g_*T_*^4$. We consider H_i to be a factor of a few larger than H_*,

take g_* to be on the order of a hundred, and guess $T_* \approx 10^{-4} G^{-1/2}$ (i.e. GUT-scale reheating). Putting all this together gives

$$\Omega_k^0 \approx e^{123-2N_e}, \tag{4.16}$$

where we have also input the present temperature $T_0 = 2.34 \times 10^{-4}$ eV and Hubble rate $H_0 = 1.53 \times 10^{-33}$ eV. We comment on the effect of changing our guess of T_* at the end of Section 4.2.

4.1.2 Structure formation in an open FRW Universe

Anthropic selection in favor of structure formation may be an important effect modulating the distribution of Ω_k. Therefore, we take interest in the details of structure formation in universes in which Ω_k may deviate significantly from zero (the work here builds upon that of Refs. [46, 12, 50]). In this section, we describe the relevant aspects of structure formation by looking at the evolution within a single bubble like ours. In Section 4.2, we incorporate these results into the complete picture involving a diverging number of bubbles that nucleate throughout the evolution of the multiverse.

In the context of estimating anthropic selection for structure formation, one often studies the asymptotic collapse fraction. This is because one is interested in *explaining*, say, the observed value of Λ, and one anticipates that observers like us could arise at times somewhat different than the present cosmic time, and in galaxies with mass somewhat different than that of the Milky Way (see for example Refs. [57, 82]). If one were instead interested in the best possible *prediction* of Λ, one would use as much information as is relevant to constrain it [83]. In this case, we would take interest in the fraction of matter in halos with mass similar to that of the Milky Way, since it is in this halo that we perform the measurement.

We denote the collapse fraction into halos of mass greater than or equal to M_G at time τ as $F_{\rm c}(M_G, \tau)$. The collapse fraction into only halos of mass equal to M_G is better known as the mass function (evaluated at M_G), and we denote this $F_{\rm m}(M_G, \tau)$. The collapse fraction $F_{\rm c}$ can be approximated using the Press-Schechter formalism [65], which gives

$$F_{\rm c} = \mathrm{erfc}\left[\frac{\delta_c}{\sqrt{2}\,\sigma_{\rm rms}(M_G, \tau)}\right]. \tag{4.17}$$

Here δ_c is the collapse density threshold — the amplitude reached by the linear evolution of an overdensity at the time when a non-linear analysis would reveal that it has collapsed — and $\sigma_{\rm rms}(M_G, \tau)$ is the root-mean-square (rms) density contrast on the comoving scale enclosing a mass M_G and evaluated at proper time τ. The collapse density threshold δ_c is not constant in time when $\Omega_k \neq 0$, nor when $\Lambda \neq 0$; however it changes by less than 10% over the course of big bang evolution [12, 67] and the collapse fraction $F_{\rm c}$ (as well as the mass function $F_{\rm m}$) is well-approximated by taking $\delta_c = 1.69$.

According to the Press-Schechter formalism, the mass function $F_{\rm m}$ can be obtained

by differentiation, $F_{\rm m} = (dF_{\rm c}/d\ln M_G)$ — this corresponds to the distribution of halo masses at any given time. Note that the only M_G dependence of $F_{\rm c}$ comes from $\sigma_{\rm rms}$. Meanwhile, the M_G dependence of $\sigma_{\rm rms}$ factors out of its time evolution, i.e.

$$\sigma_{\rm rms}(M_G,\tau) = \bar{\sigma}_{\rm rms}(M_G)\, G_\Omega(\tau)\,, \tag{4.18}$$

where $\bar{\sigma}_{\rm rms}(M_G)$ is related to the rms primordial density contrast on comoving scales enclosing mass M_G. At fixed M_G, $d\sigma_{\rm rms}/d\ln M_G = (d\bar{\sigma}_{\rm rms}/d\ln M_G)\, G_\Omega \propto \sigma_{\rm rms}$, and so we write

$$F_{\rm m} \propto \frac{1}{\sigma_{\rm rms}(M_G,\tau)} \exp\left[\frac{\delta_{\rm c}^2}{2\,\sigma_{\rm rms}^2(M_G,\tau)}\right]\,, \tag{4.19}$$

and interpret this as the mass fraction in halos with mass M_G. Both $F_{\rm c}$ and $F_{\rm m}$ are functions of $\sigma_{\rm rms}$, and so we now turn to describing this quantity.

The factor $G_\Omega(\tau)$ in Eq. (4.18) is called the growth factor, and an integral expression for it may be obtained by analyzing the first order Einstein field equation [84]. It is convenient to first define a new time variable,

$$x = \rho_\Lambda/\rho_m \propto \tilde{a}^3(\tau)\,, \tag{4.20}$$

where ρ_Λ is the energy density in cosmological constant, ρ_m is the matter density, and $\tilde{a}$ is the scale-factor (of the open FRW coordinates of the bubble, see Eqs. (4.4) and (4.5)). The growth function is then

$$G_\Omega(x) \propto \sqrt{1+\frac{1}{x}+\frac{k}{x^{2/3}}} \int_0^x \frac{y^{-1/6}\,dy}{(1+y+k\,y^{1/3})^{3/2}}\,, \tag{4.21}$$

where the curvature term k is defined by matching onto the Einstein field equation,

$$H^2 = H_\Lambda^2(1+x^{-1}+k\,x^{-2/3})\,, \tag{4.22}$$

where again $H_\Lambda^2 \equiv 8\pi G\rho_\Lambda/3$. Thus, the curvature term k is related to Ω_k by

$$\Omega_k = \frac{k\,x^{1/3}}{1+x+k\,x^{1/3}}\,. \tag{4.23}$$

In Eq. (4.22) we have ignored the presence of radiation in our universe, since its effect on our analysis is negligible. Even with this simplification, Eq. (4.22) cannot be solved in closed form. Instead, the evolution of x with time is given by the integral expression

$$H_\Lambda\tau = \frac{1}{3}\int_0^x \frac{dz}{\sqrt{z^2+z+k\,z^{4/3}}}\,. \tag{4.24}$$

This relation defines a function $\tau(x)$ relating the proper time in the bubble to the new time variable x. The function $\tau(x)$ can be obtained by numerical interpolation

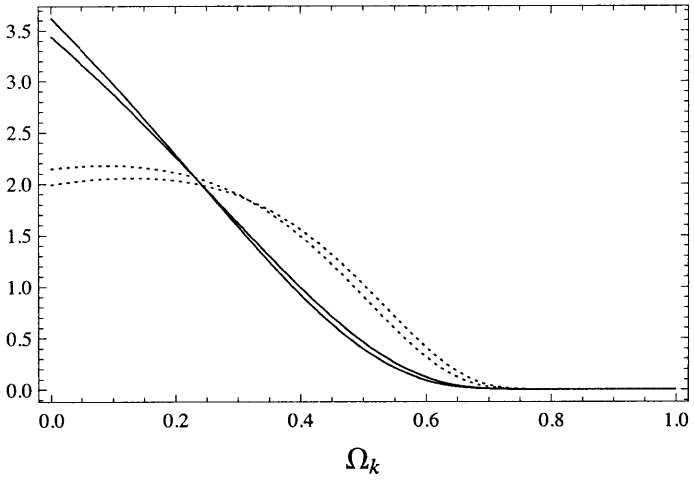

Figure 4-3: The collapse fraction $F_{\rm c}(\Omega_k)$ (solid) and mass function $F_{\rm m}(\Omega_k)$ (dotted); see the text for details.

and (numerically) inverted to give $x(\tau)$.

The functions $F_{\rm c}$ and $F_{\rm m}$ are in a sense anthropic factors, as they are approximately proportional to the number of observers that arise in a fixed comoving volume of some bubble at (or before) some specified time. Note that we here use the term "anthropic factor" loosely, as we are only looking at a single bubble and the scale-factor cutoff will introduce an additional selection effect when we account for all of the bubbles in the multiverse. Nevertheless, it is worthwhile to study the distributions $F_{\rm c}(\Omega_k)$ and $F_{\rm m}(\Omega_k)$. Of course, both of these depend on the time at which they are evaluated. As we are ultimately interested in imposing a global time cutoff, we first evaluate $F_{\rm c}$ and $F_{\rm m}$ at a fixed proper time $\Delta\tau$ before the present "time" $x_0 = 2.88$. The rationale behind this is to allow sufficient time after halo collapse for planet formation and the evolution of observers, while at the same time increasing predictive power by restricting attention to observers who perform the measurement of Ω_k at the same time that we do.

The resulting distributions $F_{\rm c}(\Omega_k)$ and $F_{\rm m}(\Omega_k)$ are displayed in Fig. 4-3, where we have used $M_G = 10^{12} M_\odot$, $M_\odot$ being the solar mass, and have chosen $\Delta\tau = 5 \times 10^9$ years. Alongside these are displayed the same distributions but ignoring the proper time lapse $\Delta\tau$, i.e. setting $\Delta\tau = 0$. We have normalized the distributions to integrate to unity. Here and throughout the Chapter we use WMAP-5 mean value parameters [5] (see footnote 1 in Chapter 3) and compute the rms density contrast on the scale M_G using Ref. [72] and the CMBFAST program. For both $F_{\rm c}$ and $F_{\rm m}$, the curve with $\Delta\tau = 0$ is the one that is slightly higher at larger Ω_k. Note that the distributions do not depend significantly on the choice of $\Delta\tau$. For this reason, and because it dramatically simplifies our calculations, henceforth we set $\Delta\tau = 0$.

Fig. 4-3 reveals that, although anthropic selection prevents an observer from measuring too large a value of Ω_k, it does not select values of Ω_k as small as the observational bound ($\Omega_k^0 \leq 0.013$ at 95% confidence level [5]) much more strongly than it

selects values, say, ten times larger than this. We return to this point in Section 4.3.

4.2 The Distribution of Ω_k

We can now describe what value of Ω_k we might expect to measure, given certain assumptions about the multiverse. In any given bubble, the value of Ω_k is a function of the expansion history along the comoving geodesic passing through the spacetime point at which Ω_k is measured. This expansion history is well-understood only during (a portion of) the big bang evolution following reheating. Although many factors contribute to the expansion history before this big bang evolution, we bundle our ignorance into a single parameter: the number of e-folds of slow-roll inflation in our bubble, N_e. This is to say, we make guesses at relevant quantities such as the scale of inflation and the reheating temperature (see the end of Section 4.1.1), and consider that our errors are offset by (small) changes in the number of e-folds N_e. The distribution of N_e is of course crucial to the analysis, yet in this aspect of the calculation that we must rely on a high degree of speculation.

As indicated from the onset of this Chapter, we consider our universe to be a thermalized bubble in an eternally inflating multiverse. Furthermore, we consider the multiverse to be populated by a landscape of vacua so large that we may consider the early dynamics of our bubble as independent of the low-energy physics that describes the subsequent big bang evolution. In this picture, we expect the value of N_e in our bubble to be typical of values across the multiverse, modulo any selection effects. To guess at this distribution, we follow Freivogel, Kleban, Rodriguez Martinez, and Susskind (FKRMS) [50].

These authors consider the dominant contribution to N_e to come from the slow-roll of a single scalar field over an approximately linear potential,

$$V(\varphi) \approx V_0 \left(1 - \frac{y}{\Delta}\varphi\right) , \quad \varphi_i \leq \varphi \leq \varphi_f , \tag{4.25}$$

where V_0, y, and $\Delta \equiv \varphi_f - \varphi_i$ are free parameters that are assumed to scan across the landscape, taking values between zero and one (in Planck units) with uniform probability distribution. The primordial density contrast can be calculated from Eq. (4.25), and is a function of the parameters V_0, y, and Δ. Since the primordial density contrast is known, we consider the slice of the landscape of $V(\varphi)$ for which it is fixed to the value we measure. The resulting distribution of N_e is [50]

$$dP_0(N_e) \propto N_e^{-4}\, dN_e , \tag{4.26}$$

where here the subscript "0" emphasizes that we have not yet accounted for all of the selection effects. Eq. (4.26) is converted into a distribution of Ω_k^0 using Eq. (4.16), which gives

$$\frac{dP_0(\Omega_k)}{d\ln\Omega_k^0} \propto \left[61.5 - \frac{1}{2}\ln\Omega_k^0\right]^{-4} \equiv f(\Omega_k^0) . \tag{4.27}$$

We now take into account the other selection effects, namely the effect of the scale-factor measure over the multiverse and the effect of anthropic selection in favor of structure formation. Let us first write the result in a somewhat cumbersome form, in order to explain the various contributions, and then simplify it. The distribution of Ω_k^0 can be written

$$\begin{aligned}\frac{dP(\Omega_k^0)}{d\ln\Omega_k^0} \;\propto\; & \lim_{t_c\to\infty}\int_{-\infty}^{t_c} e^{\gamma t_{\rm nuc}} dt_{\rm nuc} \\ & \times \int_0^{\xi_c} e^{3(H_i\tau_i+N_e)}\sinh^2\xi\, d\xi \\ & \times F_{\rm m}(M_G,x_0)\, f(\Omega_k^0)\,. \end{aligned} \tag{4.28}$$

The integral on the second line is proportional to the total amount of matter on the hypersurface Σ_0, given by Eq. (4.12), while the mass function $F_{\rm m}$ selects for the fraction of matter than has collapsed into halos of mass M_G. Collectively, these terms are proportional to the number of observers like us in bubbles that nucleate at scale-factor time $t_{\rm nuc}$ (the dependence on $t_{\rm nuc}$ is in the limit of integration ξ_c, see Eq. (4.10)). The first line of Eq. (4.28) integrates over all bubble nucleation times $t_{\rm nuc}$, with the appropriate volume weighting coming from eternal inflation with the scale-factor measure, see for example Eq. (2.16). This integration ignores the very small probability that a given vacuum might decay during slow-roll inflation or big bang evolution up to the hypersurface Σ_0. Finally, the last term in the last line of Eq. (4.28) gives the distribution of Ω_k^0 coming from the dependence on the number of e-folds of slow-roll inflation, Eq. (4.27).

As explained in Section 4.1.2, we here use the mass function $F_{\rm m}$ instead of the collapse fraction $F_{\rm c}$ because we are interested in making a prediction, so we include as much relevant information as is practical — in this case that we live in a halo with mass equal to that of the Milky Way. Thus, we set $M_G = 10^{12} M_\odot$. Although the difference between $F_{\rm c}$ and $F_{\rm m}$ is conceptually relevant, Fig. 4-3 indicates that the two distrubutions differ at most by a factor of order unity, which does not significantly affect the anthropic constraints. Similarly, we evaluate the mass function at the present ratio of energy density in cosmological constant to that in matter, $x_0 = 2.88$.[1] One might wonder how the prediction of Ω_k is affected if we do not so strongly condition the calculation. We return to this question in Section 4.3.

To proceed, we first evaluate the inside integral over ξ. Note that all of the dependence on ξ is in the factor $\sinh^2\xi$. The integration can be performed analytically,

$$\int_0^{\xi_c}\sinh^2\xi\, d\xi = \sinh(2\xi_c) - 2\xi_c\,, \tag{4.29}$$

[1] We should include a time lapse $\Delta\tau$ to allow for planet formation and biological evolution after halo collapse. However, as mentioned in Section 4.1.2, this complicates the analysis but does not significantly affect the results, so for simplicity we neglect it.

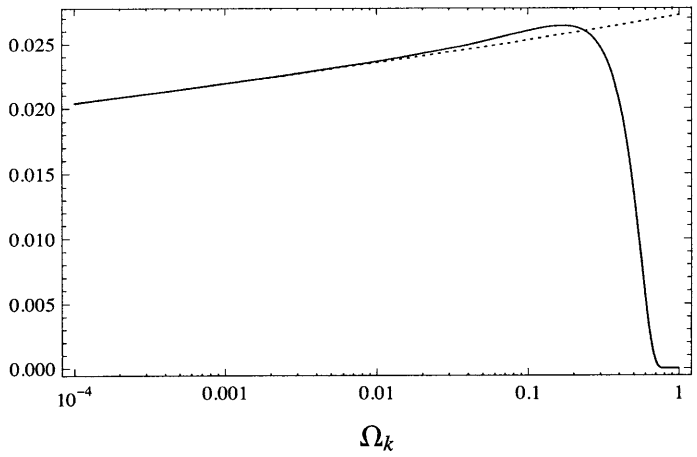

Figure 4-4: The relevant portion of the distribution of Ω_k^0 (solid), along with a simple approximation, Eq. (4.32) (dotted).

with ξ_c given by Eq. (4.10). It is convenient perform a variable redefinition,

$$z = t_c - t_{\rm nuc} - H_0\tau_0 - N_e - N_O\,, \tag{4.30}$$

and exchange integration over $t_{\rm nuc}$ for integration over z. The integration over z just gives a constant prefactor (here and below we use $\gamma = 3$). Dropping the other constant factors, Eq. (4.28) becomes

$$\frac{dP(\Omega_k^0)}{d\ln\Omega_k^0} \propto F_{\rm m}(M_G, x_0)\, f(\Omega_k^0)\,. \tag{4.31}$$

Note that Eq. (4.31), which includes the effect of the scale-factor cutoff, is exactly what one would naively expect if the issue of measure were ignored.

The distribution Eq. (4.31) is displayed (in part) in Fig. 4-4. Interestingly, the distribution is quite flat all the way up to rather large values of Ω_k^0, falling off at $\Omega_k^0 \approx 0.6$. We know from CMB measurements that $\Omega_k^0 \leq 0.013$ [5] (for simplicity we take this 95% confidence level to be a hard bound), so to produce the best prediction we should cut the distribution at that value. The distribution in Fig. 4-4 is normalized as if this cut were in place, and the small amplitude of the distribution (~ 0.02) indicates that it has broad support over values of Ω_k^0 much smaller than those displayed in the figure. This can also be seen by examining the approximation,

$$\frac{dP(\Omega_k^0)}{d\ln\Omega_k^0} \sim \left[61.5 - \frac{1}{2}\ln\Omega_k^0\right]^{-4}\,. \tag{4.32}$$

which (after proper normalization) is very accurate for small Ω_k^0. As another illustration of how broad is the distribution, note that the median sits at about $10^{-16.5}$ (corresponding to about 80 e-folds of slow-roll inflation).

Because of the broad support of the distribution Eq. (4.32), it is most likely that Ω_k^0 is dominated by cosmic variance — which is of order 10^{-5} [80] — instead of the relic contribution calculated above. Nevertheless, it is exciting that the distribution of Ω_k^0 leaves reasonable hope for future detection. In particular, there is a 6% chance to measure $\Omega_k^0 \geq 10^{-3}$, and an 11% chance to measure $\Omega_k^0 \geq 10^{-4}$ (both of these percentiles are calculated using a distribution cut off at $\Omega_k^0 = 0.013$). These results are in agreement with the estimates made in Ref. [50].

Recall that our analysis guessed at certain cosmological parameters, for example the reheating temperature, which was set at $T_* \approx 10^{-4} G^{-1/2}$ (c.f. the end of Section 4.1.2). As a quick check of the effect of our guesses, consider a very different guess at the reheating temperature, $T_* \approx 10^{-16} G^{-1/2}$ (corresponding to TeV-scale reheating). For simplicity we keep our other guesses fixed. In this case, the quantity "123" appearing in Eq. (4.16) becomes about 68. Performing an analysis analogous to that above, we find there is a 10% chance to measure $\Omega_k^0 \geq 10^{-3}$, and an 18% chance to measure $\Omega_k^0 \geq 10^{-4}$. Decreasing T_* shifts the distribution of Ω_k toward larger values, but apparently the effect is not very strong. The most important factor determining our expectations for Ω_k is the distribution of N_e over the landscape.

4.3 Anthropic considerations and the "prior" distribution of N_e

The calculation of the last section was made in the spirit of a prediction, and as such it was conditioned by certain details about our location in our universe, namely that we inhabit a galaxy with Milky Way mass and perform our measurement at $x_0 = 2.88$. Taking a different perspective, we can ask under what conditions can the landscape picture explain why the curvature is observed to be as small as it is, $\Omega_k^0 \leq 0.013$. In this case, we consider ourselves observers belonging to a more general reference class, and ask what values of Ω_k typical observers in this reference class measure. We consider here the more general reference class to be observers in bubbles with the same low-energy physics as ours, the same value of the cosmological constant, and in galaxies like the Milky Way, however these observers can arise at any time over the course of bubble evolution.

To proceed in analogy to the calculation of Section 4.2 introduces a number of unnecessary complications. Instead, we follow the methods introduced in Ref. [32]. Specifically, we take as our "reference objects" not entire bubbles, but small patches of comoving volume, whose transverse boundaries are bubble walls (or the cutoff hypersurface at scale-factor time t_c). If these patches are sufficiently small in spacelike extent, they may be chosen so that both scale-factor time t and proper time τ are nearly constant over slicings of the patch. These patches, like any reference object, arise in the multiverse at a rate that scales like that of Eq. (2.16). Integrating over these patches is equivalent to taking as the reference objects entire bubbles (cut off at t_c), and integrating over bubble nucleation times, as was done in Section 4.2.

The curvature parameter Ω_k is a function of the FRW proper time τ inside each

bubble. Therefore, to calculate what values of Ω_k typical observers measure, one must know the density of these observers as a function of time. Alternatively, one can define a time-invariant quantity k, related to Ω_k, and count the total number of observers inhabiting bubbles with different values of k. We use

$$k = \left(\frac{\Omega_k^3}{\Omega_\Lambda \Omega_m^2}\right)^{1/3}, \tag{4.33}$$

which corresponds to the quantity k used in Eq. (4.22). Note that the observational bound $\Omega_k^0 \leq 0.013$ corresponds to $k \leq 0.035$ [5].

To begin the calculation, consider a spacetime volume that is bound from below by a small patch of some bubble wall at scale-factor time $t_{\rm w}$. The number of observers in this volume is proportional to the collapse fraction evaluated at a proper time cutoff τ_c, where τ_c is defined by the relation

$$t_c - t_{\rm w} = N_e + \int_{\tau_*}^{\tau_c} H(\tau)\, d\tau = N_e + \ln\left[\frac{\tilde{a}(\tau_c)}{\tilde{a}(\tau_*)}\right], \tag{4.34}$$

where τ_* is (proper) time of reheating and N_e is the number of e-folds of expansion between the bubble wall and reheating. As our notation indicates, we assume the latter expansion comes entirely from slow-roll inflation; i.e. we neglect the contribution coming from the initial curvature-dominated phase.

The number of observers in such a patch can then be approximated as proportional to

$$e^{3N_e} F_{\rm c}(M_G, \tau_c)\,, \tag{4.35}$$

where the exponential gives the volume expansion factor coming from slow-roll inflation, and the second term evaluates the collapse fraction at the proper time cutoff. The collapse fraction counts matter collapsed into halos of mass M_G or greater; however halos with mass greater than M_G at time τ_c had mass equal to M_G at some time $\tau < \tau_c$, so these halos contribute to our reference class. As we have already noted, one might instead evaluate $F_{\rm c}$ at some time $\Delta\tau$ before τ_c, in order to give time for galaxies and observers to evolve between the time of collapse and the proper time cutoff. However, including this effect significantly complicates the calculation, whereas in Section 4.1.1 we found that it does not significantly affect the collapse fraction. Therefore, we here neglect it.

Summing over all patches gives

$$\frac{dP(k)}{d\ln k} \propto \lim_{t_c \to \infty} \int_{-\infty}^{t_c} e^{3N_e + \gamma t_{\rm w}} F_{\rm c}(M_G, \tau_c)\, \tilde{f}(k)\, dt_{\rm w}\,, \tag{4.36}$$

where as before we have neglected the small probability that a given vacuum may decay during slow-roll inflation or during big bang evolution. As was the case with Eq. (4.28), the exponential dependence on N_e is an illusion. Note that the cutoff τ_c corresponds to a cutoff x_c, where as before $x \equiv \rho_\Lambda/\rho_m$. Eq. (4.34) gives $\ln x_c =$

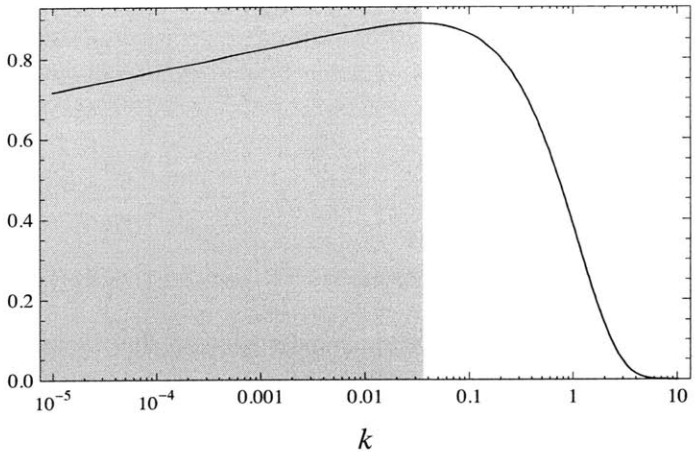

Figure 4-5: The distribution $dP(k)/dk$; see the text for details. The present observationally acceptable region, $k \leq 0.035$, is indicated by shading.

$3(t_c - t_{\rm w} - N_e) + \text{const}$, which can be used to change the variable of integration from $t_{\rm w}$ to x_c. This gives

$$\frac{dP(k)}{d\ln k} \propto \int_0^\infty x_c^{-2} F_{\rm c}(M_G, x_c)\, \tilde{f}(k)\, dx_c\,, \tag{4.37}$$

where we have used $\gamma = 3$. Note that the "prior" distribution $\tilde{f}(k)$ factors out of the integration.

The argument of Eq. (4.37) contains a factor of x_c^{-2}. This factor induces the "youngness bias" of the scale-factor cutoff measure, which prefers bubbles that nucleate nearer to the cutoff (for which x_c is smaller). As shown in Ref. [32], this bias is rather mild. It does not appear in the calculation of Section 4.2, c.f. Eq. (4.31), because that calculation was performed at fixed x, $x = x_0$.

Whereas $f(\Omega_k^0)$ of Eq. (4.31) corresponds to the distribution of $\Omega_k(x)$ at fixed $x = x_0$, the function $\tilde{f}(k)$ of Eq. (4.37) corresponds to the distribution of k, which is independent of x. Using $T \propto 1/\tilde{a} \propto x^{-1/3}$ and Eqs. (4.15) and (4.33), we find

$$k = e^{124 - 2N_e}\,, \tag{4.38}$$

where the additional factors of Ω_Λ and Ω_m essentially change the "123" of Eq. (4.16) to "124." In the case $dP_0(N_e) \propto N_e^{-4} dN_e$, this gives the distribution

$$\tilde{f}(k) \equiv \frac{dP_0(k)}{d\ln k} \propto \left[62 - \frac{1}{2}\ln k\right]^{-4}. \tag{4.39}$$

In Fig. 4-5 we display $dP(k)/dk$, using Eq. (4.37) with $\tilde{f}(k)$ given by Eq. (4.39). As in Fig. 4-4, we have cropped the figure to more clearly illustrate the region of interest (the cropped portion very closely follows the distribution $dP_0(k)/dk$). The

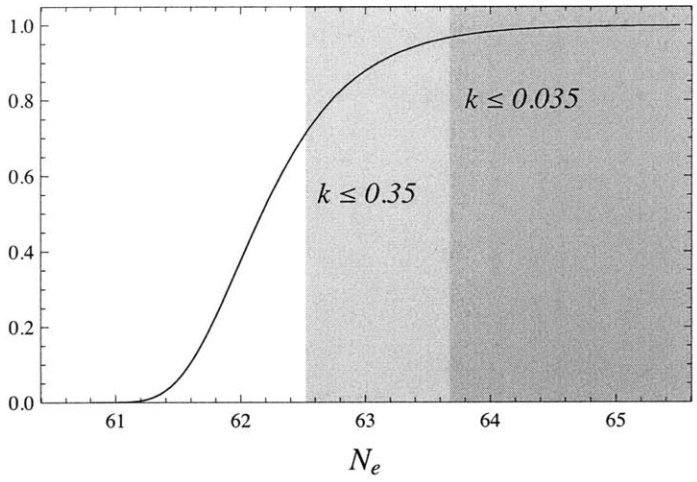

Figure 4-6: The distribution $dP(N_e)/dN_e$ assuming a flat "prior" for N_e, i.e. $dP_0(N_e)/dN_e$ = constant. The shaded regions correspond to the observatinal bound $k \leq 0.035$, and a bound ten times larger, translated to number of e-folds.

observationally acceptable region, $k \leq 0.035$, is indicated by shading. Clearly, values of k satisfying our observational bound are not atypical in the FKRMS landscape model of inflation; in fact 93% of observers measure k to satisfy this bound.

Although typical observers measure $k \leq 0.035$, note that anthropic selection for structure formation, which causes the distribution of k to fall off at large k, does not select for values of k satisfying the observational bound much more strongly than it selects for values, say, ten times larger. This is more clearly illustrated if we plot the distribution $dP(N_e)/dN_e$ — i.e. the distribution of the observed number of e-folds N_e — using a flat "prior" for N_e, in other words setting $dP_0(N_e)/dN_e$ = constant. This is done in Fig. 4-6. The observational bound on k, and a bound ten times larger, are converted to e-folds of inflation and represented by the shaded regions.

A flat prior for N_e is unrealistic, but it serves to illustrate the effect of anthropic selection. As expected, the distribution of N_e is exponentially suppressed for small values of N_e, where Fig. 4-6 reveals that in this context "small" means $N_e \lesssim 61$. The present observational bound, $k \leq 0.035$, corresponds to $N_e \geq 63.7$. Although the lower limit of this bound is not much larger than the anthropic cutoff at $N_e \approx 61$, k depends exponentially on N_e, and we can see from Fig. 4-6 that values of k over ten times larger than the present bound are not strongly suppressed. This, in principle, allows us to exclude hypothetical landscape models of inflation, based on their predicting k to be larger than the observational bound.

In particular, if a hypothetical model of inflation in the landscape predicts a distribution of N_e that too strongly prefers smaller values of N_e, then it is possible for us to exclude this model based on the measurement $k \leq 0.035$. This is enticing because models of inflation in string theory tend to prefer a smaller number of e-folds of slow-roll inflation. On the other hand, it is important to recognize that in order to exclude a landscape model of inflation, we require a certain "fortuitous" shape to

the "prior" distribution $dP_0(N_e)/dN_e$. For example, many classes of potentials will strongly prefer smaller values of N_e when N_e is small, but this region of the parameter space is not relevant to our observations, because values $N_e \lesssim 61$ are exponentially suppressed and do not contribute to the full distribution $dP(N_e)/dN_e$.

Let us illustrate this with an example. Consider a landscape model of inflation that predicts a power-law prior distribution of N_e,

$$dP_0(N_e) \propto N_e^{-\alpha} dN_e \,. \tag{4.40}$$

According to our assumptions, such a distribution is ruled out at greater than 95% confidence level when $\int_0^{0.035} (dP(k)/dk)\, dk < 0.025$, where $dP(k)/dk$ is here presumed to be normalized to unity. Performing the calculation, we find $\alpha \geq 114$ is ruled out. That only such a strong power-law dependence can be ruled out may be striking, but it is easy to understand in light of our above remarks. The observationally excluded region is, roughly speaking, $N_e < 64$; however anthropic selection suppresses all contributions from the interval $N_e < 61$. Therefore a landscape model of inflation is ruled out only if the prior distribution $dP_0(N_e)/dN_e$ has much more weight in the interval $61 \leq N_e \leq 64$ than in the interval $64 < N_e$. In the context of the power-law distribution of Eq.(4.40), we require

$$1 \ll \frac{\int_{61}^{64} N_e^{-\alpha} dN_e}{\int_{64}^{\infty} N_e^{-\alpha} dN_e} \approx \frac{3(\alpha - 1)}{64} \,. \tag{4.41}$$

Thus, roughly speaking, we expect to rule out power-law distributions only if $\alpha \gg 20$. The large power is explained by the fact that the prior distribution must have sharp behavior at large values of N_e.

Although it is hard to imagine how a landscape model of inflation could give such a strong power-law prior distribution of N_e, it is not implausible that a more realistic model of inflation, which could give a much more complicated prior distribution of N_e, could have the necessary sharp behavior at large N_e. Let us note, for instance, that potential energy barriers — as are necessary in the bubble-nucleation model we are considering — will give a sharp cutoff at large N_e.

Finally, we emphasize that the above analysis, which refers specifically to numbers like $N_e = 63.7$, etc., relies implicitly on a number of assumptions in addition to the form of the prior distribution of N_e, for example the reheating temperature. These are described at the end of Section 4.1.1. Yet, different assumptions would merely shift the specific values of N_e mentioned above, and our conclusions would be unchanged.

4.4 The distribution of Ω_k using the "local" scale-factor cutoff measure

We here repeat the analysis of Sections 4.2 and 4.3, but performing a cutoff on the "local" scale-factor time t' (see Section 2.2.1), where we use the prime to help distinguish the results here from those of the "FRW" scale-factor time t. It is convenient to

approach the problem in the manner of Section 4.3; that is we take as our reference objects small patches of comoving volume, with transverse boundaries corresponding to bubble walls (or the scale-factor cutoff hypersurface at t'_c). Again, if these patches are sufficiently small in their spacelike extent, the scale-factor time t' and the proper time τ are nearly constant over spacelike slicings of the patches. Analogous to in Section 4.3, if we label each patch by the scale-factor time of reheating in the patch, t'_*, then such patches arise in the multiverse at a rate proportional to $e^{\gamma t'_*}$.

The scale-factor time t' probes expansion on infinitesimal scales. However, we take the number of observers to be proportional to the number of Milky Way–like galaxies, and we model such galaxies using spherical top-hat overdensities with mass $M_G = 10^{12} M_\odot$, so there is no need to probe scales smaller than the comoving volume that encloses mass M_G.[2] The probability that a comoving patch enclosing mass M_G contains an observer is then proportional to the probability that such a patch begins to collapse before the scale-factor time cutoff t'_c. (Recall that we have defined the scale factor cutoff such that geodesics in collapsing regions are extended unless or until they hit a singularity.) This probability can be parametrized in terms of the spacetime curvature of the patch at, say, the reheating time t'_*.

By Birkhoff's theorem, the evolution of a comoving patch enclosing a spherical top-hat overdensity is equivalent to that of a closed FRW universe with field equation

$$(\dot{y}/3y)^2 = H_\Lambda^2 (1 + y^{-1} - \kappa y^{-2/3}) \,. \tag{4.42}$$

The "local scale factor cube root" y is defined so as to coincide with the "bubble scale factor cube root" x of Eq. (4.22) (c.f. Eq. (4.20)) at early times. The total spacetime curvature κ is the sum of the bubble curvature k (coming from the global bubble geometry) and the primordial curvature perturbation $\mathcal{R}$ (coming from quantum fluctuations during inflation). We define $\mathcal{R}$ to be positive for overdensities, so that

$$\kappa = \mathcal{R} - k \,. \tag{4.43}$$

The spherical overdensity will turn around and begin to collapse before the scale-factor time cutoff t'_c only if the curvature exceeds some minimum value $\kappa_{\rm min}(t'_c, t'_*)$. For a bubble with given value of k, the probability for this to occur is

$$\mathcal{A}(k; t'_c, t'_*) \;\propto\; \int_{\kappa_{\rm min}}^{\infty} \exp\left[-\frac{(\kappa + k)^2}{\mathcal{R}_{\rm rms}^2} \right] d\kappa$$

[2]Realistically, structure formation is hierarchical: small scales turn around and collapse before larger scales. When the region surrounding a given geodesic collapses, its scale-factor time becomes frozen. Thus, it would seem we cannot ignore structure formation on such small scales. However, whether or not any observers arise in some small collapsed structure depends on whether that structure combines with others to form a larger structure — ultimately a large galaxy. We model the requirement that small structures coalesce into larger ones as equivalent to requiring that structure formation occurs on the largest necessary scale, using a spherical top-hot model for the initial overdensity.

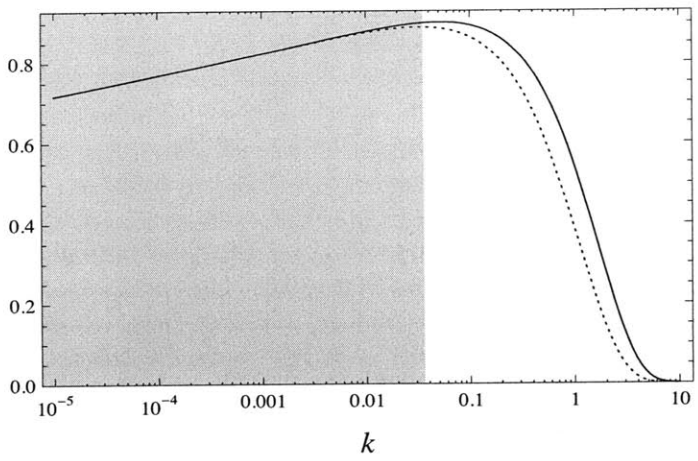

Figure 4-7: The distribution $dP(k)/dk$ using scale-factor times t' (solid) and t (dashed); see text for details. The normalizations are chosen for clear comparison, while the shaded region indicates the observed bound $k \leq 0.035$.

$$\propto \ \mathrm{erfc}\left[\frac{\kappa_{\min}(t'_c, t'_*) + k}{\sqrt{2}\,\mathcal{R}_{\rm rms}}\right] , \tag{4.44}$$

where we assume $\mathcal{R}$ has a Gaussian distribution with rms value $\mathcal{R}_{\rm rms}$. As our notation suggests, $\mathcal{A}$ can be interpreted as an anthropic factor, giving the probability that a given patch contains an observer. The probability to observe a given value of k is thus

$$\frac{dP(k)}{d\ln k} \propto \lim_{t'_c \to \infty} \int_{-\infty}^{t'_c} \mathcal{A}(k; t'_c, t'_*)\, \tilde{f}(k)\, e^{\gamma t'_*}\, dt'_* , \tag{4.45}$$

where, as in Eq. (4.39), $\tilde{f}(k)$ is the (logarithmic) distribution of k among universes with big bang evolution like ours, and $e^{\gamma t'_*}$ is proportional to the number of patches at scale-factor time t'_*.

It is left to solve for $\kappa_{\min}(t'_c, t'_*)$. First note that a spherical overdensity described by Eq. (4.42) turns around and begins to collapse when $\dot{y} = 0$, or when $1 + y^{-1} - \kappa\, y^{-2/3} = 0$. Thus we can write

$$\kappa(y_{\rm turn}) = y_{\rm turn}^{-1/3}\,(1 + y_{\rm turn}) \ . \tag{4.46}$$

Meanwhile, $\kappa_{\min}$ is simply the value of κ for which $t'_c - t'_* = (1/3)\ln(y_{\rm turn}/y_*)$, where y_* is the local scale factor at the time of reheating. (Here we use the definition of scale-factor time, $t' = \ln a$, along with $y \propto a^{1/3}$.) Thus we can write

$$\kappa_{\min}(t'_c, t'_*) = y_*^{-1/3} e^{t'_* - t'_c} \left[1 + y_* e^{3(t'_c - t'_*)}\right] . \tag{4.47}$$

The distribution of observed values of the bubble curvature k is obtained by

combining Eq. (4.45) with Eq. (4.44) and Eq. (4.47). The resulting expression is simplified if we change the integration variable from t'_* to $y_{\rm turn} = y_*^{1/3} e^{t'_c - t'_*}$. Then we can write

$$\frac{dP(k)}{d\ln k} \propto \int_{y_*}^{\infty} \mathrm{erfc}\left[\frac{1 + k y_{\rm turn} + y_{\rm turn}^3}{\sqrt{2}\,\mathcal{R}_{\rm rms}\, y_{\rm turn}}\right] \frac{\tilde{f}(k)}{y_{\rm turn}^4}\, dy_{\rm turn}\,, \tag{4.48}$$

where we have used $\gamma = 3$. It makes no difference if we simply set $y_* \to 0$ in the lower limit of integration. This expression corresponds to the analogue of Eq. (4.37), but for the local scale-factor time t', as opposed to the FRW scale-factor time t. $\mathcal{R}_{\rm rms}$ is the rms primordial curvature perturbation on comoving scales enclosing mass M_G — it is related to, say, the rms density contrast $\sigma_{\rm rms}$ by

$$\mathcal{R}_{\rm rms} = (5/3)\sigma_{\rm rms}(M_G, \tau_F)\, x_F^{-1/3}\,, \tag{4.49}$$

where the quantities on the right-hand side are evaluated at some fiducial time τ_F during matter domination, i.e. before vacuum energy or curvature become significant. (This relation is obtained from matching the linearized Einstein field equation onto Eq. (4.42).)

Fig. 4-7 displays $dP(k)/d\ln k$ using the scale-factor cutoff measure for both scale-factor time t' and scale-factor time t. We use Eq. (4.39) to determine $\tilde{f}(k)$ for clear comparison, and the shaded region indicates the bound $k \leq 0.035$. As advertised in the introduction, the two definitions of scale-factor time give qualitatively similar results, however the anthropic suppression of large values of k kicks in at larger k when using the locally-defined scale-factor time t'. The two distributions are very similar for k less than the observed bound, indicating that the predictions of Section 4.2 are essentially unchanged when using the local scale-factor time. On the other hand, since the local scale-factor time measure permits larger values of k before strong anthropic suppression, if this is the correct measure then it would be somewhat easier (than indicated in Section 4.3) to rule out landscape models of inflation that prefer smaller values of N_e.

4.5 Conclusions

In this Chapter we have studied the distribution of the curvature parameter Ω_k using the the scale-factor cutoff measure of the multiverse.

In a large landscape, the vacuum of our bubble might be reached by tunneling from a number of different "parent" vacua. Then, depending on in which parent vacuum our bubble nucleates, we in general expect different early universe dynamics, including different possibilities for the number of e-folds of slow-roll inflation N_e. In a very large landscape, as is expected from string theory, we also expect a large number of vacua with low-energy physics indistinguishable from our own. In this case, one expects a smooth distribution of possible values of N_e describing our bubble. One of the features of the scale-factor cutoff measure is that it does not reward bubbles for having a longer duration of slow-roll inflation. This raises the possibility that N_e may

not be too much larger than is needed to pave the way for structure formation, and therefore that Ω_k^0 may be large enough to distinguish from the value expected from cosmic variance, $\sim 10^{-5}$.

Freivogel, Kleban, Rodriguez Martinez, and Susskind (FKRMS) have proposed a toy model of inflation in the landscape, which gives a "prior" distribution of N_e of the form $dP_0(N_e) \propto N_e^{-4}\, dN_e$ (on the slice of the parameter space corresponding to a fixed primordial density contrast Q). Using the scale-factor cutoff measure, we find this distribution predicts a 6% chance to observe $\Omega_k^0 \geq 10^{-3}$, and an 11% chance to observe $\Omega_k^0 \geq 10^{-4}$, thus confirming the results of FKRMS [50].

Although in the FKRMS model of inflation in the landscape observers typically measure $k = (\Omega_k^3/\Omega_\Lambda \Omega_m^2)^{1/3}$ to satisfy our observational bound, $k \leq 0.035$, anthropic selection does not strongly suppress values of k over ten times larger than this (when asking what typical observers measure, it is convenient to refer to the time-independent curvature term k rather than the time-dependent curvature parameter Ω_k). Thus, we may use the observed bound on k to rule out hypothetical landscape models of inflation that too strongly prefer smaller values of N_e.

Anthropic selection is not strong in the vicinity of the observational bound $k \leq 0.035$, however sufficiently large values of k are strongly suppressed. Put in another way, with some assumptions about inflation $k \leq 0.035$ corresponds to $N_e \geq 63.7$. Anthropic selection is not strong in the vicinity of $N_e = 63.7$, but exponentially suppresses $N_e \lesssim 61$. This is to say a hypothetical model of inflation that very strongly prefers smaller values of N_e for $N_e \lesssim 61$ does not conflict with our observational bound, since this range of N_e is strongly anthropically suppressed. On the other hand, if a hypothetical model of inflation gives a prior distribution of N_e that strongly prefers N_e in the interval $61 \lesssim N_e < 63.7$, relative to it being in the interval $63.7 < N_e$, then such a model can be ruled out using our observational bound.

Chapter 5

The Boltzmann Brain problem

The simplest interpretation of the observed accelerating expansion of the universe is that it is driven by a constant vacuum energy density ρ_Λ, which is about three times greater than the present density of nonrelativistic matter. While ordinary matter becomes more dilute as the universe expands, the vacuum energy density remains the same, and in another ten billion years or so the universe will be completely dominated by vacuum energy. The subsequent evolution of the universe is accurately described as de Sitter space.

It was shown by Gibbons and Hawking [85] that an observer in de Sitter space would detect thermal radiation with a characteristic temperature $T_{\rm dS} = H_\Lambda/2\pi$, where

$$H_\Lambda = \sqrt{\frac{8\pi}{3} G\rho_\Lambda} \tag{5.1}$$

is the de Sitter Hubble expansion rate. For the observed value of ρ_Λ, the de Sitter temperature is extremely low, $T_{\rm dS} = 2.3 \times 10^{-30}$ K. Nevertheless, complex structures will occasionally emerge from the vacuum as quantum fluctuations, at a small but nonzero rate per unit spacetime volume. An intelligent observer, like a human, could be one such structure. Or, short of a complete observer, a disembodied brain may fluctuate into existence, with a pattern of neuron firings creating a perception of being on Earth and, for example, observing the cosmic microwave background radiation. Such freak observers are collectively referred to as "Boltzmann brains" [35, 36]. Of course, the nucleation rate $\Gamma_{\rm BB}$ of Boltzmann brains is extremely small, its magnitude depending on how one defines a Boltzmann brain. The important point, however, is that $\Gamma_{\rm BB}$ is always nonzero.

De Sitter space is eternal to the future. Thus, if the accelerating expansion of the universe is truly driven by the energy density of a stable vacuum state, then Boltzmann brains will eventually outnumber normal observers, no matter how small the value of $\Gamma_{\rm BB}$ [86, 38, 39, 40, 41] might be.

To define the problem more precisely, we use the term "normal observers" to refer to those that evolve as a result of non-equilibrium processes that occur in the wake of the hot big bang. If our universe is approaching a stable de Sitter spacetime, then the total number of normal observers that will ever exist in a fixed comoving volume

of the universe is finite. On the other hand, the cumulative number of Boltzmann brains grows without bound over time, growing roughly as the volume, proportional to $e^{3H_\Lambda t}$. When extracting the predictions of this theory, such an infinite preponderance of Boltzmann brains cannot be ignored.

For example, suppose that some normal observer, at some moment in her lifetime, tries to make a prediction about her next observation. According to the theory there would be an infinite number of Boltzmann brains, distributed throughout the space-time, that would happen to share exactly all her memories and thought processes at that moment. Since all her knowledge is shared with this set of Boltzmann brains, for all she knows she could equally likely be any member of the set. The probability that she is a normal observer is then arbitrarily small, and all predictions would be based on the proposition that she is a Boltzmann brain. The theory would predict, therefore, that the next observations that she shall make, if she survives to make any at all, shall be totally incoherent, with no logical relationship to the world that she thought she knew. (While it is of course true that some Boltzmann brains might experience coherent observations, for example by living in a Boltzmann solar system, it is easy to show that Boltzmann brains with such dressing would be vastly outnumbered by Boltzmann brains without any coherent environment.) Thus, the continued orderliness of the world that we observe is distinctly at odds with the predictions of a Boltzmann-brain-dominated cosmology.[1]

This problem was recently addressed by Page [40], who concluded that the least unattractive way to produce more normal observers than Boltzmann brains is to require that our vacuum should be rather unstable. More specifically, it should decay within a few Hubble times of vacuum energy domination; that is, in 20 billion years or so.

In the context of inflationary cosmology, however, this problem acquires a new twist. Inflation is generically eternal, with the physical volume of false-vacuum inflating regions increasing exponentially with time and "pocket universes" like ours constantly nucleating out of the false vacuum. In an eternally inflating multiverse, the numbers of normal observers and Boltzmann brains produced over the course of eternal inflation are both infinite. They can be meaningfully compared only after one adopts some prescription to regulate the infinities.

The problem of regulating the infinities in an eternally inflating multiverse is known as the measure problem [87], and has been under discussion for some time. It is crucially important in discussing predictions for any kind of observation. A number of measures have been proposed [88, 7, 8, 9, 10, 11, 89, 90, 12, 13, 14, 15, 16, 17, 20, 21, 91], and some of them have already been disqualified, as they make predictions

[1]Here we are taking a completely mechanistic view of the brain, treating it essentially as a highly sophisticated computer. Thus, the normal observer and the Boltzmann brains can be thought of as a set of logically equivalent computers running the same program with the same data, and hence they behave identically until they are affected by further input, which might be different. Since the computer program cannot determine whether it is running inside the brain of one of the normal observers or one of the Boltzmann brains, any intelligent probabilistic prediction that the program makes about the next observation would be based on the assumption that it is equally likely to be running on any member of that set.

that conflict with observations.

In particular, if one uses the proper-time cutoff measure [88, 7, 8, 9, 10], one encounters the "youngness paradox," predicting that humans should have evolved at a very early cosmic time, when the conditions for life were rather hostile [92]. The youngness problem, as well as the Boltzmann brain problem, can be avoided in the stationary measure [90, 91], which is an improved version of the proper-time cutoff measure. However, the stationary measure, as well as the pocket-based measure, is afflicted with a runaway problem, suggesting that we should observe extreme values (either very small or very large) of the primordial density contrast Q [27, 28] and the gravitational constant G [29], while these parameters appear to sit comfortably in the middle of their respective anthropic ranges [30, 29]. Some suggestions to get around this issue have been described in Refs. [93, 28, 94, 31]. In addition, the pocket-based measure seems to suffer from the Boltzmann brain problem. The comoving coordinate measure [95, 88] and the causal-patch measures [16, 17] are free from these problems, but have an unattractive feature of depending sensitively on the initial state of the multiverse. This does not seem to mix well with the attractor nature of eternal inflation: the asymptotic late-time evolution of an eternally inflating universe is independent of the starting point, so it seems appealing for the measure to maintain this property. Since the scale-factor cutoff measure[2] [7, 8, 9, 11, 89, 96] has been shown to be free of all of the above issues [32], we consider it to be a promising candidate for the measure of the multiverse.

As we have indicated, the relative abundance of normal observers and Boltzmann brains depends on the choice of measure over the multiverse. This means the predicted ratio of Boltzmann brains to normal observers can be used as yet another criterion to evaluate a prescription to regulate the diverging volume of the multiverse: regulators that predict normal observers are greatly outnumbered by Boltzmann brains should be ruled out. This criterion has been studied in the context of several multiverse measures, including a causal patch measure [41], several measures associated with globally defined time coordinates [89, 97, 90, 26, 91], and the pocket-based measure [98]. In this work, we apply this criterion to the scale-factor cutoff measure, extending the investigation that was initiated in Ref. [89]. We show that the scale-factor cutoff measure gives a finite ratio of Boltzmann brains to normal observers; if certain assumptions about the landscape are valid, the ratio can be small.[3]

The remainder of this Chapter is organized as follows. In Section 5.1 we calculate the ratio of Boltzmann brains to normal observers in terms of multiverse volume fractions and transition rates. The volume fractions are discussed in Section 5.2, in the context of toy landscapes, and the section ends with a general description of the con-

[2]This measure is sometimes referred to as the volume-weighted scale-factor cutoff measure, but we shall define it below in terms of the counting of events in spacetime, so the concept of weighting will not be relevant. The term "volume-weighted" is relevant when a measure is described as a prescription for defining the probability distribution for the value of a field. In Ref. [89], this measure is called the "pseudo-comoving volume-weighted measure."

[3]In a paper that appeared simultaneously with version 1 [34], Raphael Bousso, Ben Freivogel, and I-Sheng Yang independently analyzed the Boltzmann brain problem for the scale-factor cutoff measure [33].

ditions necessary to avoid Boltzmann brain domination. The rate of Boltzmann brain production and the rate of vacuum decay play central roles in our calculations, and these are estimated in Section 5.3. Concluding remarks are provided in Section 5.4.

5.1 The abundance of normal observers and Boltzmann brains

Let us now calculate the relative abundances of Boltzmann brains and normal observers, in terms of the vacuum transition rates and the asymptotic volume fractions.

Estimates for the numerical values of the Boltzmann brain nucleation rates and vacuum decay rates will be discussed in Section 5.3, but it is important at this stage to be aware of the kind of numbers that will be considered. We shall be able to give only rough estimates of these rates, but the numbers that will be mentioned in Section 5.3 will range from $\exp(-10^{120})$ to $\exp(-10^{16})$. Thus, when we calculate the ratio $\mathcal{N}^{\rm BB}/\mathcal{N}^{\rm NO}$ of Boltzmann brains to normal observers, the natural logarithm of this ratio will always include one term with a magnitude of at least 10^{16}. Consequently, the presence or absence of any term in $\ln(\mathcal{N}^{\rm BB}/\mathcal{N}^{\rm NO})$ that is small compared to 10^{16} is of no relevance. We therefore refer to any factor f for which

$$|\ln f| < 10^{14} \tag{5.2}$$

as "roughly of order one." In the calculation of $\mathcal{N}^{\rm BB}/\mathcal{N}^{\rm NO}$ such factors — although they may be minuscule or colossal by ordinary standards — can be ignored. It will not be necessary to keep track of factors of 2, π, or even 10^{10^8}. Dimensionless coefficients, factors of H, and factors coming from detailed aspects of the geometry are unimportant, and in the end all of these will be ignored. We nonetheless include some of these factors in the intermediate steps below simply to provide a clearer description of the calculation.

We begin by estimating the number of normal observers that will be counted in the sample spacetime region specified by the scale-factor cutoff measure. Normal observers arise during the big bang evolution in the aftermath of slow-roll inflation and reheating. The details of this evolution depend not only on the vacuum of the pocket in question, but also on the parent vacuum from which it nucleated [99]. That is, if we view each vacuum as a local minimum in a multidimensional field space, then the dynamics of inflation in general depend on the direction from which the field tunneled into the local minimum. We therefore label pockets with two indices, ik, indicating the pocket and parent vacua respectively.

To begin, we restrict our attention to a single "anthropic" pocket — i.e., one that produces normal observers — which nucleates at scale-factor time $t_{\rm nuc}$. The internal geometry of the pocket is that of an open FRW universe. We assume that, after a brief curvature-dominated period $\Delta\tau \sim H_k^{-1}$, slow-roll inflation inside the pocket gives N_e e-folds of expansion before thermalization. Furthermore, we assume that all normal observers arise at a fixed number N_O of e-folds of expansion after thermalization. (Note that N_e and N_O are both measured along FRW comoving geodesics inside the

pocket, which do not initially coincide with, but rapidly asymptote to, the "global" geodesic congruence that originated outside the pocket.) We denote the fixed-internal-time hypersurface on which normal observers arise by $\Sigma^{\rm NO}$, and call the average density of observers on this hypersurface $n_{ik}^{\rm NO}$.

The hypersurface $\Sigma^{\rm NO}$ would have infinite volume, due to the constant expansion of the pocket, but this divergence is regulated by the scale-factor cutoff t_c, because the global scale-factor time t is not constant over the $\Sigma^{\rm NO}$ hypersurface. For the pocket described above, the regulated physical volume of $\Sigma^{\rm NO}$ can be written as

$$V_O^{(ik)}(t_{\rm nuc}) = H_k^{-3} e^{3(N_e+N_O)}\, w(t_c - t_{\rm nuc} - N_e - N_O)\,, \tag{5.3}$$

where the exponential gives the volume expansion factor coming from slow-roll inflation and big bang evolution to the hypersurface $\Sigma^{\rm NO}$, and $H_k^{-3} w(t_c - t_{\rm nuc} - N_e - N_O)$ describes the comoving volume of the part of the $\Sigma^{\rm NO}$ hypersurface that is underneath the cutoff. The function $w(t)$ was calculated, for example, in Refs. [46] and [26], and is applied to scale-factor cutoff measure in Ref. [34]. Its detailed form will not be needed to determine the answer up to a factor that is roughly of order one, but to avoid mystery we mention that $w(t)$ can be written as

$$w(t) = \frac{\pi}{2} \int_0^{\bar\xi(t)} \sinh^2(\xi)\, d\xi = \frac{\pi}{8} \left[\sinh(2\bar\xi(t)) - 2\bar\xi(t)\right]\,, \tag{5.4}$$

where $\bar\xi(t_c - t_{\rm nuc} - N_e - N_O)$ is the maximum value of the Robertson-Walker radial coordinate ξ that lies under the cutoff. If the pocket universe begins with a moderate period of inflation ($\exp(N_e) \gg 1$) with the same vacuum energy as outside, then

$$\bar\xi(t) \approx 2\cosh^{-1}\left(e^{t/2}\right)\,. \tag{5.5}$$

Eq. (5.3) gives the physical volume on the $\Sigma^{\rm NO}$ hypersurface for a single pocket of type ik, which nucleates at time $t_{\rm nuc}$. The number of ik-pockets that nucleate between time $t_{\rm nuc}$ and $t_{\rm nuc} + dt_{\rm nuc}$ is

$$\begin{aligned} dn_{\rm nuc}^{(ik)}(t_{\rm nuc}) &= (3/4\pi) H_k^3 \kappa_{ik}\, V_k(t_{\rm nuc})\, dt_{\rm nuc} \\ &= (3/4\pi) H_k^3 \kappa_{ik} s_k\, V_0\, e^{(3-q)\, t_{\rm nuc}}\, dt_{\rm nuc}\,, \end{aligned} \tag{5.6}$$

where we use Eq. (2.16) to give $V_k(t_{\rm nuc})$. The total number of normal observers in the sample region is then

$$\begin{aligned} \mathcal{N}_{ik}^{\rm NO} &= n_{ik}^{\rm NO} \int^{t_c - N_e - N_O} V_O^{(ik)}(t_{\rm nuc})\, dn_{\rm nuc}^{(ik)}(t_{\rm nuc}) \\ &\approx n_{ik}^{\rm NO} \kappa_{ik} s_k\, V_0\, e^{(3-q)\, t_c} \int_0^\infty w(z)\, e^{-(3-q)\, z}\, dz\,. \end{aligned} \tag{5.7}$$

In the first expression we have ignored the (very small) probability that pockets of type ik may transition to other vacua during slow-roll inflation or during the subsequent period N_O of big bang evolution. In the second line, we have changed the integration

variable to $z = t_c - t_{\rm nuc} - N_e - N_O$ (reversing the direction of integration) and have dropped the $\mathcal{O}(1)$ prefactors, and also the factor $e^{q(N_e+N_O)}$, since q is expected to be extraordinarily small. We have kept e^{-qt_c}, since we are interested in the limit $t_c \to \infty$. We have also kept the factor e^{qz} long enough to verify that the integral converges with or without the factor, so we can carry out the integral using the approximation $q \approx 0$, resulting in an $\mathcal{O}(1)$ prefactor that we shall drop.

Finally,

$$\mathcal{N}_{ik}^{\rm NO} \approx n_{ik}^{\rm NO} \kappa_{ik}\, s_k\, V_0\, e^{(3-q)\,t_c}\ . \tag{5.8}$$

Note that the expansion factor $e^{3(N_e+N_O)}$ in Eq. (5.3) was canceled when we integrated over nucleation times, illustrating the mild youngness bias of the scale-factor cutoff measure. The expansion of the universe is canceled, so objects that form at a certain density per physical volume in the early universe will have the same weight as objects that form at the same density per physical volume at a later time, despite the naive expectation that there is more volume at later times.

To compare, we now need to calculate the number of Boltzmann brains that will be counted in the sample spacetime region. Boltzmann brains can be produced in any anthropic vacuum, and presumably in many non-anthropic vacua as well. Suppose Boltzmann brains are produced in vacuum j at a rate $\Gamma_j^{\rm BB}$ per unit spacetime volume. The number of Boltzmann brains $\mathcal{N}_j^{\rm BB}$ is then proportional to the total four-volume in that vacuum. Imposing the cutoff at scale-factor time t_c, this four-volume is

$$\begin{aligned} \mathcal{V}_j^{(4)} &= \int^{t_c} V_j(t)\, d\tau \,=\, H_j^{-1} \int^{t_c} V_j(t)\, dt \\ &= \frac{1}{3-q} H_j^{-1} s_j\, V_0\, e^{(3-q)\,t_c}\,, \end{aligned} \tag{5.9}$$

where we have used Eq. (2.16) for the asymptotic volume fraction. By setting $d\tau = H_j^{-1}\, dt$, we have ignored the time-dependence of $H(\tau)$ in the earlier stages of cosmic evolution, assuming that only the late-time de Sitter evolution is relevant. In a similar spirit, we shall assume that the Boltzmann brain nucleation rate $\Gamma_j^{\rm BB}$ can be treated as time-independent, so the total number of Boltzmann brains nucleated in vacua of type j, within the sample volume, is given by

$$\mathcal{N}_j^{\rm BB} \,\approx\, \Gamma_j^{\rm BB} H_j^{-1} s_j\, V_0\, e^{(3-q)\,t_c}\,, \tag{5.10}$$

where we have dropped the $\mathcal{O}(1)$ numerical factor.

For completeness, we may want to consider the effects of early universe evolution on Boltzmann brain production, effects which were ignored in Eq. (5.10). We shall separate the effects into two categories: the effects of slow-roll inflation at the beginning of a pocket universe, and the effects of reheating.

To account for the effects of slow-roll inflation, we argue that, within the approximations used here, there is no need for an extra calculation. Consider, for example, a pocket universe A which begins with a period of slow-roll inflation during which $H(\tau) \approx H_{\text{slow roll}} = \text{const}$. Consider also a pocket universe B, which throughout its evolution has $H = H_{\text{slow roll}}$, and which by hypothesis has the same formation rate,

Boltzmann brain nucleation rate, and decay rates as pocket A. Then clearly the number of Boltzmann brains formed in the slow roll phase of pocket A will be smaller than the number formed throughout the lifetime of pocket B. Since we shall require that generic bubbles of type B do not overproduce Boltzmann brains, there will be no need to worry about the slow-roll phase of bubbles of type A.

To estimate how many Boltzmann brains might form as a consequence of reheating, we can make use of the calculation for the production of normal observers described above. We can assume that the Boltzmann brain nucleation rate has a spike in the vicinity of some particular hypersurface in the early universe, peaking at some value $\Gamma^{\rm BB}_{{\rm reheat},ik}$ which persists roughly for some time interval $\Delta\tau^{\rm BB}_{{\rm reheat},ik}$, producing a density of Boltzmann brains equal to $\Gamma^{\rm BB}_{{\rm reheat},ik}\,\Delta\tau^{\rm BB}_{{\rm reheat},ik}$. This spatial density is converted into a total number for the sample volume in exactly the same way that we did for normal observers, leading to

$$\mathcal{N}^{\rm BB,reheat}_{ik} \approx \Gamma^{\rm BB}_{{\rm reheat},ik}\,\Delta\tau^{\rm BB}_{{\rm reheat},ik}\,\kappa_{ik}\,s_k\,V_0\,e^{(3-q)\,t_c}\ . \tag{5.11}$$

Thus, the dominance of normal observers is assured if

$$\sum_{i,k}\Gamma^{\rm BB}_{{\rm reheat},ik}\,\Delta\tau^{\rm BB}_{{\rm reheat},ik}\kappa_{ik}\,s_k \ll \sum_{i,k} n^{\rm NO}_{ik}\kappa_{ik}\,s_k\,. \tag{5.12}$$

If Eq. (5.12) did not hold, it seems likely that we would suffer from Boltzmann brain problems regardless of our measure. We leave numerical estimates for Section 5.3, but we shall see that Boltzmann brain production during reheating is not a danger.

Ignoring the Boltzmann brains that form during reheating, the ratio of Boltzmann brains to normal observers can be found by combining Eqs. (5.8) and (5.10), giving

$$\frac{\mathcal{N}^{\rm BB}}{\mathcal{N}^{\rm NO}} \approx \frac{\sum_j H_j^3\kappa_j^{\rm BB}\,s_j}{\sum_{i,\,k} n^{\rm NO}_{ik}\kappa_{ik}\,s_k}\,, \tag{5.13}$$

where the summation in the numerator covers only the vacua in which Boltzmann brains can arise, the summation over i in the denominator covers only anthropic vacua, and the summation over k includes all of their possible parent vacua. $\kappa_j^{\rm BB}$ is the dimensionless Boltzmann brain nucleation rate in vacuum j, related to $\Gamma_j^{\rm BB}$ by Eq. (2.8). The expression can be further simplified by dropping the factors of H_j and $n_i^{\rm NO}$, which are roughly of order one, as defined by Eq. (5.2). We can also replace the sum over j in the numerator by the maximum over j, since the sum is at least as large as the maximum term and no larger than the maximum term times the number of vacua. Since the number of vacua (perhaps 10^{500}) is roughly of order one, the sum over j is equal to the maximum up to a factor that is roughly of order one. We similarly replace the sum over i in the denominator by its maximum, but we choose to leave the sum over k. Thus we can write

$$\frac{\mathcal{N}^{\rm BB}}{\mathcal{N}^{\rm NO}} \sim \frac{\max_j\{\kappa_j^{\rm BB}\,s_j\}}{\max_i\left\{\sum_k \kappa_{ik}\,s_k\right\}}\,, \tag{5.14}$$

where the sets of j and i are restricted as for Eq. (5.13).

In dropping $n_i^{\rm NO}$, we are assuming that $n_i^{\rm NO} H_i^3$ is roughly of order one, as defined at the beginning of this section. It is hard to know what a realistic value for $n_i^{\rm NO} H_i^3$ might be, as the evolution of normal observers may require some highly improbable events. For example, it was argued in Ref. [100] that the probability for life to evolve in a region of the size of our observable universe per Hubble time may be as low as $\sim 10^{-1000}$. But even the most pessimistic estimates cannot compete with the small numbers appearing in estimates of the Boltzmann brain nucleation rate, and hence by our definition they are roughly of order one. Nonetheless, it is possible to imagine vacua for which $n_i^{\rm NO}$ might be negligibly small, but still nonzero. We shall ignore the normal observers in these vacua; for the remainder of this Chapter we shall use the phrase "anthropic vacuum" to refer only to those vacua for which $n_i^{\rm NO} H_i^3$ is roughly of order one.

For any landscape that satisfies Eq. (2.9), which includes any irreducible landscape, Eq. (5.14) can be simplified by using Eq. (2.10):

$$\frac{\mathcal{N}^{\rm BB}}{\mathcal{N}^{\rm NO}} \sim \frac{\max_j\{\kappa_j^{\rm BB}\, s_j\}}{\max_i\{(\kappa_i - q)\, s_i\}}\,, \tag{5.15}$$

where the numerator is maximized over all vacua j that support Boltzmann brains, and the denominator is maximized over all anthropic vacua i.

In order to learn more about the ratio of Boltzmann brains to normal observers, we need to learn more about the volume fractions s_j, a topic that will be pursued in the next section.

5.2 Toy landscapes and the general conditions to avoid Boltzmann brain domination

In this section we study a number of simple models of the landscape, in order to build intuition for the volume fractions that appear in Eqs. (5.14) and (5.15). The reader uninterested in the details may skip the pedagogical examples given in Subsections 5.2.1–5.2.5, and continue with Subsection 5.2.6, where we state the general conditions that must be enforced in order to avoid Boltzmann brain domination.

5.2.1 The FIB landscape

Let us first consider a very simple model of the landscape, described by the schematic

$$F \to I \to B\,, \tag{5.16}$$

where F is a high-energy false vacuum, I is a positive-energy anthropic vacuum, and B is a terminal vacuum. This model, which we call the FIB landscape, was analyzed in Ref. [14] and was discussed in relation to the abundance of Boltzmann brains in Ref. [89]. As in Ref. [89], we assume that both Boltzmann brains and normal observers

reside only in vacuum I.

Note that the FIB landscape ignores upward transitions from I to F. The model is constructed in this way as an initial first step, and also in order to more clearly relate our analysis to that of Ref. [89]. Although the rate of upward transitions is exponentially suppressed relative the other rates, its inclusion is important for the irreducibility of the landscape, and hence the nondegeneracy of the dominant eigenvalue and the independence of the late-time asymptotic behavior from the initial conditions of the multiverse. The results of this subsection will therefore not always conform to the expectations outlined in Section 2.2.1, but this shortcoming is corrected in the next subsection and all subsequent work in this Chapter.

We are interested in the eigenvectors and eigenvalues of the rate equation, Eq. (2.6). In the FIB landscape the rate equation gives

$$\begin{aligned} \dot{f}_F &= -\kappa_{IF} f_F \\ \dot{f}_I &= -\kappa_{BI} f_I + \kappa_{IF} f_F \,. \end{aligned} \tag{5.17}$$

We ignore the volume fraction in the terminal vacuum as it is not relevant to our analysis. Starting with the ansatz,

$$\mathbf{f}(t) = \mathbf{s}\, e^{-qt} \,, \tag{5.18}$$

we find two eigenvalues of Eqs. (5.17). These are, with their corresponding eigenvectors,

$$\begin{aligned} q_1 &= \kappa_{IF} \,, \qquad & \mathbf{s}_1 &= (1, C) \,, \\ q_2 &= \kappa_{BI} \,, \qquad & \mathbf{s}_2 &= (0, 1) \,, \end{aligned} \tag{5.19}$$

where the eigenvectors are written in the basis $\mathbf{s} \equiv (s_F, s_I)$ and

$$C = \frac{\kappa_{IF}}{\kappa_{BI} - \kappa_{IF}} \,. \tag{5.20}$$

Suppose that we start in the false vacuum F at $t = 0$, i.e. $\mathbf{f}(t = 0) = (1, 0)$. Then the solution of the FIB rate equation, Eq. (5.17), is

$$\begin{aligned} f_F(t) &= e^{-\kappa_{IF} t} \,, \\ f_I(t) &= C \left(e^{-\kappa_{IF} t} - e^{-\kappa_{BI} t} \right) \,. \end{aligned} \tag{5.21}$$

The asymptotic evolution depends on whether $\kappa_{IF} < \kappa_{BI}$ (case I) or not (case II). In case I,

$$\mathbf{f}(t \to \infty) = \mathbf{s}_1 e^{-\kappa_{IF} t} \qquad (\kappa_{IF} < \kappa_{BI}) \,, \tag{5.22}$$

where $\mathbf{s}_1$ is given in Eq. (5.19), while in case II

$$\mathbf{f}(t \to \infty) = \left(e^{-\kappa_{IF} t} \,, |C| e^{-\kappa_{BI} t} \right) \qquad (\kappa_{BI} < \kappa_{IF}) \,. \tag{5.23}$$

In the latter case, the inequality of the rates of decay for the two volume fractions

arises from the reducibility of the FIB landscape, stemming from our ignoring upward transitions from I to F.

For case I ($\kappa_{IF} < \kappa_{BI}$), we find the ratio of Boltzmann brains to normal observers by evaluating Eq. (5.14) for the asymptotic behavior described by Eq. (5.22):

$$\frac{\mathcal{N}^{\rm BB}}{\mathcal{N}^{\rm NO}} \sim \frac{\kappa^{\rm BB} s_I}{\kappa_{IF} s_F} \sim \frac{\kappa^{\rm BB}}{\kappa_{IF}} \frac{\kappa_{IF}}{\kappa_{BI} - \kappa_{IF}} \sim \frac{\kappa^{\rm BB}}{\kappa_{BI}}, \tag{5.24}$$

where we drop κ_{IF} compared to κ_{BI} in the denominator, as we are only interested in the overall scale of the solution. We find that the ratio of Boltzmann brains to normal observers is finite, depending on the relative rate of Boltzmann brain production to the rate of decay of vacuum I. Meanwhile, in case II (where $\kappa_{BI} < \kappa_{IF}$) we find

$$\frac{\mathcal{N}^{\rm BB}}{\mathcal{N}^{\rm NO}} \sim \frac{\kappa^{\rm BB}}{\kappa_{IF}} e^{(\kappa_{IF} - \kappa_{BI})t} \to \infty. \tag{5.25}$$

In this situation, the number of Boltzmann brains overwhelms the number of normal observers; in fact the ratio diverges with time.

The unfavorable result of case II stems from the fact that, in this case, the volume of vacuum I grows faster than that of vacuum F. Most of this I-volume is in large pockets that formed very early; and this volume dominates because the F-vacuum decays faster than I, and is not replenished due to the absence of upward transitions. This leads to Boltzmann brain domination, in agreement with the conclusion reached in Ref. [89]. Thus, the FIB landscape analysis suggests that Boltzmann brain domination can be avoided only if the decay rate of the anthropic vacuum is larger than both the decay rate of its parent false vacuum F and the rate of Boltzmann brain production. Moreover, the FIB analysis suggests that Boltzmann brain domination in the multiverse can be avoided only if the first of these conditions is satisfied for all vacua in which Boltzmann brains exist. This is a very stringent requirement, since low-energy vacua like I typically have lower decay rates than high-energy vacua (see Section 5.3). We shall see, however, that the above conditions are substantially relaxed in more realistic landscape models.

5.2.2 The FIB landscape with recycling

The FIB landscape of the preceding section is reducible, since vacuum F cannot be reached from vacuum I. We can make it irreducible by simply allowing upward transitions,

$$F \leftrightarrow I \to B. \tag{5.26}$$

This "recycling FIB" landscape is more realistic than the original FIB landscape, because upward transitions out of positive-energy vacua are allowed in semi-classical quantum gravity [44]. The rate equation of the recycling FIB landscape gives the

eigenvalue system,

$$\begin{aligned} -qs_F &= -\kappa_{IF}s_F + \kappa_{FI}s_I\,, \\ -qs_I &= -\kappa_I s_I + \kappa_{IF}s_F\,, \end{aligned} \tag{5.27}$$

where $\kappa_I \equiv \kappa_{BI} + \kappa_{FI}$ is the total decay rate of vacuum I, as defined in Eq. (2.11). Thus, the eigenvalues q_1 and q_2 correspond to the roots of

$$(\kappa_{IF} - q)(\kappa_I - q) = \kappa_{IF}\kappa_{FI}\,. \tag{5.28}$$

Further analysis is simplified if we note that upward transitions from low-energy vacua like ours are very strongly suppressed, even when compared to the other exponentially suppressed transition rates, i.e. $\kappa_{FI} \ll \kappa_{IF}, \kappa_{BI}$. We are interested mostly in how this small correction modifies the dominant eigenvector in the case where $\kappa_{BI} < \kappa_{IF}$ (case II), which led to an infinite ratio of Boltzmann brains to normal observers. To the lowest order in κ_{FI}, we find

$$q \approx \kappa_I - \frac{\kappa_{IF}\kappa_{FI}}{\kappa_{IF} - \kappa_I}\,, \tag{5.29}$$

and

$$s_I \approx \frac{\kappa_{IF} - \kappa_I}{\kappa_{FI}} s_F \gg s_F\,. \tag{5.30}$$

The above equation is a consequence of the second of Eqs. (5.27), but it also follows directly from Eq. (2.10), which holds in any irreducible landscape. In this case $f_I(t)$ and $f_F(t)$ have the same asymptotic time dependence, $\propto e^{-qt}$, so the ratio $f_I(t)/f_F(t)$ approaches a constant limit, $s_I/s_F \equiv R$. However, due to the smallness of κ_{FI}, this ratio is extremely large. Note that the ratio of Boltzmann brains to normal observers is proportional to R. Although it is also proportional to the minuscule Boltzmann brain nucleation rate (estimated in Section 5.3), the typically huge value of R will still lead to Boltzmann brain domination (again, see Section 5.3 for relevant details). But the story is not over, since the recycling FIB landscape is still far from realistic.

5.2.3 A more realistic landscape

In the recycling model of the preceding section, the anthropic vacuum I was also the dominant vacuum, while in a realistic landscape this is not likely to be the case. To see how it changes the situation to have a non-anthropic vacuum as the dominant one, we consider the model

$$A \leftarrow D \leftrightarrow F \rightarrow I \rightarrow B\,, \tag{5.31}$$

which we call the "ADFIB landscape." Here, D is the dominant vacuum and A and B are both terminal vacua. The vacuum I is still an anthropic vacuum, and the vacuum F has large, positive vacuum energy. As explained in Section 5.3, the

dominant vacuum is likely to have very small vacuum energy; hence we consider that at least one upward transition (here represented as the transition to F) is required to reach an anthropic vacuum.

Note that the ADFIB landscape ignores the upward transition rate from vacuum I to F; however this is exponentially suppressed relative the other transition rates pertinent to I and, unlike the situation in Subsection 5.2.1, ignoring the upward transition does not significantly affect our results. The important property is that all vacuum fractions have the same late-time asymptotic behavior, and this property is assured whenever there is a unique dominant vacuum, and all inflating vacua are accessible from the dominant vacuum via a sequence of tunneling transitions. The uniformity of asymptotic behaviors is sufficient to imply Eq. (2.10), which implies immediately that

$$\frac{s_I}{s_F} = \frac{\kappa_{IF}}{\kappa_{BI} - q} \approx \frac{\kappa_{IF}}{\kappa_{BI} - \kappa_D} \approx \frac{\kappa_{IF}}{\kappa_{BI}}, \tag{5.32}$$

where we used $q \approx \kappa_D \equiv \kappa_{AD} + \kappa_{FD}$, and assumed that $\kappa_D \ll \kappa_{BI}$.

This holds even if the decay rate of the anthropic vacuum I is smaller than that of the false vacuum F.

Even though the false vacuum F may decay rather quickly, it is constantly being replenished by upward transitions from the slowly-decaying vacuum D, which overwhelmingly dominates the physical volume of the multiverse. Note that, in light of these results, our constraints on the landscape to avoid Boltzmann brain domination are considerably relaxed. Specifically, it is no longer required that the anthropic vacua decay at a faster rate than their parent vacua. Using Eq. (5.32) with Eq. (5.14), the ratio of Boltzmann brains to normal observers in vacuum I is found to be

$$\frac{\mathcal{N}_I^{\rm BB}}{\mathcal{N}_I^{\rm NO}} \sim \frac{\kappa_I^{\rm BB} s_I}{\kappa_{IF} s_F} \sim \frac{\kappa_I^{\rm BB}}{\kappa_{BI}}. \tag{5.33}$$

If Boltzmann brains can also exist in the dominant vacuum D, then they are a much more severe problem. By applying Eq. (2.10) to the F vacuum, we find

$$\frac{s_F}{s_D} = \frac{\kappa_{FD}}{\kappa_F - q} \approx \frac{\kappa_{FD}}{\kappa_F - \kappa_D} \approx \frac{\kappa_{FD}}{\kappa_F}, \tag{5.34}$$

where $\kappa_F = \kappa_{IF} + \kappa_{DF}$, and where we have assumed that $\kappa_D \ll \kappa_F$. The ratio of Boltzmann brains in vacuum D to normal observers in vacuum I is then

$$\frac{\mathcal{N}_D^{\rm BB}}{\mathcal{N}_I^{\rm NO}} \sim \frac{\kappa_D^{\rm BB} s_D}{\kappa_{IF} s_F} \sim \frac{\kappa_D^{\rm BB}}{\kappa_{FD}} \frac{\kappa_F}{\kappa_{IF}}. \tag{5.35}$$

Since we expect that the dominant vacuum has very small vacuum energy, and hence a heavily suppressed upward transition rate κ_{FD}, the requirement that $\mathcal{N}_D^{\rm BB}/\mathcal{N}_I^{\rm NO}$ be small could be a very stringent one. Note that compared to s_D, both s_F and s_I are suppressed by the small factor κ_{FD}; however the ratio s_I/s_F is independent of this factor.

Since s_D is so large, one should ask whether Boltzmann brain domination can be more easily avoided by allowing vacuum D to be anthropic. The answer is no, because

the production of normal observers in vacuum D is proportional (see Eq. (5.8)) to the rate at which bubbles of D nucleate, which is not large. D dominates the spacetime volume due to slow decay, not rapid nucleation. If we assume that D is anthropic and restrict Eq. (5.14) to vacuum D, we find using Eq. (5.34) that

$$\frac{\mathcal{N}_D^{\rm BB}}{\mathcal{N}_D^{\rm NO}} \sim \frac{\kappa_D^{\rm BB} s_D}{\kappa_{DF} s_F} \sim \frac{\kappa_D^{\rm BB}}{\kappa_{FD}} \frac{\kappa_F}{\kappa_{DF}}\,, \tag{5.36}$$

so again the ratio is enhanced by the extremely small upward tunneling rate κ_{FD} in the denominator.

Thus, in order to avoid Boltzmann brain domination, it seems we have to impose two requirements: (1) the Boltzmann brain nucleation rate in the anthropic vacuum I must be less than the decay rate of that vacuum, and (2) the dominant vacuum D must either not support Boltzmann brains at all, or must produce them with a dimensionless rate $\kappa_D^{\rm BB}$ that is small even compared to the upward tunneling rate κ_{FD}. If the vacuum D is anthropic then it would support Boltzmann brains, so the domination by Boltzmann brains could be avoided only by the stringent requirement $\kappa_D^{\rm BB} \ll \kappa_{FD}$.

5.2.4 A further generalization

The conclusions of the last subsection are robust to more general considerations. To illustrate, let us generalize the ADFIB landscape to one with many low-vacuum-energy pockets, described by the schematic

$$A \leftarrow D \leftrightarrow F_j \rightarrow I_i \rightarrow B\,, \tag{5.37}$$

where each high energy false vacuum F_j decays into a set of vacua $\{I_i\}$, all of which decay (for simplicity) to the same terminal vacuum B. The vacua I_i are taken to be a large set including both anthropic vacua and vacua that host only Boltzmann brains. Eq. (2.10) continues to apply, so Eqs. (5.32) and (5.34) are easily generalized to this case, giving

$$s_{I_i} \approx \frac{1}{\kappa_{I_i}} \sum_j \kappa_{I_i F_j}\, s_{F_j} \tag{5.38}$$

and

$$s_{F_j} \approx \frac{1}{\kappa_{F_j}} \kappa_{F_j D}\, s_D\,, \tag{5.39}$$

where we have assumed that $q \ll \kappa_{I_i}, \kappa_{F_j}$, as we expect for vacua other than the dominant one. Using these results with Eq. (5.14), the ratio of Boltzmann brains in vacua I_i to normal observers in vacua I_i is given by

$$\frac{\mathcal{N}_{\{I_i\}}^{\rm BB}}{\mathcal{N}_{\{I_i\}}^{\rm NO}} \sim \frac{\max_i \left\{\kappa_{I_i}^{\rm BB}\, s_{I_i}\right\}}{\max_i \left\{\sum_j \kappa_{I_i F_j}\, s_{F_j}\right\}}$$

$$\sim \frac{\max_i \left\{ \kappa_{I_i}^{\rm BB} \frac{1}{\kappa_{I_i}} \sum_j \kappa_{I_i F_j} \frac{1}{\kappa_{F_j}} \kappa_{F_j D}\, s_D \right\}}{\max_i \left\{ \sum_j \kappa_{I_i F_j} \frac{1}{\kappa_{F_j}} \kappa_{F_j D}\, s_D \right\}}$$

$$\sim \frac{\max_i \left\{ \frac{\kappa_{I_i}^{\rm BB}}{\kappa_{I_i}} \sum_j \frac{\kappa_{I_i F_j}}{\kappa_{F_j}} \kappa_{F_j D} \right\}}{\max_i \left\{ \sum_j \frac{\kappa_{I_i F_j}}{\kappa_{F_j}} \kappa_{F_j D} \right\}}, \tag{5.40}$$

where the denominators are maximized over the restricted set of anthropic vacua i (and the numerators are maximized without restriction). The ratio of Boltzmann brains in the dominant vacuum (vacuum D) to normal observers in vacua I_i is given by

$$\frac{\mathcal{N}_D^{\rm BB}}{\mathcal{N}_{\{I_i\}}^{\rm NO}} \sim \frac{\kappa_D^{\rm BB}\, s_D}{\max_i \left\{ \sum_j \kappa_{I_i F_j}\, s_{F_j} \right\}}$$

$$\sim \frac{\kappa_D^{\rm BB}}{\max_i \left\{ \sum_j \frac{\kappa_{I_i F_j}}{\kappa_{F_j}} \kappa_{F_j D} \right\}}, \tag{5.41}$$

and, if vacuum D is anthropic, then the ratio of Boltzmann brains in vacuum D to normal observers in vacuum D is given by

$$\frac{\mathcal{N}_D^{\rm BB}}{\mathcal{N}_D^{\rm NO}} \sim \frac{\kappa_D^{\rm BB}}{\sum_j \frac{\kappa_{DF_j}}{\kappa_{F_j}} \kappa_{F_j D}}. \tag{5.42}$$

In this case our answers are complicated by the presence of many different vacua. We can in principle determine whether Boltzmann brains dominate by evaluating Eqs. (5.40)–(5.42) for the correct values of the parameters, but this gets rather complicated and model-dependent. The evaluation of these expressions can be simplified significantly, however, if we make some very plausible assumptions.

For tunneling out of the high-energy vacua F_j, one can expect the transition rates into different channels to be roughly comparable, so that $\kappa_{I_i F_j} \sim \kappa_{DF_j} \sim \kappa_{F_j}$. That is, we assume that the branching ratios $\kappa_{I_i F_j}/\kappa_{F_j}$ and $\kappa_{DF_j}/\kappa_{F_j}$ are roughly of order one in the sense of Eq. (5.2). These factors (or their inverses) will therefore be unimportant in the evaluation of $\mathcal{N}^{\rm BB}/\mathcal{N}^{\rm NO}$, and may be dropped. Furthermore, the upward transition rates from the dominant vacuum D into F_j are all comparable to one another, as can be seen by writing [44]

$$\kappa_{F_j D} \sim e^{A_{F_j D}} e^{-S_D}, \tag{5.43}$$

where $A_{F_j D}$ is the action of the instanton responsible for the transition and S_D is the

action of the Euclideanized de Sitter 4-sphere,

$$S_D = \frac{8\pi^2}{H_D^2} \,. \tag{5.44}$$

But generically $|A_{F_j D}| \sim 1/\rho_{F_j}$. If we assume that

$$\left| \frac{1}{\rho_{F_j}} - \frac{1}{\rho_{F_k}} \right| < 10^{14} \tag{5.45}$$

for every pair of vacua F_j and F_k, then $\kappa_{F_j D} = \kappa_{F_k D}$ up to a factor that can be ignored because it is roughly of order one. Thus, up to subleading factors, the transition rates $\kappa_{F_j D}$ cancel out[4] in the ratio $\mathcal{N}^{\rm BB}_{\{I_i\}}/\mathcal{N}^{\rm NO}$.

Returning to Eq. (5.40) and keeping only the leading factors, we have

$$\frac{\mathcal{N}^{\rm BB}_{\{I_i\}}}{\mathcal{N}^{\rm NO}} \sim \max_i \left\{ \frac{\kappa^{\rm BB}_{I_i}}{\kappa_{I_i}} \right\} \,, \tag{5.46}$$

where the index i runs over all (non-dominant) vacua in which Boltzmann brains can nucleate. For the dominant vacuum, our simplifying assumptions[5] convert Eqs. (5.41) and (5.42) into

$$\frac{\mathcal{N}^{\rm BB}_D}{\mathcal{N}^{\rm NO}} \sim \frac{\kappa^{\rm BB}_D}{\kappa_{\rm up}} \sim \kappa^{\rm BB}_D \, e^{S_D} \,, \tag{5.47}$$

where $\kappa_{\rm up} \equiv \sum_j \kappa_{F_j D}$ is the upward transition rate out of the dominant vacuum.

Thus, the conditions needed to avoid Boltzmann brain domination are essentially the same as what we found in Subsection 5.2.3. In this case, however, we must require that in any vacuum that can support Boltzmann brains, the Boltzmann brain nucleation rate must be less than the decay rate of that vacuum.

5.2.5 A dominant vacuum system

In the next to last paragraph of Section 2.2.1, we described a scenario where the dominant vacuum was not the vacuum with the smallest decay rate. Let us now

[4]Depending on the range of vacua F_j that are considered, the bound of Eq. (5.45) may or may not be valid. If it is not, then the simplification of Eq. (5.46) below is not justified, and the original Eq. (5.40) has to be used. Of course one should remember that there was significant arbitrariness in the choice of 10^{14} in the definition of "roughly of order one." 10^{14} was chosen to accommodate the largest estimate that we discuss in Sec. 5.3 for the Boltzmann brain nucleation rate, $\Gamma_{\rm BB} \sim \exp(-10^{16})$. In considering the other estimates of $\Gamma_{\rm BB}$, one could replace 10^{14} by a much larger number, thereby increasing the applicability of Eq. (5.45).

[5]The dropping of the factor $e^{A_{F_j D}}$ is a more reliable approximation in this case than it was in Eq. (5.46) above. In this case the factor e^{-S_D} does not cancel between the numerator and denominator, so the factor $e^{A_{F_j D}}$ can be dropped if it is unimportant compared to e^{-S_D}. We of course do not know the value of S for the dominant vacuum, but for our vacuum it is of order 10^{122}, and it is plausible that the value for the dominant vacuum is similar or even larger. Thus as long as $1/\rho_{F_j}$ is small compared to 10^{122}, it seems safe to drop the factor $e^{A_{F_j D}}$.

study a simple landscape to illustrate this situation. Consider the toy landscape

$$\begin{array}{ccccccc} & & & F_j & \to & I_i & \to & B \\ & & \swarrow & & \searrow & & & \\ A & \leftarrow & D_1 & \longleftrightarrow & & D_2 & \to & A \\ & & \nwarrow & & \swarrow & & & \\ & & & S & \to & A\,, & & \end{array} \tag{5.48}$$

where as in Subsection 5.2.4 the vacua I_i are taken to include both anthropic vacua and vacua that support only Boltzmann brains. Vacua A and B are terminal vacua and the F_j have large, positive vacuum energies. Assume that vacuum S has the smallest total decay rate.

We have in mind the situation in which D_1 and D_2 are nearly degenerate, and transitions from D_1 to D_2 (and vice versa) are rapid, even though the transition in one direction is upward. With this in mind, we divide the decay rates of D_1 and D_2 into two parts,

$$\kappa_1 = \kappa_{21} + \kappa_1^{\rm out} \tag{5.49}$$

$$\kappa_2 = \kappa_{12} + \kappa_2^{\rm out}\,, \tag{5.50}$$

with $\kappa_{12}, \kappa_{21} \gg \kappa_{1,2}^{\rm out}$. We assume as in previous sections that the rates for large upward transitions (S to D_1 or D_2, and D_1 or D_2 to F_j) are extremely small, so that we can ignore them in the calculation of q. The rate equation, Eq. (2.10), then admits a solution with $q \simeq \kappa_D$, but it also admits solutions with

$$q \simeq \frac{1}{2}\left[\kappa_1 + \kappa_2 \pm \sqrt{(\kappa_1 - \kappa_2)^2 + 4\kappa_{12}\kappa_{21}}\right]\,. \tag{5.51}$$

Expanding the smaller root to linear order in $\kappa_{1,2}^{\rm out}$ gives

$$q \simeq \alpha_1 \kappa_1^{\rm out} + \alpha_2 \kappa_2^{\rm out}\,, \tag{5.52}$$

where

$$\alpha_1 \equiv \frac{\kappa_{12}}{\kappa_{12} + \kappa_{21}}\,, \qquad \alpha_2 \equiv \frac{\kappa_{21}}{\kappa_{12} + \kappa_{21}}\,. \tag{5.53}$$

In principle this value for q can be smaller than κ_D, which is the case that we wish to explore.

In this case the vacua D_1 and D_2 dominate the volume fraction of the multiverse, even if their total decay rates κ_1 and κ_2 are not the smallest in the landscape. We can therefore call the states D_1 and D_2 together a dominant vacuum system, which we denote collectively as D. The rate equation (Eq. (2.10)) shows that

$$s_{D_1} \approx \alpha_1\, s_D\,, \qquad s_{D_2} \approx \alpha_2\, s_D\,, \tag{5.54}$$

where $s_D \equiv s_{D_1} + s_{D_2}$, and the equations hold in the approximation that $\kappa_{1,2}^{\rm out}$ and the upward transition rates from D_1 and D_2 can be neglected. To see that these vacua

dominate the volume fraction, we calculate the modified form of Eq. (5.39):

$$\frac{s_{F_j}}{s_D} \approx \frac{\alpha_1 \kappa_{F_j D_1} + \alpha_2 \kappa_{F_j D_2}}{\kappa_{F_j}} . \tag{5.55}$$

Thus the volume fractions of the F_j, and hence also the I_j and B vacua, are suppressed by the very small rate for large upward jumps from low energy vacua, namely $\kappa_{F_j D_1}$ and $\kappa_{F_j D_2}$. The volume fraction for S depends on κ_{AD_1} and κ_{AD_2}, but it is maximized when these rates are negligible, in which case it is given by

$$\frac{s_S}{s_D} \approx \frac{q}{\kappa_S - q} . \tag{5.56}$$

This quantity can in principle be large, if q is just a little smaller than κ_S, but that would seem to be a very special case. Generically, we would expect that since q must be smaller than κ_S (see Eq. (2.12)), it would most likely be many orders of magnitude smaller, and hence the ratio in Eq. (5.56) would be much less than one. There is no reason, however, to expect it to be as small as the ratios that are suppressed by large upward jumps. For simplicity, however, we shall assume in what follows that s_S can be neglected.

To calculate the ratio of Boltzmann brains to normal observers in this toy landscape, note that Eqs. (5.40) and (5.41) are modified only by the substitution

$$\kappa_{F_j D} \to \bar{\kappa}_{F_j D} \equiv \alpha_1 \kappa_{F_j D_1} + \alpha_2 \kappa_{F_j D_2} . \tag{5.57}$$

Thus, the dominant vacuum transition rate is simply replaced by a weighted average of the dominant vacuum transition rates. If we assume that neither of the vacua D_1 nor D_2 are anthropic, and make the same assumptions about magnitudes used in Subsection 5.2.4, then Eqs. (5.46) and (5.47) continue to hold as well, where we have redefined $\kappa_{\rm up}$ by $\kappa_{\rm up} \equiv \sum_j \bar{\kappa}_{F_j D}$.

If, however, we allow D_1 or D_2 to be anthropic, then new questions arise. Transitions between D_1 and D_2 are by assumption rapid, so they copiously produce new pockets and potentially new normal observers. We must recall, however (as discussed in Section 5.1), that the properties of a pocket universe depend on both the current vacuum and the parent vacuum. In this case, the unusual feature is that the vacua within the D system are nearly degenerate, and hence very little energy is released by tunnelings within D. For pocket universes created in this way, the maximum particle energy density during reheating will be only a small fraction of the vacuum energy density. Such a big bang is very different from the one that took place in our pocket, and presumably much less likely to produce life. We shall call a vacuum in the D system "strongly anthropic" if normal observers are produced by tunnelings from within D, and "mildly anthropic" if normal observers can be produced, but only by tunnelings from higher energy vacua outside D.

If either of the vacua in D were strongly anthropic, then the normal observers in D would dominate the normal observers in the multiverse. Normal observers in the vacua I_i would be less numerous by a factor proportional to the extremely small

rate $\bar{\kappa}_{F_j D}$ for large upward transitions . This situation would itself be a problem, however, similar to the Boltzmann brain problem. It would mean that observers like ourselves, who arose from a hot big bang with energy densities much higher than our vacuum energy density, would be extremely rare in the multiverse. We conclude that if there are any models which give a dominant vacuum system that contains a strongly anthropic vacuum, such models would be considered unacceptable in the context of the scale-factor cutoff measure.

On the other hand, if the D system included one or more mildly anthropic vacua, then the situation is very similar to that discussed in Subsections 5.2.3 and 5.2.4. In this case the normal observers in the D system would be comparable in number to the normal observers in the vacua I_i, so they would have no significant effect on the ratio of Boltzmann brains to normal observers in the multiverse. If any of the D vacua were mildly anthropic, however, then the stringent requirement $\kappa_D^{\rm BB} \ll \kappa_{\rm up}$ would have to be satisfied without resort to the simple solution $\kappa_D^{\rm BB} = 0$.

Thus, we find that the existence of a dominant vacuum system does not change our conclusions about the abundance of Boltzmann brains, except insofar as the Boltzmann brain nucleation constraints that would apply to the dominant vacuum must apply to every member of the dominant vacuum system. Probably the most important implication of this example is that the dominant vacuum is not necessarily the vacuum with the lowest decay rate, so the task of identifying the dominant vacuum could be very difficult.

5.2.6 General conditions to avoid Boltzmann brain domination

In constructing general conditions to avoid Boltzmann brain domination, we are guided by the toy landscapes discussed in the previous subsections. Our goal, however, is to construct conditions that can be justified using only the general equations of Sections 2.2.1 and 5.1, assuming that the landscape is irreducible, but without relying on the properties of any particular toy landscape. We shall be especially cautious about the treatment of the dominant vacuum and the possibility of small upward transitions, which could be rapid. The behavior of the full landscape of a realistic theory may deviate considerably from that of the simplest toy models.

To discuss the general situation, it is useful to divide vacuum states into four classes. We are only interested in vacua that can support Boltzmann brains. These can be

(1) anthropic vacua for which the total dimensionless decay rate satisfies $\kappa_i \gg q$,

(2) non-anthropic vacua that can transition to anthropic vacua via unsuppressed transitions,

(3) non-anthropic vacua that can transition to anthropic vacua only via suppressed transitions,

(4) anthropic vacua for which the total dimensionless decay rate is $\kappa_i \approx q$.

Here q is the smallest-magnitude eigenvalue of the rate equation (see Eqs. (2.6)–(2.9)). We call a transition "unsuppressed" if its branching ratio is roughly of order one in the sense of Eq. (5.2). If the branching ratio is smaller than this, it is "suppressed." As before, when calculating $\mathcal{N}^{\rm BB}/\mathcal{N}^{\rm NO}$ we assume that factors that are roughly of order one can be ignored. Note that Eq. (2.12) forbids κ_i from being less than q, so the above four cases are exhaustive.

We first discuss conditions that are sufficient to guarantee that Boltzmann brains will not dominate, postponing until later the issue of what conditions are necessary.

We begin with the vacua in the first class. Very likely all anthropic vacua belong to this class. For an anthropic vacuum i, the Boltzmann brains produced in vacuum i cannot dominate the multiverse if they do not dominate the normal observers in vacuum i, so we can begin with this comparison. Restricting Eq. (5.15) to this single vacuum, we obtain

$$\frac{\mathcal{N}_i^{\rm BB}}{\mathcal{N}_i^{\rm NO}} \sim \frac{\kappa_i^{\rm BB}}{\kappa_i}\,, \tag{5.58}$$

a ratio that has appeared in many of the simple examples. If this ratio is small compared to one, then Boltzmann brains created in vacuum i are negligible.

Let us now study a vacuum j in the second class. First note that Eq. (2.10) implies the rigorous inequality

$$\kappa_i\, s_i \geq \kappa_{ij}\, s_j \quad \text{(no sum on repeated indices)}\,, \tag{5.59}$$

which holds for any two states i and j. (Intuitively, Eq. (5.59) is the statement that, in steady state, the total rate of loss of volume fraction must exceed the input rate from any one channel.) To simplify what follows, it will be useful to rewrite Eq. (5.59) as

$$(\kappa_i s_i) \geq (\kappa_j s_j)\, B_{j\to i}\,, \tag{5.60}$$

where $B_{j\to i} \equiv \kappa_{ij}/\kappa_j$ is the branching ratio for the transition $j \to i$.

Suppose that we are trying to bound the Boltzmann brain production in vacuum j, and we know that it can undergo unsuppressed transitions

$$j \to k_1 \to \ldots \to k_n \to i\,, \tag{5.61}$$

where i is an anthropic vacuum. We begin by using Eqs. (5.8) and (5.10) to express $\mathcal{N}_j^{\rm BB}/\mathcal{N}_i^{\rm NO}$, dropping irrelevant factors as in Eq. (5.14), and then we can iterate the above inequality:

$$\begin{aligned}
\frac{\mathcal{N}_j^{\rm BB}}{\mathcal{N}_i^{\rm NO}} &\sim \frac{\kappa_j^{\rm BB}\, s_j}{\sum_k \kappa_{ik}\, s_k} \leq \frac{\kappa_j^{\rm BB}\, s_j}{\kappa_i\, s_i} \\
&\leq \frac{\kappa_j^{\rm BB}\, s_j}{(\kappa_j s_j) B_{j\to k_1} B_{k_1\to k_2} \cdots B_{k_n\to i}} \\
&= \frac{\kappa_j^{BB}}{\kappa_j}\, \frac{1}{B_{j\to k_1} B_{k_1\to k_2} \cdots B_{k_n\to i}}\,,
\end{aligned} \tag{5.62}$$

where again there is no sum on repeated indices, and Eq. (2.10) was used in the last step on the first line. Each inverse branching ratio on the right of the last line is greater than or equal to one, but by our assumptions can be considered to be roughly of order one, and hence can be dropped. Thus, the multiverse will avoid domination by Boltzmann brains in vacuum j if $\kappa_j^{\rm BB}/\kappa_j \ll 1$, the same criterion found for the first class.

The third class — non-anthropic vacua that can only transition to an anthropic state via at least one suppressed transition — presumably includes many states with very low vacuum energy density. The dominant vacuum of our toy landscape models certainly belongs to this class, but we do not know of anything that completely excludes the possibility that the dominant vacuum might belong to the second or fourth classes. That is, perhaps the dominant vacuum is anthropic, or decays to an anthropic vacuum. If there is a dominant vacuum system, as described in Subsection 5.2.5, then $\kappa_i \gg q$, and the dominant vacua could belong to the first class, as well as to either of classes (2) and (3).

To bound the Boltzmann brain production in this class, we consider two possible criteria. To formulate the first, we can again use Eqs. (5.61) and (5.62), but this time the sequence must include at least one suppressed transition, presumably an upward jump. Let us therefore denote the branching ratio for this suppressed transition as $B_{\rm up}$, noting that $B_{\rm up}$ will appear in the denominator of Eq. (5.62). Of course, the sequence of Eq. (5.61) might involve more than one suppressed transition, but in any case the product of these very small branching ratios in the denominator can be called $B_{\rm up}$, and all the other factors can be taken as roughly of order one. Thus, a landscape containing a vacuum j of the third class avoids Boltzmann brain domination if

$$\frac{\kappa_j^{\rm BB}}{B_{\rm up}\,\kappa_j} \ll 1\,, \tag{5.63}$$

in agreement with the results obtained for the dominant vacua in the toy landscape models in the previous subsections.

A few comments are in order. First, if the only suppressed transition is the first, then $B_{\rm up} = \kappa_{\rm up}/\kappa_j$, and the above criterion simplifies to $\kappa_j^{\rm BB}/\kappa_{\rm up} \ll 1$. Second, we should keep in mind that the sequence of Eq. (5.61) is presumably not unique, so other sequences will produce other bounds. All the bounds will be valid, so the strongest bound is the one of maximum interest. Finally, since the vacua under discussion are not anthropic, a likely method for Eq. (5.63) to be satisfied would be for $\kappa_j^{\rm BB}$ to vanish, as would happen if the vacuum j did not support the complex structures needed to form Boltzmann brains.

The criterion above can be summarized by saying that if $\kappa_j^{\rm BB}/(B_{\rm up}\kappa_j) \ll 1$, then the Boltzmann brains in vacuum j will be overwhelmingly outnumbered by the normal observers living in pocket universes that form in the decay chain starting from vacuum j. We now describe a second, alternative criterion, based on the idea that the number of Boltzmann brains in vacuum j can be compared with the number of normal observers in vacuum i if the two types of vacuum have a common ancestor.

Denoting the common ancestor vacuum as A, we assume that it can decay to an

anthropic vacuum i by a chain of transitions

$$A \to k_1 \to \ldots \to k_n \to i\,, \tag{5.64}$$

and also to a Boltzmann-brain-producing vacuum j by a chain

$$A \to \ell_1 \to \ldots \to \ell_m \to j\,. \tag{5.65}$$

From the sequence of Eq. (5.64) and the bound of Eq. (5.60), we can infer that

$$(\kappa_i s_i) \geq (k_A s_A) B_{A\to k_1} B_{k_1 \to k_2} \cdots B_{k_n \to i}\,. \tag{5.66}$$

To make use of the sequence of Eq. (5.65) we shall want a bound that goes in the opposite direction, for which will need to require additional assumptions. Starting with Eq. (2.10), we first require $q \ll \kappa_i$, which is plausible provided that vacuum i is not the dominant vacuum. Next we look at the sum over j on the right-hand side, and we call the transition $j \to i$ "significant" if its contribution to the sum is within a factor roughly of order one of the entire sum. (The sum over j is the sum over sources for vacuum i, so a transition $j \to i$ is "significant" if pocket universes of vacuum j are a significant source of pocket universes of vacuum i.) It follows that for any significant transition $j \to i$ for which $q \ll \kappa_i$,

$$(\kappa_i s_i) \leq (\kappa_j s_j) Z_{\max} B_{j\to i} \leq (\kappa_j s_j) Z_{\max}\,, \tag{5.67}$$

where $Z_{\max}$ denotes the largest number that is roughly of order one. By our conventions, $Z_{\max} = \exp(10^{14})$. If we assume now that all the transitions in the sequence of Eq. (5.65) are significant, and that q is negligible in each case, then

$$(\kappa_j s_j) \leq (k_A s_A) Z_{\max}^{m+1}\,. \tag{5.68}$$

Using the bounds from Eqs. (5.66) and (5.68), the Boltzmann brain ratio is bounded by

$$\begin{aligned} \frac{\mathcal{N}_j^{\rm BB}}{\mathcal{N}_i^{\rm NO}} &\sim \frac{\kappa_j^{\rm BB}\, s_j}{\sum_k \kappa_{ik}\, s_k} \leq \frac{\kappa_j^{\rm BB}\, s_j}{\kappa_i\, s_i} \\ &\leq \frac{Z_{\max}^{m+1}}{B_{A\to k_1} B_{k_1\to k_2} \cdots B_{k_n \to i}} \frac{\kappa_j^{\rm BB}}{\kappa_j}\,. \end{aligned} \tag{5.69}$$

But all the factors on the right are roughly of order one, except that some of the branching ratios in the denominator might be smaller, if they correspond to suppressed transitions. If $B_{\rm up}$ denotes the product of branching ratios for all the suppressed transitions shown in the denominator (i.e., all suppressed transitions in the sequence of Eq. (5.64)), then the bound reduces to Eq. (5.63).[6]

[6]Note, however, that the argument breaks down if the sequences in either of Eqs. (5.64) or (5.65) become too long. For the choices that we have made, a factor of $Z_{\max}$ is unimportant in the calculation of $\mathcal{N}^{\rm BB}/\mathcal{N}^{\rm NO}$, but $Z_{\max}^{100} = \exp(10^{16})$ can be significant. Thus, for our choices we can

To summarize, the Boltzmann brains in a non-anthropic vacuum j can be bounded if there is an ancestor vacuum A that can decay to j through a chain of significant transitions for which $q \ll \kappa_\ell$ for each vacuum, as in the sequence of Eq. (5.65), and if the same ancestor vacuum can decay to an anthropic vacuum through a sequence of transitions as in Eq. (5.64). The Boltzmann brains will never dominate provided that $\kappa_j^{\rm BB}/(B_{\rm up}\,\kappa_j) \ll 1$, where $B_{\rm up}$ is the product of all suppressed branching ratios in the sequence of Eq. (5.64).

Finally, the fourth class of vacua consists of anthropic vacua i with decay rate $\kappa_i \simeq q$, a class which could be empty. For this class Eq. (5.15) may not be very useful, since the quantity $(\kappa_i - q)$ in the denominator could be very small. Yet, as in the two previous classes, this class can be treated by using Eq. (5.62), where in this case the vacuum i can be the same as j or different, although the case $i = j$ requires $n \geq 1$. Again, if the sequence contains only unsuppressed transitions, then the multiverse avoids domination by Boltzmann brains in vacuum i if $\kappa_i^{\rm BB}/\kappa_i \ll 1$. If upward jumps are needed to reach an anthropic vacuum, whether it is the vacuum i again or a distinct vacuum j, then the Boltzmann brains in vacuum i will never dominate if $\kappa_i^{\rm BB}/(B_{\rm up}\,\kappa_i) \ll 1$.

The conditions described in the previous paragraph are very difficult to meet, so if the fourth class is not empty, Boltzmann brain domination is hard to avoid. These vacua have the slowest decay rates in the landscape, $\kappa_i \approx q$, so it seems plausible that they have very low energy densities, precluding the possibility of decaying to an anthropic vacuum via unsuppressed transitions; in that case Boltzmann brain domination can be avoided if

$$\kappa_i^{\rm BB} \ll B_{\rm up}\kappa_i\,. \tag{5.70}$$

However, as pointed out in Ref. [33], $B_{\rm up} \propto e^{-S_D}$ (see Eq. (5.43)) is comparable to the inverse of the recurrence time, while in an anthropic vacuum one would expect the Boltzmann brain nucleation rate to be much faster than once per recurrence time.

To summarize, the domination of Boltzmann brains can be avoided by first of all requiring that all vacuum states in the landscape obey the relation

$$\frac{\kappa_j^{\rm BB}}{\kappa_j} \ll 1\,. \tag{5.71}$$

That is, the rate of nucleation of Boltzmann brains in each vacuum must be less than the rate of nucleation, in that same vacuum, of bubbles of other phases. For anthropic vacua i with $\kappa_i \gg q$, this criterion is enough. Otherwise, the Boltzmann brains that might be produced in vacuum j must be bounded by the normal observers forming in some vacuum i, which must be related to j through decay chains. Specifically, there must be a vacuum A that can decay through a chain to an anthropic vacuum i, i.e.

$$A \to k_1 \to \ldots \to k_n \to i\,, \tag{5.72}$$

justify the dropping of $\mathcal{O}(100)$ factors that are roughly of order one, but not more than that. For choices appropriate to smaller estimates of $\Gamma_{\rm BB}$, however, the number of factors that can be dropped will be many orders of magnitude larger.

where either $A = j$, or else A can decay to j through a sequence

$$A \to \ell_1 \to \ldots \to \ell_m \to j\,. \tag{5.73}$$

In the above sequence we insist that $\kappa_j \gg q$ and that $\kappa_l \gg q$ for each vacuum ℓ_p in the chain, and that each transition must be "significant," in the sense that pockets of type ℓ_p must be a significant source of pockets of type ℓ_{p+1}. (More precisely, a transition from vacuum j to i is "significant" if it contributes a fraction that is roughly of order one to $\sum_j \kappa_{ij} s_j$ in Eq. (2.10).) For these cases, the bound which ensures that the Boltzmann brains in vacuum j are dominated by the normal observers in vacuum i is given by

$$\frac{\kappa_j^{\rm BB}}{B_{\rm up}\,\kappa_j} \ll 1\,, \tag{5.74}$$

where $B_{\rm up}$ is the product of any suppressed branching ratios in the sequence of Eq. (5.72). If all the transitions in Eq. (5.72) are unsuppressed, this bound reduces to Eq. (5.71). If j is anthropic, the case $A = j = i$ is allowed, provided that $n \geq 1$.

The conditions described above are sufficient to guarantee that Boltzmann brains do not dominate over normal observers in the multiverse, but without further assumptions there is no way to know if they are necessary. All of the conditions that we have discussed are quasi-local, in the sense that they do not require any global picture of the landscape of vacua. For each of the above arguments, the Boltzmann brains in one type of vacuum j are bounded by the normal observers in some type of vacuum i that is either the same type, or directly related to it through decay chains. Thus, there was no need to discuss the importance of the vacua j and i compared to the rest of the landscape as a whole. The quasi-local nature of these conditions, however, guarantees that they cannot be necessary to avoid the domination by Boltzmann brains. If two vacua j and i are both totally insignificant in the multiverse, then it will always be possible for the Boltzmann brains in vacuum j to overwhelm the normal observers in vacuum i, while the mulitverse as a whole could still be dominated by normal observers in other vacua.

We have so far avoided making global assumptions about the landscape of vacua, because such assumptions are generally hazardous. While it may be possible to make statements that are true for the bulk of vacua in the landscape, in this context the statements are not useful unless they are true for **all** the vacua of the landscape. Although the number of vacua in the landscape, often estimated at 10^{500} [101], is usually considered to be incredibly large, the number is nonetheless roughly of order one compared to the numbers involved in the estimates of Boltzmann brain nucleation rates and vacuum decay rates. Thus, if a single vacuum produces Boltzmann brains in excess of required bounds, the Boltzmann brains from that vacuum could easily overwhelm all the normal observers in the multiverse.

Recognizing that our conclusions could be faulty, we can nonetheless adopt some reasonable assumptions to see where they lead. We can assume that the multiverse is sourced by either a single dominant vacuum, or by a dominant vacuum system. We can further assume that every anthropic and/or Boltzmann-brain-producing vacuum

i can be reached from the dominant vacuum (or dominant vacuum system) by a single significant upward jump, with a rate proportional to e^{-S_D}, followed by some number of significant, unsuppressed transitions, all of which have rates $\kappa_k \gg q$ and branching ratios that are roughly of order one:

$$D \to k_1 \to \ldots \to k_n \to i\,. \tag{5.75}$$

We shall further assume that each non-dominant anthropic and/or Boltzmann-brain-producing vacuum i has a decay rate $\kappa_i \gg q$, but we need not assume that all of the κ_i are comparable to each other. With these assumptions, the estimate of $\mathcal{N}^{\rm BB}/\mathcal{N}^{\rm NO}$ becomes very simple.

Applying Eq. (2.10) to the first transition of Eq. (5.75),

$$\kappa_{k_1}\, s_{k_1} \sim \kappa_{k_1 D}\, s_D \sim \kappa_{\rm up} s_D\,, \tag{5.76}$$

where we use $\kappa_{\rm up}$ to denote the rate of a typical transition $D \to k$, assuming that they are all equal to each other up to a factor roughly of order one. Here $\sim$ indicates equality up to a factor that is roughly of order one. If there is a dominant vacuum system, then $\kappa_{k_1 D}$ is replaced by $\bar\kappa_{k_1 D} \equiv \sum_\ell \alpha_\ell \kappa_{k_1 D_\ell}$, where the D_ℓ are the components of the dominant vacuum system, and the α_ℓ are defined by generalizing Eqs. (5.53) and (5.54).[7] Applying Eq. (2.10) to the next transition, $k_1 \to k_2$ we find

$$\kappa_{k_2}\, s_{k_2} = B_{k_1 \to k_2} \kappa_{k_1} s_{k_1} + \ldots \sim \kappa_{k_1}\, s_{k_1}\,, \tag{5.77}$$

where we have used the fact that $B_{k_1 \to k_2}$ is roughly of order one, and that the transition is significant. Iterating, we have

$$\kappa_i\, s_i \sim \kappa_{k_n}\, s_{k_n} \sim \kappa_{\rm up}\, s_D\,. \tag{5.78}$$

Since the expression on the right is independent of i, we conclude that under these assumptions any two non-dominant anthropic and/or Boltzmann-brain-producing vacua

[7] In more detail, the concept of a dominant vacuum system is relevant when there is a set of vacua ℓ that can have rapid transitions within the set, but only very slow transitions connecting these vacua to the rest of the landscape. As a zeroth order approximation one can neglect all transitions connecting these vacua to the rest of the landscape, and assume that $\kappa_\ell \gg q$, so Eq. (2.10) takes the form

$$\kappa_\ell\, s_\ell = \sum_{\ell'} B_{\ell\ell'}\, \kappa_{\ell'}\, s_{\ell'}\,.$$

Here $B_{\ell\ell'} \equiv \kappa_{\ell\ell'}/\kappa_{\ell'}$ is the branching ratio within this restricted subspace, where $\kappa_\ell = \sum_{\ell'} \kappa_{\ell'\ell}$ is summed only within the dominant vacuum system, so $\sum_\ell B_{\ell\ell'} = 1$ for all ℓ'. $B_{\ell\ell'}$ is nonnegative, and if we assume also that it is irreducible, then the Perron-Frobenius theorem guarantees that it has a nondegenerate eigenvector v_ℓ of eigenvalue 1, with positive components. From the above equation $\kappa_\ell\, s_\ell \propto v_\ell$, and then

$$\alpha_\ell = \frac{s_\ell}{\sum_{\ell'} s_{\ell'}} = \frac{v_\ell}{\kappa_\ell \sum_{\ell'} \frac{v_{\ell'}}{\kappa_{\ell'}}}\,.$$

i and j have equal values of κs, up to a factor that is roughly of order one:

$$\kappa_j s_j \sim \kappa_i s_i \ . \tag{5.79}$$

Using Eq. (5.8) and assuming as always that $n_{ik}^{\rm NO}$ is roughly of order one, Eq. (5.79) implies that any two non-dominant anthropic vacua i and j have comparable numbers of ordinary observers, up to a factor that is roughly of order one:

$$\mathcal{N}_j^{\rm NO} \sim \mathcal{N}_i^{\rm NO} \ . \tag{5.80}$$

The dominant vacuum could conceivably be anthropic, but we begin by considering the case in which it is not. In that case all anthropic vacua are equivalent, so the Boltzmann brains produced in any vacuum j will either dominate the multiverse or not depending on whether they dominate the normal observers in an arbitrary anthropic vacuum i. Combining Eqs. (5.8), (5.10), (2.10), and (5.79), and omitting irrelevant factors, we find that for any non-dominant vacuum j

$$\frac{\mathcal{N}_j^{\rm BB}}{\mathcal{N}_i^{\rm NO}} \sim \frac{\kappa_j^{\rm BB} s_j}{\sum_k \kappa_{ik}\, s_k} \sim \frac{\kappa_j^{\rm BB} s_j}{\kappa_i s_i} \sim \frac{\kappa_j^{\rm BB}}{\kappa_j} \ . \tag{5.81}$$

Thus, given the assumptions described above, for any non-dominant vacuum j the necessary and sufficient condition to avoid the domination of the multiverse by Boltzmann brains in vacuum j is given by

$$\frac{\kappa_j^{\rm BB}}{\kappa_j} \ll 1 \ . \tag{5.82}$$

For Boltzmann brains formed in the dominant vacuum, we can again find out if they dominate the multiverse by determining whether they dominate the normal observers in an arbitrary anthropic vacuum i. Repeating the above analysis for vacuum D instead of vacuum j, using Eq. (5.78) to relate s_i to s_D, we have

$$\frac{\mathcal{N}_D^{\rm BB}}{\mathcal{N}_i^{\rm NO}} \sim \frac{\kappa_D^{\rm BB} s_D}{\sum_k \kappa_{ik}\, s_k} \sim \frac{\kappa_D^{\rm BB} s_D}{\kappa_i s_i} \sim \frac{\kappa_D^{\rm BB}}{\kappa_{\rm up}} \ . \tag{5.83}$$

Thus, for a single dominant vacuum D or a dominant vacuum system with members D_i, the necessary and sufficient conditions to avoid the domination of the multiverse by these Boltzmann brains is given by

$$\frac{\kappa_D^{\rm BB}}{\kappa_{\rm up}} \ll 1 \ \ \text{or} \ \ \frac{\kappa_{D_i}^{\rm BB}}{\kappa_{\rm up}} \ll 1 \ . \tag{5.84}$$

As discussed after Eq. (5.70), probably the only way to satisfy this condition is to require that $\kappa_D^{\rm BB} = 0$.

If the dominant vacuum is anthropic, then the conclusions are essentially the same, but the logic is more involved. For the case of a dominant vacuum system, we distinguish between the possibility of vacua being "strongly" or "mildly" anthropic, as

discussed in Subsection 5.2.5. "Strongly anthropic" means that normal observers are formed by tunneling within the dominant vacuum system D, while "mildly anthropic" implies that normal observers are formed by tunneling, but only from outside D. Any model that leads to a strongly anthropic dominant vacuum would be unacceptable, because almost all observers would live in pockets with a maximum reheat energy density that is small compared to the vacuum energy density. With a single anthropic dominant vacuum, or with one or more mildly anthropic vacua within a dominant vacuum system, the normal observers in the dominant vacuum would be comparable in number (up to factors roughly of order one) to those in other anthropic vacua, so they would have no significant effect on the ratio of Boltzmann brains to normal observers in the multiverse. An anthropic vacuum would also produce Boltzmann brains, however, so Eq. (5.84) would have to somehow be satisfied for $\kappa_D^{\rm BB} \neq 0$.

5.3 Boltzmann brain nucleation and vacuum decay rates

5.3.1 Boltzmann brain nucleation rate

Boltzmann brains emerge from the vacuum as large quantum fluctuations. In particular, they can be modeled as localized fluctuations of some mass M, in the thermal bath of a de Sitter vacuum with temperature $T_{\rm dS} = H_\Lambda/2\pi$ [85]. The Boltzmann brain nucleation rate is then roughly estimated by the Boltzmann suppression factor [38, 41],

$$\Gamma_{\rm BB} \sim e^{-M/T_{\rm dS}}\,, \tag{5.85}$$

where our goal is to estimate only the exponent, not the prefactor. Eq. (5.85) gives an estimate for the nucleation rate of a Boltzmann brain of mass M in any particular quantum state, but we shall normally describe the Boltzmann brain macroscopically. Thus $\Gamma_{\rm BB}$ should be multiplied by the number of microstates $e^{S_{\rm BB}}$ corresponding to the macroscopic description, where $S_{\rm BB}$ is the entropy of the Boltzmann brain. Thus we expect

$$\Gamma_{\rm BB} \sim e^{-M/T_{\rm dS}} e^{S_{\rm BB}} = e^{-F/T_{\rm dS}}\,, \tag{5.86}$$

where $F = M - T_{\rm dS}\, S_{\rm BB}$ is the free energy of the Boltzmann brain.

Eq. (5.86) should be accurate as long as the de Sitter temperature is well-defined, which will be the case as long as the Schwarzschild horizon is small compared to the de Sitter horizon radius. Furthermore, we shall neglect the effect of the gravitational potential energy of de Sitter space on the Boltzmann brain, which requires that the Boltzmann brain be small compared to the de Sitter horizon. Thus we assume

$$M/4\pi < R \ll H_\Lambda^{-1}\,, \tag{5.87}$$

where the first inequality assumes that Boltzmann brains cannot be black holes. The general situation, which allows for $M \sim R \sim H_\Lambda^{-1}$, will be discussed in Appendix C.

While the nucleation rate is proportional to $e^{S_{\rm BB}}$, this factor is negligible for any

Boltzmann brain made of atoms like those in our universe. The entropy of such atoms is bounded by

$$S \lesssim 3M/m_n\,, \tag{5.88}$$

where m_n is the nucleon mass. Indeed, the actual value of $S_{\rm BB}$ is much smaller than this upper bound because of the complex organization of the Boltzmann brain. Meanwhile, to prevent the Boltzmann brain from being destroyed by pair production, we require that $T_{\rm dS} \ll m_n$. Thus, for these Boltzmann brains the entropy factor $e^{S_{\rm BB}}$ is irrelevant compared to the Boltzmann suppression factor.

To estimate the nucleation rate for Boltzmann brains, we need at least a crude description of what constitutes a Boltzmann brain. There are many possibilities. We argued in the introduction to this Chapter that a theory that predicts the domination of Boltzmann brains over normal observers would be overwhelmingly disfavored by our continued observation of an orderly world, in which the events that we observe have a logical relationship to the events that we remember. In making this argument, we considered a class of Boltzmann brains that share exactly the memories and thought processes of a particular normal observer at some chosen instant. For these purposes the memory of the Boltzmann brain can consist of random bits that just happen to match those of the normal observer, so there are no requirements on the history of the Boltzmann brain. Furthermore, the Boltzmann brain need only survive long enough to register one observation after the chosen instant, so it is not required to live for more than about a second. We shall refer to Boltzmann brains that meet these requirements as minimal Boltzmann brains.

While an overabundance of minimal Boltzmann brains is enough to cause a theory to be discarded, we nonetheless find it interesting to discuss a wide range of Boltzmann brain possibilities. We shall start with very large Boltzmann brains, discussing the minimal Boltzmann brains last.

We first consider Boltzmann brains much like us, who evolved in stellar systems like ours, in vacua with low-energy particle physics like ours, but allowing for a de Sitter Hubble radius as small as a few astronomical units or so. These Boltzmann brains evolved in their stellar systems on a time scale similar to the evolution of life on Earth, so they are in every way like us, except that, when they perform cosmological observations, they find themselves in an empty, vacuum-dominated universe. These "Boltzmann solar systems" nucleate at a rate of roughly

$$\Gamma_{\rm BB} \sim \exp(-10^{85})\,, \tag{5.89}$$

where we have set $M \sim 10^{30}$ kg and $H_\Lambda^{-1} = (2\pi T_{\rm dS})^{-1} \sim 10^{12}$ m. This nucleation rate is fantastically small; we found it, however, by considering the extravagant possibility of nucleating an entire Boltzmann solar system.

Next, we can consider the nucleation of an isolated brain, with a physical construction that is roughly similar to our own brains. If we take $M \sim 1$ kg and $H_\Lambda^{-1} = (2\pi T_{\rm dS})^{-1} \sim 1$ m, then the corresponding Boltzmann brain nucleation rate is

$$\Gamma_{\rm BB} \sim \exp(-10^{43})\,. \tag{5.90}$$

If the construction of the brain is similar to ours, however, then it could not function if the tidal forces resulted in a relative acceleration from one end to the other that is much greater than the gravitational acceleration g on the surface of the Earth. This requires $H_\Lambda^{-1} \gtrsim 10^8$ m, giving a Boltzmann brain nucleation rate

$$\Gamma_{\rm BB} \sim \exp(-10^{51})\,. \tag{5.91}$$

Until now, we have concentrated on Boltzmann brains that are very similar to human brains. However a common assumption in the philosophy of mind is that of substrate-independence. Therefore, pressing onward, we study the possibility that a Boltzmann brain can be any device capable of emulating the thoughts of a human brain. In other words, we treat the brain essentially as a highly sophisticated computer, with logical operations that can be duplicated by many different systems of hardware.

With this in mind, from here out we drop the assumption that Boltzmann brains are made of the same materials as human brains. Instead, we attempt to find an upper bound on the probability of creation of a more generalized computing device, specified by its information content $I_{\rm BB}$, which is taken to be comparable to the information content of a human brain.

To clarify the meaning of information content, we can model an information storage device as a system with N possible microstates. $S_{\rm max} = \ln N$ is then the maximum entropy that the system can have, the entropy corresponding to the state of complete uncertainty of microstate. To store B bits of information in the device, we can imagine a simple model in which 2^B distinguishable macroscopic states of the system are specified, each of which will be used to represent one assignment of the bits. Each macroscopic state can be modeled as a mixture of $N/2^B$ microstates, and hence has entropy $S = \ln(N/2^B) = S_{\rm max} - B\ln 2$. Motivated by this simple model, one defines the information content of any macroscopic state of entropy S as the difference between $S_{\rm max}$ and S, where $S_{\rm max}$ is the maximum entropy that the device can attain. Applying this definition to a Boltzmann brain, we write

$$I_{\rm BB} = S_{\rm BB,max} - S_{\rm BB}\,, \tag{5.92}$$

where $I_{\rm BB}/\ln 2$ is the information content measured in bits.

As discussed in Ref. [102], the only known substrate-independent limit on the storage of information is the Bekenstein bound. It states that, for an asymptotically flat background, the entropy of any physical system of size R and energy M is bounded by

$$S \leq S_{\rm Bek} \equiv 2\pi MR\,. \tag{5.93}$$

One can use this bound in de Sitter space as well if the size of the system is sufficiently small, $R \ll H_\Lambda^{-1}$, so that the system does not "know" about the horizon. A possible generalization of the Bekenstein bound for $R = \mathcal{O}(H_\Lambda^{-1})$ was proposed in Ref. [103]; we shall study this and other possibilities in Appendix C. To begin, however, we shall discuss the simplest case, $R \ll H_\Lambda^{-1}$, so that we can focus on the most important issues before dealing with the complexities of more general results.

Using Eq. (5.92), the Boltzmann brain nucleation rate of Eq. (5.86) can be rewritten as

$$\Gamma_{\rm BB} \sim \exp\left(-\frac{2\pi M}{H_\Lambda} + S_{\rm BB,max} - I_{\rm BB}\right) , \tag{5.94}$$

which is clearly maximized by choosing M as small as possible. The Bekenstein bound, however, implies that $S_{\rm BB,max} \leq S_{\rm Bek}$ and therefore $M \geq S_{\rm BB,max}/(2\pi R)$. Thus

$$\Gamma_{\rm BB} \leq \exp\left(-\frac{S_{\rm BB,max}}{RH_\Lambda} + S_{\rm BB,max} - I_{\rm BB}\right) . \tag{5.95}$$

Since $R < H_\Lambda^{-1}$, the expression above is maximized by taking $S_{\rm BB,max}$ equal to its smallest possible value, which is $I_{\rm BB}$. Finally, we have

$$\Gamma_{\rm BB} \leq \exp\left(-\frac{I_{\rm BB}}{RH_\Lambda}\right) . \tag{5.96}$$

Thus, the Boltzmann brain production rate is maximized if the Boltzmann brain saturates the Bekenstein bound, with $I_{\rm BB} = S_{\rm BB,max} = 2\pi MR$. Simultaneously, we should make RH_Λ as large as possible, which means taking our assumption $R \ll H_\Lambda^{-1}$ to the boundary of its validity. Thus we write the Boltzmann brain production rate

$$\Gamma_{\rm BB} \leq e^{-aI_{\rm BB}} , \tag{5.97}$$

where $a \equiv (RH_\Lambda)^{-1}$, the value of which is of order a few. In Appendix C we explore the case in which the Schwarzschild radius, the Boltzmann brain radius, and the de Sitter horizon radius are all about equal, in which case Eq. (5.97) holds with $a = 2$.

The bound of Eq. (5.97) can be compared to the estimate of the Boltzmann brain production rate, $\Gamma_{\rm BB} \sim e^{-S_{\rm BB}}$, which follows from Eq. (2.13) of Freivogel and Lippert, in Ref. [104]. The authors of Ref. [104] explained that by $S_{\rm BB}$ they mean not the entropy, but the number of degrees of freedom, which is roughly equal to the number of particles in a Boltzmann brain. This estimate appears similar to our result, if one equates $S_{\rm BB}$ to $I_{\rm BB}$, or to a few times $I_{\rm BB}$. Freivogel and Lippert describe this relation as a lower bound on the nucleation rate for Boltzmann brains, commenting that it can be used as an estimate of the nucleation rate for vacua with "reasonably cooperative particle physics." Here we shall explore in some detail the question of whether this bound can be used as an estimate of the nucleation rate. While we shall not settle this issue here, we shall discuss evidence that Eq. (5.97) is a valid estimate for at most a small fraction of the vacua of the landscape, and possibly none at all.

So far, the conditions to reach the upper bound in Eq. (5.97) are $R = (aH_\Lambda)^{-1} \sim \mathcal{O}(H_\Lambda^{-1})$ and $I_{\rm BB} = S_{\rm max,BB} = S_{\rm Bek}$. However these are not enough to ensure that a Boltzmann brain of size $R \sim H_\Lambda^{-1}$ is stable and can actually compute. Indeed, the time required for communication between two parts of a Boltzmann brain separated by a distance $\mathcal{O}(H_\Lambda^{-1})$ is at least comparable to the Hubble time. If the Boltzmann brain can be stretched by cosmological expansion, then after just a few operations the different parts will no longer be able to communicate. Therefore we need a stabilization mechanism by which the brain is protected against expansion.

A potential mechanism to protect the Boltzmann brain against de Sitter expansion is the self-gravity of the brain. A simple example is a black hole, which does not expand when the universe expands. It seems unlikely that black holes can think,[8] but one can consider objects of mass approaching that of a black hole with radius R. This, together with our goal to keep R as close as possible to H_Λ^{-1}, leads to the following condition:

$$M \sim R \sim H_\Lambda^{-1} . \tag{5.98}$$

If the Bekenstein bound is saturated, this leads to the following relations between $I_{\rm BB}$, H_Λ, and M:

$$I_{\rm BB} \sim MR \sim MH_\Lambda^{-1} \sim H_\Lambda^{-2} . \tag{5.99}$$

A second potential mechanism of Boltzmann brain stabilization is to surround it by a domain wall with a surface tension σ, which would provide pressure preventing the exponential expansion of the brain. An investigation of this situation reveals that one cannot saturate the Bekenstein bound using this mechanism unless there is a specific relation between $I_{\rm BB}$, H_Λ, and σ:

$$\sigma \sim I_{\rm BB}\, H_\Lambda^3 . \tag{5.100}$$

If σ is less than this magnitude, it cannot prevent the expansion, while a larger σ increases the mass and therefore prevents saturation of the Bekenstein bound.

Regardless of the details leading to Eqs. (5.99) and (5.100), the important point is that both of them lead to constraints on the vacuum hosting the Boltzmann brain.

For example, the Boltzmann brain stabilized by gravitational attraction can be produced at a rate approaching $e^{-aI_{\rm BB}}$ only if $I_{\rm BB} \sim H_\Lambda^{-2}$. For a given value of $I_{\rm BB}$, say $I_{\rm BB} \sim 10^{16}$ (see the discussion below), this result applies only to vacua with a particular vacuum energy, $\Lambda \sim 10^{-16}$. Similarly, according to Eq. (5.100), for Boltzmann brains with $I_{\rm BB} \sim 10^{16}$ contained inside a domain wall in a vacuum with $\Lambda \sim 10^{-120}$, the Bekenstein bound on $\Gamma_{\rm BB}$ cannot be reached unless the tension of the domain wall is incredibly small, $\sigma \sim 10^{-164}$. Thus, the maximal Boltzmann brain production rate $\sim e^{-aI_{\rm BB}}$ saturating the Bekenstein bound cannot be reached unless Boltzmann brains are produced on a narrow hypersurface in the landscape.

This conclusion by itself does not eliminate the danger of a rapid Boltzmann brain production rate, $\Gamma_{\rm BB} \sim e^{-aI_{\rm BB}}$. Given the vast number of vacua in the landscape, it seems plausible that this bound could actually be met. If this is the case, Eq. (5.97) offers a stunning increase over previous estimates of $\Gamma_{\rm BB}$.

Setting aside the issue of Boltzmann brain stability, one can also question the assumption of Bekenstein bound saturation that is necessary to achieve the rather high nucleation rate that is indicated by Eq. (5.97). Of course black holes saturate this bound, but we assume that a black hole cannot think. Even if a black hole can

[8]The possibility of a black hole computer is not excluded, however, and has been considered in Ref. [102]. Nonetheless, if black holes can compute, our conclusions would not be changed, provided that the Bekenstein bound can be saturated for the near-black hole computers that we discuss. At this level of approximation, there would be no significant difference between a black hole computer and a near-black hole computer.

think, it would still be an open question whether this information processing could make use of a substantial fraction of the degrees of freedom associated with the black hole entropy. A variety of other physical systems are considered in Ref. [105], where the validity of $S_{\max}(E) \leq 2\pi ER$ is studied as a function of energy E. In all cases, the bound is saturated in a limit where $S_{\max} = \mathcal{O}(1)$. Meanwhile, as we shall argue below, the required value of $S_{\max}$ should be greater than 10^{16}.

The present authors are aware of only one example of a physical system that may saturate the Bekenstein bound and at the same time store sufficient information I to emulate a human brain. This may happen if the total number of particle species with mass smaller than H_Λ is greater than $I_{\rm BB} \gtrsim 10^{16}$. No realistic examples of such theories are known to us, although some authors have speculated about similar possibilities [106].

If Boltzmann brains cannot saturate the Bekenstein bound, they will be more massive than indicated in Eq. (5.96), and their rate of production will be smaller than $e^{-aI_{\rm BB}}$.

To put another possible bound on the probability of Boltzmann brain production, let us analyze a simple model based on an ideal gas of massless particles. Dropping all numerical factors, we consider a box of size R filled with a gas with maximum entropy $S_{\max} = (RT)^3$ and energy $E = R^3T^4 = S_{\max}^{4/3}/R$, where T is the temperature and we assume there is not an enormous number of particle species. The probability of its creation can be estimated as follows:

$$\Gamma_{\rm BB} \sim e^{-E/H_\Lambda}\, e^{S_{\rm BB}} \sim \exp\left(-\frac{S_{\max}^{4/3}}{H_\Lambda R}\right), \tag{5.101}$$

where we have neglected the Boltzmann brain entropy factor, since $S_{\rm BB} \leq S_{\max} \ll S_{\max}^{4/3}$. This probability is maximized by taking $R \sim H_\Lambda^{-1}$, which yields

$$\Gamma_{\rm BB} \lesssim e^{-S_{\max}^{4/3}}\ . \tag{5.102}$$

In case the full information capacity of the gas is used, one can also write

$$\Gamma_{\rm BB} \lesssim e^{-I_{\rm BB}^{4/3}}\ . \tag{5.103}$$

For $I_{\rm BB} \gg 1$, this estimate leads to a much stronger suppression of Boltzmann brain production as compared to our previous estimate, Eq. (5.97).

Of course, such a hot gas of massless particles cannot think — indeed it is not stable in the sense outlined below Eq. (5.97) — so we must add more parts to this construction. Yet it seems likely that this will only decrease the Boltzmann brain production rate. As a partial test of this conjecture, one can easily check that if instead of a gas of massless particles we consider a gas of massive particles, the resulting suppression of Boltzmann brain production will be stronger. Therefore in our subsequent estimates we shall assume that Eq. (5.103) represents our next "line of defense" against the possibility of Boltzmann brain domination, after the one given by Eq. (5.97).

Having related $\Gamma_{\rm BB}$ to the information content $I_{\rm BB}$ of the brain, we now need to estimate $I_{\rm BB}$. How much information storage must a computer have to be able to perform all the functions of the human brain? Since no one can write a computer program that comes close to imitating a human brain, this is not an easy question to answer.

One way to proceed is to examine the human brain, with the goal of estimating its capacities based on its biological structure. The human brain contains $\sim 10^{14}$ synapses that may in principle connect to any of $\sim 10^{11}$ neurons [107], suggesting that its information content[9] might be roughly $I_{\rm BB} \sim 10^{15}$–10^{16}. (We are assuming here that the logical functions of the brain depend on the connections among neurons, and not for example on their precise locations, cellular structures, or other information that might be necessary to actually construct a brain.) A minimal Boltzmann brain is only required to simulate the workings of a real brain for about a second, but with neurons firing typically at 10 to 100 times a second, it is plausible that a substantial fraction of the brain is needed even for only one second of activity. Of course the actual number of required bits might be somewhat less.

An alternative approach is to try to determine how much information the brain processes, even if one does not understand much about what the processing involves.

In Ref. [108], Landauer attempted to estimate the total content of a person's long-term memory, using a variety of experiments. He concluded that a person remembers only about 2 bits/second, for a lifetime total in the vicinity of 10^9 bits. In a subsequent paper [109], however, he emphatically denied that this number is relevant to the information requirements of a "real or theoretical cognitive processor," because such a device "would have so much more to do than simply record new information."

Besides long-term memory, one might be interested in the total amount of information a person receives but does not memorize. A substantial part of this information is visual; it can be estimated by the information stored on high definition DVDs watched continuously on several monitors over the span of a hundred years. The total information received would be about 10^{16} bits.

Since this number is similar to the number obtained above by counting synapses, it is probably as good an estimate as we can make for a minimal Boltzmann brain. If the Bekenstein bound can be saturated, then the estimated Boltmann brain nucleation rate for the most favorable vacua in the landscape would be given by Eq. (5.97):

$$\Gamma_{\rm BB} \lesssim e^{-10^{16}} . \tag{5.104}$$

If, however, the Bekenstein bound cannot be reached for systems with $I_{\rm BB} \gg 1$, then it might be more accurate to use instead the ideal gas model of Eq. (5.103), yielding

$$\Gamma_{\rm BB} \lesssim e^{-10^{21}} . \tag{5.105}$$

Obviously, there are many uncertainties involved in the numerical estimates of the required value of $I_{\rm BB}$. Our estimate $I_{\rm BB} \sim 10^{16}$ concerns the information stored in the human brain that appears to be relevant for cognition. It certainly does not include

[9]Note that the specification of one out of 10^{11} neurons requires $\log_2\left(10^{11}\right) = 36.5$ bits.

all the information that would be needed to physically construct a human brain, and it therefore does not allow for the information that might be needed to physically construct a device that could emulate the human brain. [10] It is also possible that extra mass might be required for the mechanical structure of the emulator, to provide the analogues of a computer's wires, insulation, cooling systems, etc. On the other hand, it is conceivable that a Boltzmann brain can be relevant even if it has fewer capabilities than what we called the minimal Boltzmann brain. In particular, if our main requirement is that the Boltzmann brain is to have the same "perceptions" as a human brain for just one second, then one may argue that this can be achieved using much less than 10^{14} synapses. And if one decreases the required time to a much smaller value required for a single computation to be performed by a human brain, the required amount of information stored in a Boltzmann brain may become many orders of magnitude smaller than 10^{16}.

We find that regardless of how one estimates the information in a human brain, if Boltzmann brains can be constructed so as to come near the limit of Eq. (5.97), their nucleation rate would provide stringent requirements on vacuum decay rates in the landscape. On the other hand, if no such physical construction exists, we are left with the less dangerous bound of Eq. (5.103), perhaps even further softened by the speculations described in Footnote 10. Note that none of these bounds is based upon a realistic model of a Boltzmann brain. For example, the nucleation of an actual human brain is estimated at the vastly smaller rate of Eq. (5.91). The conclusions of this paragraph apply to the causal patch measures [16, 17] as well as the scale-factor cutoff measure.

In Section 5.1 we discussed the possibility of Boltzmann brain production during reheating, stating that this process would not be a danger. We postponed the numerical discussion, however, so we now return to that issue. According to Eq. (5.12), the multiverse will be safe from Boltzmann brains formed during reheating provided

[10] That is, the actual construction of a brain-like device would presumably require large amounts of information that are not part of the schematic "circuit diagram" of the brain. Thus there may be some significance to the fact that a billion years of evolution on Earth has not produced a human brain with fewer than about 10^{27} particles, and hence of order 10^{27} units of entropy. In counting the information in the synapses, for example, we counted only the information needed to specify which neurons are connected to which, but nothing about the actual path of the axons and dendrites that complete the connections. These are nothing like nearest-neighbor couplings, but instead axons from a single neuron can traverse large fractions of the brain, resulting in an extremely intertwined network [110]. To specify even the topology of these connections, still ignoring the precise locations, could involve much more than 10^{16} bits. For example, the synaptic "wiring" that connects the neurons will in many cases form closed loops. A specification of the connections would presumably require a topological winding number for every pair of closed loops in the network. The number of bits required to specify these winding numbers would be proportional to the square of the number of closed loops, which would be proportional to the square of the number of synapses. Thus, the structural information could be something like $I_{\rm struct} \sim b \times 10^{28}$, where b is a proportionality constant that is probably a few orders of magnitude less than 1. In estimating the resulting suppression of the nucleation rate, there is one further complication: since structural information of this sort presumably has no influence on brain function, these choices would contribute to the multiplicity of Boltzmann brain microstates, thereby multiplying the nucleation rate by $e^{I_{\rm struct}}$. There would still be a net suppression, however, with Eq. (5.97) leading to $\Gamma_{\rm BB} \propto e^{-(a-1)I_{\rm struct}}$, where a is generically greater than 1. See Appendix C for further discussion of the value of a.

that

$$\Gamma^{\rm BB}_{{\rm reheat},ik}\,\Delta\tau^{\rm BB}_{{\rm reheat},ik} \ll n^{\rm NO}_{ik} \tag{5.106}$$

holds for every pair of vacua i and k, where $\Gamma^{\rm BB}_{{\rm reheat},ik}$ is the peak Boltzmann brain nucleation rate in a pocket of vacuum i that forms in a parent vacuum of type k, $\Delta\tau^{\rm BB}_{{\rm reheat},ik}$ is the proper time available for such nucleation, and $n^{\rm NO}_{ik}$ is the volume density of normal observers in these pockets, working in the approximation that all observers form at the same time.

Compared to the previous discussion about late-time de Sitter space nucleation, here $\Gamma^{\rm BB}_{{\rm reheat},ik}$ can be much larger, since the temperature during reheating can be much larger than H_Λ. On the other hand, safety from Boltzmann brains requires the late-time nucleation rate to be small compared to the potentially very small vacuum decay rates, while in this case the quantity on the right-hand side of Eq. (5.106) is not exceptionally small. In discussing this issue, we shall consider in sequence three descriptions of the Boltzmann brain: a human-like brain, a near-black hole computer, and a diffuse computer.

The nucleation of human-like Boltzmann brains during reheating was discussed in Ref. [91], where it was pointed out that such brains could not function at temperatures much higher than 300 K, and that the nucleation rate for a 100 kg object at this temperature is $\sim \exp(-10^{40})$. This suppression is clearly more than enough to ensure that Eq. (5.106) is satisfied.

For a near-black hole computer with $I_{\rm BB} \approx S_{\rm BB,max} \approx 10^{16}$, the minimum mass is 600 grams. If we assume that the reheat temperature is no more than the reduced Planck mass, $m_{\rm Planck} \equiv 1/\sqrt{8\pi G} \approx 2.4 \times 10^{18}$ GeV $\approx 4.3 \times 10^{-6}$ gram, we find that $\Gamma^{\rm BB}_{\rm reheat} < \exp\left(-\sqrt{2I_{\rm BB}}\right) \sim \exp(-10^8)$. Although this is not nearly as much suppression as in the previous case, it is clearly enough to guarantee that Eq. (5.106) will be satisfied.

For the diffuse computer, we can consider an ideal gas of massless particles, as discussed in Eqs. (5.101)–(5.103). The system would have approximately $S_{\rm max}$ particles, and a total energy of $E = S_{\rm max}^{4/3}/R$, so the Boltzmann suppression factor is $\exp\left[-S_{\rm max}^{4/3}/\left(RT_{\rm reheat}\right)\right]$. The Boltzmann brain production can occur at any time during the reheating process, so there is nothing wrong with considering Boltzmann brain production in our universe at the present time. For $T_{\rm reheat} = 2.7$ K and $S_{\rm max} = 10^{16}$, this formula implies that the exponent has magnitude 1 for $R = S_{\rm max}^{4/3} T_{\rm reheat}^{-1} \approx 200$ light-years. Thus, the formula suggests that diffuse-gas-cloud Boltzmann brains of radius 200 light-years can be thermally produced in our universe, at the present time, without suppression! If this estimate were valid, then Boltzmann brains would almost certainly dominate the universe.

We argue, however, that the gas clouds described above would have no possibility of computing, because the thermal noise would preclude any storage or transfer of information. The entire device has energy of order $E \approx T_{\rm reheat}$, which is divided among approximately 10^{16} massless particles. The mean particle energy is therefore 10^{16} times smaller than that of the thermal particles in the background radiation, and the density of Boltzmann brain particles is 10^{48} times smaller than the background. To function, it seems reasonable that the diffuse computer needs an energy per particle

that is at least comparable to the background, which means that the suppression factor is $\exp(-10^{16})$ or smaller. Thus, we conclude that for all three cases, the ratio of Boltzmann brains to normal observers is totally negligible.

Finally, let us also mention the possibility that Boltzmann brains might form in stable Minkowski vacua. Quantum fluctuations in Minkowski space are certainly less classical than in de Sitter space, but they still might be relevant. If $\Gamma_{\rm BB}$ is nonzero in such vacua, regardless of how small it might be, Boltzmann brains will always dominate in the scale-factor cutoff measure as we have defined it. Even if Minkowski vacua cannot support Boltzmann brains, there might still be a serious problem with what might be called "Boltzmann islands." That is, it is conceivable that a fluctuation in a Minkowski vacuum can produce a small region of an anthropic vacuum with a Boltzmann brain inside it. If such a process has a nonvanishing probability to occur, it will also give rise to Boltzmann brain domination in the scale-factor cutoff measure. These problems would be shared by all measures that assign an infinite weight to stable Minkowski vacua. Fortunately, the estimates of thermal Boltzmann brain nucleation rates in de Sitter space approach zero in the Minkowski space limit $\Lambda \to 0$, so the issue of Boltzmann brains formed by quantum fluctuations in Minkowski space can be set aside for later study. Hopefully the vague idea that these fluctuations are less classical than de Sitter space fluctuations can be promoted into a persuasive argument that they are not relevant.

5.3.2 Vacuum decay rates

One of the most developed approaches to the string landscape scenario is based on the KKLT construction [111]. In this construction, one begins by finding a set of stabilized supersymmetric AdS and Minkowski vacua. After that, an uplifting is performed, e.g. by adding a $\overline{D3}$ brane at the tip of a conifold [111]. This uplifting makes the vacuum energy density of some of these vacua positive (AdS $\to$ dS), but in general many vacua remain AdS, and the Minkowski vacuum corresponding to the uncompactified 10d space does not become uplifted. The enormous number of the vacua in the landscape appears because of the large number of different topologies of the compactified space, and the large number of different fluxes and branes associated with it.

There are many ways in which our low-energy dS vacuum may decay. First of all, it can always decay into the Minkowski vacuum corresponding to the uncompactified 10d space [111]. It can also decay to one of the AdS vacua corresponding to the same set of branes and fluxes [112]. More generally, decays occur due to the jumps between vacua with different fluxes, or due to the brane-flux annihilation [113, 114, 115, 116, 117, 118, 104, 119], and may be accompanied by a change in the number of compact dimensions [120, 121, 122]. If one does not take into account vacuum stabilization, these transitions are relatively easy to analyze [113, 114, 115]. However, in the realistic situations where the moduli fields are determined by fluxes, branes, etc., these transitions involve a simultaneous change of fluxes and various moduli fields, which makes a detailed analysis of the tunneling quite complicated.

Therefore, we begin with an investigation of the simplest decay modes due to the

scalar field tunneling. The transition to the 10d Minkowski vacuum was analyzed in Ref. [111], where it was shown that the decay rate κ is always greater than

$$\kappa \gtrsim e^{-S_D} = \exp\left(-\frac{24\pi^2}{V_{\rm dS}}\right) . \tag{5.107}$$

Here S_D is the entropy of dS space. For our vacuum, $S_D \sim 10^{120}$, which yields

$$\kappa \gtrsim e^{-S_D} \sim \exp\left(-10^{120}\right) . \tag{5.108}$$

Because of the inequality in Eq. (5.107), we expect the slowest-decaying vacua to typically be those with very small vacuum energies, with the dominant vacuum energy density possibly being much smaller than the value in our universe.

The decay to AdS space (or, more accurately, a decay to a collapsing open universe with a negative cosmological constant) was studied in Ref. [112]. The results of Ref. [112] are based on investigation of BPS and near-BPS domain walls in string theory, generalizing the results previously obtained in $\mathcal{N} = 1$ supergravity [123, 124, 125, 126]. Here we briefly summarize the main results obtained in Ref. [112].

Consider, for simplicity, the situation where the tunneling occurs between two vacua with very small vacuum energies. For the sake of argument, let us first ignore the gravitational effects. Then the tunneling always takes place, as long as one vacuum has higher vacuum energy than the other. In the limit when the difference between the vacuum energies goes to zero, the radius of the bubble of the new vacuum becomes infinitely large, $R \to \infty$ (the thin-wall limit). In this limit, the bubble wall becomes flat, and its initial acceleration, at the moment when the bubble forms, vanishes. Therefore to find the tension of the domain wall in the thin wall approximation one should solve an equation for the scalar field describing a static domain wall separating the two vacua.

If the difference between the values of the scalar potential in the two minima is too small, and at least one of them is AdS, then the tunneling between them may be forbidden because of the gravitational effects [6]. In particular, all supersymmetric vacua, including all KKLT vacua prior to the uplifting, are absolutely stable even if other vacua with lower energy density are available [127, 128, 129, 130].

It is tempting to make a closely related but opposite statement: non-supersymmetric vacua are always unstable. However, this is not always the case. In order to study tunneling while taking account of supersymmetry (SUSY), one may start with two different supersymmetric vacua in two different parts of the universe and find a BPS domain wall separating them. One can show that if the superpotential does not change its sign on the way from one vacuum to the other, then this domain wall plays the same role as the flat domain wall in the no-gravity case discussed above: it corresponds to the wall of the bubble that can be formed once the supersymmetry is broken in either of the two minima. However, if the superpotential does change its sign, then only a sufficiently large supersymmetry breaking will lead to the tunneling [123, 112].

One should keep this fact in mind, but since we are discussing a landscape with an

extremely large number of vacua, in what follows we assume that there is at least one direction in which the superpotential does not change its sign on the way from one minimum to another. In what follows we describe tunneling in one such direction. Furthermore, we assume that at least some of the AdS vacua to which our dS vacuum may decay are uplifted much less than our vacuum. This is a generic situation, since the uplifting depends on the value of the volume modulus, which takes different values in each vacuum.

In this case the decay rate of a dS vacuum with low energy density and broken supersymmetry can be estimated as follows [112, 131]:

$$\kappa \sim \exp\left(-\frac{8\pi^2\alpha}{3m_{3/2}^2}\right) , \tag{5.109}$$

where $m_{3/2}$ is the gravitino mass in that vacuum and α is a quantity that depends on the parameters of the potential. Generically one can expect $\alpha = \mathcal{O}(1)$, but it can also be much greater or much smaller than $\mathcal{O}(1)$. The mass $m_{3/2}$ is set by the scale of SUSY breaking,

$$3m_{3/2}^2 = \Lambda_{\rm SUSY}^4 , \tag{5.110}$$

where we recall that we use reduced Planck units, $8\pi G = 1$. Therefore the decay rate can be also represented in terms of the SUSY-breaking scale $\Lambda_{\rm SUSY}$:

$$\kappa \sim \exp\left(-\frac{24\pi^2\alpha}{\Lambda_{\rm SUSY}^4}\right) , \tag{5.111}$$

Note that in the KKLT theory, $\Lambda_{\rm SUSY}^4$ corresponds to the depth of the AdS vacuum before the uplifting, so that

$$\kappa \sim \exp\left(-\frac{24\pi^2\alpha}{|V_{\rm AdS}|}\right) . \tag{5.112}$$

In this form, the result for the tunneling looks very similar to the lower bound on the decay rate of a dS vacuum, Eq. (5.107), with the obvious replacements $\alpha \to 1$ and $|V_{\rm AdS}| \to V_{\rm dS}$.

Let us apply this result to the question of vacuum decay in our universe. Clearly, the implications of Eq. (5.111) depend on the details of SUSY phenomenology. The standard requirement that the gaugino mass and the scalar masses are $\mathcal{O}(1)$ TeV leads to the lower bound

$$\Lambda_{\rm SUSY} \gtrsim 10^4\text{–}10^5 \text{ GeV} , \tag{5.113}$$

which can be reached, e.g., in the models of conformal gauge mediation [132]. This implies that for our vacuum

$$\kappa_{\rm our} \gtrsim \exp(-10^{56})\text{–}\exp(-10^{60}) . \tag{5.114}$$

Using Eq. (5.85), the Boltzmann brain nucleation rate in our universe exceeds the lower bound of the above inequality only if $M \lesssim 10^{-9}$ kg.

On the other hand, one can imagine universes very similar to ours except with much larger vacuum energy densities. The vacuum decay rate of Eq. (5.109) exceeds the Boltzmann brain nucleation rate of Eq. (5.85) when

$$\left(\frac{m_{3/2}}{10^{-2}\ \mathrm{eV}}\right)^2 \left(\frac{M}{1\ \mathrm{kg}}\right) \left(\frac{H_\Lambda^{-1}}{10^8\ \mathrm{m}}\right) \gtrsim 10^9 \alpha\,. \tag{5.115}$$

Note that $H_\Lambda^{-1} \sim 10^8$ m corresponds to the smallest de Sitter radius for which the tidal force on a 10 cm brain does not exceed the gravitational force on the surface of the earth, while $m_{3/2} \sim 10^{-2}$ eV corresponds to $\Lambda_{\mathrm{SUSY}} \sim 10^4$ GeV. Thus, it appears the decay rate of Eq. (5.109) allows for Boltzmann brain domination.

However, we do not really know whether the models with low Λ_{SUSY} can successfully describe our world. To mention one potential problem: in models of string inflation there is a generic constraint that during the last stage of inflation one has $H \lesssim m_{3/2}$ [133]. If we assume the second and third factors of Eq. (5.115) cannot be made much less than unity, then we only require $m_{3/2} \gtrsim \mathcal{O}(10^2)$ eV to avoid Boltzmann brain domination. While models of string inflation with $H \lesssim 100$ eV are not entirely impossible in the string landscape, they are extremely difficult to construct [134]. If instead of $\Lambda_{\mathrm{SUSY}} \sim 10^4$ GeV one uses $\Lambda_{\mathrm{SUSY}} \sim 10^{11}$ GeV, as in models with gravity mediation, one finds $m_{3/2} \sim 10^3$ GeV and Eq. (5.115) is easily satisfied.

These arguments apply when supersymmetry violation is as large or larger than in our universe. If supersymmetry violation is too small, atomic systems are unstable [135], the masses of some of the particles will change dramatically, etc. However, the Boltzmann computers described in the previous subsection do not necessarily rely on laws of physics similar to those in our universe (in fact, they seem to require very different laws of physics). The present authors are unaware of an argument that supersymmetry breaking must be so strong that vacuum decay is always faster than the Boltzmann brain production rate of Eq. (5.104).

On the other hand, up to this point we have used the estimates of the vacuum decay rate that were obtained in Refs. [112, 131] by investigation of the transition where only moduli fields changed. As we have already mentioned, the description of a more general class of transitions involving the change of branes or fluxes is much more complicated. Investigation of such processes, performed in Refs. [116, 117, 104], indicates that the process of vacuum decay for any vacuum in the KKLT scenario should be rather fast,

$$\kappa \gtrsim \exp(-10^{22})\,. \tag{5.116}$$

The results of Refs. [116, 117, 104], like the results of Refs. [112, 131], are not completely generic. In particular, the investigations of Refs. [116, 117, 104] apply to the original version of the KKLT scenario, where the uplifting of the AdS vacuum occurs due to $\overline{D3}$ branes, but not to its generalization proposed in Ref. [136], where the uplifting is achieved due to D7 branes. Neither does it apply to the recent version of dS stabilization proposed in Ref. [137]. Nevertheless, the results of Refs. [116, 117, 104] show that the decay rate of dS vacua in the landscape can be quite large. The rate $\kappa \gtrsim \exp(-10^{22})$ is much greater than the expected rate of Boltzmann brain production

given by Eq. (5.91). However, it is just a bit smaller than the bosonic gas Boltzmann brain production rate of Eq. (5.105) and much smaller than our most dangerous upper bound on the Boltzmann brain production rate, given by Eq. (5.104).

5.4 Conclusions

In this Chapter, we have calculated the ratio of the total number of Boltzmann brains to the number of normal observers, using the scale-factor cutoff.

The general conditions under which Boltzmann brain domination is avoided were discussed in Subsection 5.2.6, where we described several alternative criteria that can be used to ensure safety from Boltzmann brains. We also explored a set of assumptions that allow one to state conditions that are both necessary and sufficient to avoid Boltzmann brain domination. One relatively simple way to ensure safety from Boltzmann brains is to require two conditions: (1) in any vacuum, the Boltzmann brain nucleation rate must be less than the decay rate of that vacuum, and (2) for any anthropic vacuum j with a decay rate $\kappa_j \approx q$, and for any non-anthropic vacuum j, one must construct a sequence of transitions from j to an anthropic vacuum; if the sequence includes suppressed upward jumps, then the Boltzmann brain nucleation rate in vacuum j must be less than the decay rate of vacuum j times the product of all the suppressed branching ratios $B_{\rm up}$ that appear in the sequence. The condition (2) might not be too difficult to satisfy, since it will generically involve only states with very low vacuum energy densities, which are likely to be nearly supersymmetric and therefore unlikely to support the complex structures needed for Boltzmann brains or normal observers. Condition (2) can also be satisfied if there is no unique dominant vacuum, but instead a dominant vacuum system that consists of a set of nearly degenerate states, some of which are anthropic, which undergo rapid transitions to each other, but only slow transitions to other states. The condition (1) is perhaps more difficult to satisfy. Although nearly-supersymmetric string vacua can in principle be long-lived [123, 124, 125, 126, 111, 112], with decay rates possibly much smaller than the Boltzmann brain nucleation rate, recent investigations suggest that other decay channels may evade this problem [116, 117, 104]. However, the decay processes studied in [123, 124, 125, 126, 111, 112, 116, 117, 104] do not describe some of the situations which are possible in the string theory landscape, and the strongest constraints on the decay rate obtained in [104] are still insufficient to guarantee that the vacuum decay rate is always smaller than the fastest estimate of the Boltzmann brain production rate, Eq. (5.104).

One must emphasize that we are discussing a rapidly developing field of knowledge. Our estimates of the Boltzmann brain production rate are exponentially sensitive to our understanding of what exactly the Boltzmann brain is. Similarly, the estimates of the decay rate in the landscape became possible only five years ago, and this subject certainly is going to evolve. Therefore we shall mention here two logical possibilities which may emerge as a result of the further investigation of these issues.

If further investigation will demonstrate that the Boltzmann brain production rate is always smaller than the vacuum decay rate in the landscape, the probability

measure that we are investigating in this Chapter will be shown not to suffer from the Boltzmann brain problem. Conversely, if one believes that this measure is correct, the fastest Boltzmann brain production rate will give us a rather strong lower bound on the decay rate of the metastable vacua in the landscape. We expect that similar conclusions with respect to the Boltzmann brain problem should be valid for the causal-patch measures [16, 17].

On the other hand, if we do not find a sufficiently convincing theoretical reason to believe that the vacuum decay rate in all vacua in the landscape is always greater than the fastest Boltzmann brain production rate, this would motivate the consideration of other probability measures where the Boltzmann brain problem can be solved even if the probability of their production is not strongly suppressed.

In any case, our present understanding of the Boltzmann brain problem does not rule out the scale-factor cutoff measure, but the situation remains uncertain.

Chapter 6

Conclusions

Inflation is generically eternal, with the physical volume of inflating regions increasing exponentially with time and "bubble universes" like ours constantly nucleating out of the inflating false vacuum. The problem of defining a consistent way to regulate the infinities in an eternally inflating multiverse is known as the measure problem, which has been the subject of this thesis. We have introduced our proposal, the scale-factor cutoff measure, and studied some of its properties and consequences. We shall now summarize what we have learned about this measure.

First of all we have shown that the scale-factor cutoff does not suffer from pathologies that plague other proposed measures, namely the "youngness problem" and the "Q catastrophe".

Then we turned to calculate the probability distributions for two quantities varying in the multiverse: the cosmological constant and the curvature parameter. For $\Lambda > 0$, we adopted the standard assumption that the number of observers is proportional to the fraction of matter clustered in halos of mass greater than $10^{12} M_{\odot}$, and allowed a fixed proper time interval $\Delta\tau = 5 \times 10^9$ years for the evolution of observers in such halos. For $\Lambda < 0$, we considered two possibilities for the formation of observers in the contracting phase, which probably bracket the range of reasonable possibilities. Our results show that, the observed value of Λ is within one or two standard deviations from the mean, depending on the assumptions for the formation of observers in negative-Λ universes, and whether one uses the local or the nonlocal version of the scale-factor cutoff. We have verified that our results are robust with respect to changing the parameters M_G and $\Delta\tau$. As for the curvature parameter Ω_k, one of the features of the scale-factor cutoff measure is that it does not reward bubbles for having a longer duration of slow-roll inflation. This raises the possibility that N_e may not be too much larger than is needed to pave the way for structure formation, and therefore that Ω_k^0 may be large enough to distinguish from the value expected from cosmic variance, $\sim 10^{-5}$.

Finally, we have addressed the theoretical issue of avoiding an unacceptable domination of Boltzmann brains over normal observers. We have calculated the ratio of the total number of Boltzmann brains to the number of normal observers, using the scale-factor cutoff and stated the general conditions under which Boltzmann brain domination is avoided. We also explored a set of assumptions that allow one

to state conditions that are both necessary and sufficient to avoid Boltzmann brain domination.

We believe the scale-factor cutoff measure is a promising candidate solution to one of the fundamental issues of theoretical cosmology.

Appendix A

Independence of the Initial State

In Chapter 3 we assumed that the landscape is irreducible, so that any vacuum is accessible through quantum diffusion or bubble nucleation from any other (de Sitter) vacuum. If instead the landscape splits into several disconnected sectors, the scale-factor cutoff can be used to find the probability distributions $P_j^{(A)}$ in each of the sectors (labeled by A). These distributions are determined by the dominant eigenstates of the master equation, which correspond to the largest eigenvalues γ_A, and are independent of the choice of the initial hypersurfaces Σ_A that are used in implementing the scale-factor cutoff. But the question still remains, how do we compare the probabilities of vacua belonging to different sectors?

Since different sectors are inaccessible from one another, the probability P_A of being in a given sector must depend on the initial state of the universe. For definiteness, we shall assume here that the initial state is determined by the wave function of the universe, although most of the following discussion should apply to any theory of initial conditions. According to both tunneling [138] and Hartle-Hawking [139] proposals for the wave function, the universe starts as a 3-sphere S_α filled with some positive-energy vacuum α. The radius of the 3-sphere is $r_\alpha = H_\alpha^{-1}$, where H_α is the de Sitter expansion rate. The corresponding nucleation probability is

$$P_{\rm nucl}^{(\alpha)} \propto \exp\left(\pm\frac{\pi}{H_\alpha^2}\right), \tag{A.1}$$

where the upper sign is for the Hartle-Hawking and the lower is for the tunneling wave function. Once the universe has nucleated, it immediately enters de Sitter inflationary expansion, transitions from α to other vacua, and populates the entire sector of the landscape to which the vacuum α belongs. We thus have an ensemble of eternally inflating universes with initial conditions at 3-surfaces S_α and the probability distribution $P_{\rm nucl}^{(\alpha)}$ given by Eq. (A.1).

If the landscape were not disconnected, we could apply the scale factor cutoff measure to any single component α of the initial wave function, and the result would be the same in all cases. To generalize the scale-factor cutoff measure to the disconnected landscape, the most straightforward prescription is to apply the scale factor

cutoff directly to the initial probability ensemble. In that case,

$$P_{j,A} \propto \lim_{t_c \to \infty} \sum_{\alpha \in A} P^{(\alpha)}_{\rm nucl} \mathcal{N}^{(\alpha)}_j(t_c)\,. \tag{A.2}$$

Here,

$$\mathcal{N}^{(\alpha)}_j(t_c) = R^{(A)}_\alpha P^{(A)}_j e^{\gamma_A t_c} \tag{A.3}$$

is the number of relevant observations in the entire closed universe, starting from the hypersurface S_α, with a cutoff at scale-factor time t_c. The $R^{(A)}_\alpha$ are determined by the initial volume of the 3-surface S_α, and also by the efficiency with which this initial state couples to the leading eigenvector of Eq. (2.16). In other words, the $\mathcal{N}^{(\alpha)}_j(t_c)$ are calculated using S_α as the initial hypersurface Σ_A. Note that only the overall normalization of $\mathcal{N}^{(\alpha)}_j$ depends on the initial vacuum α; the relative probabilities of different vacua in the sector do not. In the limit of $t_c \to \infty$, only the sectors corresponding to the largest of all dominant eigenvalues, $\gamma_{\rm max} = \max\{\gamma_A\}$, have a nonzero probability. If there is only one sector with this eigenvalue, this selects the sector uniquely.

Since the issue of initial state dependence is new, one might entertain an alternative method of dealing with the issue, in which the probability P_A for each sector is determined immediately by the initial state, with

$$P_A \propto \sum_{\alpha \in A} P^{(\alpha)}_{\rm nucl}\,. \tag{A.4}$$

Then one could calculate any probability of interest within each sector, using the standard scale factor cutoff method, and weight the different sectors by P_A. However, although this prescription is well-defined, we would advocate the first method that we described as the natural extension of the scale factor cutoff measure. First, it seems to be more closely related to the description of the scale-factor cutoff measure in a connected landscape: the only change is to replace the initial state by an ensemble of states, determined in principle by one's theory of the initial wave function. Second, in a toy theory, one could imagine approaching a disconnected landscape from a connected one, by gradually decreasing all the cross-sector tunneling rates to zero. In that case, the limit clearly corresponds to the first description, where one sector is selected uniquely if it has the largest dominant eigenvalue.

Assuming the first of these prescriptions, the conclusion is that the probability distribution (A.2) defined by the scale-factor measure is essentially independent of the initial distribution (A.1). Some dependence on $P^{(\alpha)}_{\rm nucl}$ survives only in a restricted class of models where the landscape splits into a number of sectors with strictly zero probability of transitions between them and, in addition, where the maximum eigenvalue $\gamma_{\rm max}$ is degenerate. Even then, this dependence is limited to the relative probability of the sectors characterized by the eigenvalue $\gamma_{\rm max}$.

Appendix B

The Collapse Density Threshold δ_C

The collapse density threshold δ_c is determined by comparing the linearized evolution of matter perturbations with the nonlinear evolution of a spherical top-hat density perturbation, which can be treated as a closed FRW universe. The collapse density threshold $\delta_c(\tau)$ is defined as the amplitude reached by the linear evolution of an overdensity $\delta \equiv \delta\rho_m/\rho_m$ that has the same initial amplitude as a top-hat density perturbation that collapses to a singularity in proper time τ. In a matter-dominated universe with zero cosmological constant, δ_c is a constant; however, it is well known that δ_c depends on the collapse time when Λ is nonzero (see e.g. Refs. [66, 67]). In this appendix we first outline the calculation of the time evolution of δ_c, then display the results for positive and negative Λ, and finally describe how we apply it in our analysis of the collapse fraction F of Eq. (3.7).

As suggested by the definition above, both linear and nonlinear analyses are involved at different stages of the calculation of the collapse density. Arbitrarily small perturbations obey linearized equations of motion, and their evolution defines the linear growth function $G_\Lambda(\tau)$:

$$\delta(\tau) \propto G_\Lambda(\tau)\,, \tag{B.1}$$

where $G_\Lambda(\tau)$ is normalized so that the behavior for small τ is given by $G_\Lambda(\tau) \sim (3H_\Lambda\tau/2)^{2/3}$, where $H_\Lambda = \sqrt{|\Lambda|/3}$. The exact nonlinear analysis is used to determine the time at which an overdensity with a given initial amplitude will collapse to a singularity. For simplicity, this is worked out for the "top-hat" model, where the overdensity is assumed to be uniform and spherically symmetric. Such a region is embedded in a flat FRW universe containing only non-relativistic matter and cosmological constant.

By Birkhoff's theorem, the evolution of the spherical overdensity is equivalent to that of a closed FRW universe. The Friedmann equation for a closed FRW universe, with scale factor a, may be written as:

$$H^2 = H_\Lambda^2\left[\mathrm{sign}(\Lambda) + \frac{B(\kappa)}{a^3} - \frac{\kappa}{a^2}\right], \tag{B.2}$$

where $H = d\ln a/d\tau = \dot{a}/a$ and $B(\kappa)$ is an arbitrary quantity that fixes the nor-

malization of a. We will always choose $B(0) = 1$, so for $\kappa = 0$ the scale factor is normalized in such a way that $\rho_m = |\rho_\Lambda|$ at $a = 1$, where $\rho_\Lambda = \Lambda/(8\pi)$ is the vacuum energy density.

Let us first focus our attention on the evolution of a linearized density perturbation in a flat FRW universe with positive cosmological constant; the case with negative cosmological constant proceeds similarly. Consider a closed FRW universe obtained by "perturbing" the flat universe with a small curvature term $\delta\kappa$. The proper time parameter $\hat{\tau}$ in such a universe, as a function of the scale factor, is given by an expansion with respect to the flat background: $\hat{\tau}(a) = \tau(a) + \delta\tau(a)$, where to linear order in $\delta\kappa$

$$\delta\tau(a) = \frac{\delta\kappa}{2H_\Lambda} \int_0^a \frac{\sqrt{a'}\left[a' - \frac{dB}{d\kappa}(0)\right] da'}{(1 + a'^3)^{3/2}} \,. \tag{B.3}$$

The scale factor of the closed universe is obtained by inverting the function $\hat{\tau}(a)$:

$$\hat{a}(\tau) = a(\tau) - \dot{a}(\tau)\, \delta\tau(a(\tau)) \,. \tag{B.4}$$

As mentioned above, the evolution of this closed FRW universe also gives the evolution of a small density perturbation. Using $\rho_m = (3/8\pi)H_\Lambda^2 B(\kappa)/a^3$, one has

$$\delta = \frac{\delta\rho_m}{\rho_m} = -3\frac{\delta a}{a} + \frac{dB}{d\kappa}(0) = 3H\delta\tau + \frac{dB}{d\kappa}(0) \,, \tag{B.5}$$

where the last equality follows from Eq. (B.4). From here on, unless noted otherwise, we normalize a so that $B(\kappa) = 1$. It is convenient to introduce the "time" variable

$$x \equiv \frac{|\rho_\Lambda|}{\rho_m} = a^3 \,, \tag{B.6}$$

for both choices of the sign of Λ. To be consistent with Eq. (B.2), the solutions for $\kappa = 0$ are not normalized as in Eq. (3.4), but instead are given by

$$a(\tau) = \begin{cases} \sinh^{2/3}(\frac{3}{2}H_\Lambda\tau) & \text{for } \Lambda > 0 \\ \sin^{2/3}(\frac{3}{2}H_\Lambda\tau) & \text{for } \Lambda < 0 \,. \end{cases} \tag{B.7}$$

We can then find the evolution function $\delta(x)$ from Eq. (B.5), using Eq. (B.3) and also Eq. (B.2) with $\kappa = 0$:

$$\begin{aligned} \delta(x) &= \frac{1}{2}\delta\kappa\sqrt{1 + \frac{1}{x}} \int_0^x \frac{dy}{y^{1/6}(1+y)^{3/2}} \\ &= \frac{3}{5}\,\delta\kappa\, G^+(x) \,, \end{aligned} \tag{B.8}$$

where the linear growth function (for $\Lambda > 0$),

$$G^+(x) = \frac{5}{6}\sqrt{1+\frac{1}{x}}\int_0^x \frac{dy}{y^{1/6}(1+y)^{3/2}}\,, \tag{B.9}$$

is normalized so that the behavior for small x is given by $G^+(x) \sim x^{1/3} = a \sim (3H_\Lambda\tau/2)^{2/3}$.

In the $\Lambda < 0$ case, the calculation proceeds along the same steps as before and the formula (B.8) is indeed valid also for negative Λ, after replacing the growth function with $G^-(x)$. This function now has two branches $G^-_{\rm I}(x)$ and $G^-_{\rm II}(x)$, corresponding to the expanding and contracting phases of the universe, respectively. The first branch of the growth function introduces no new complications, and is found to be

$$G^-_{\rm I}(x) = \frac{5}{6}\sqrt{\frac{1}{x}-1}\int_0^x \frac{dy}{y^{1/6}(1-y)^{3/2}}\,. \tag{B.10}$$

For the second branch, the integration is first performed over the whole history of the universe, from $x = 0$ to $x = 1$ and back to $x = 0$, and then one integrates back to the value of interest x. There is a complication, however, because for this case the denominator in Eq. (B.3) is $(1-a'^3)^{3/2}$, so the integral diverges when the upper limit is equal to 1. The cause of the problem is that for $\delta\kappa \neq 0$, $a_{\rm max}$ is no longer equal to 1. A simple cure is to choose $B(\kappa) = 1+\kappa$ for this case, which ensures that $a_{\rm max} = 1$ for any κ, and which correspondingly provides an additional term in Eq. (B.3) which causes the integral to converge. After some manipulation of the integrals, the result can be written as

$$G^-_{\rm II}(x) = \frac{5}{6}\sqrt{\frac{1}{x}-1}\left[\frac{4\sqrt{\pi}\,\Gamma\left(\frac{5}{6}\right)}{\Gamma\left(\frac{1}{3}\right)} + \int_0^x \frac{dy}{y^{1/6}(1-y)^{3/2}}\right]. \tag{B.11}$$

The time dependence of the linear growth functions can be made explicit by expressing x as a function of τ, through Eqs. (B.6) and (B.7).

In practice, we carry out our calculations using fitting functions for the growth functions, which were devised by Peacock [61], and which are accurate to better than 0.1%. These give

$$\begin{aligned} G^+_\Lambda(\tau) &\simeq \tanh^{2/3}(\tfrac{3}{2}H_\Lambda\tau)\Big[1-\tanh^{1.27}(\tfrac{3}{2}H_\Lambda\tau)\Big]^{0.82} \\ &\quad +1.437\,H_\Lambda^{-2/3}\Big[1-\cosh^{-4/3}(\tfrac{3}{2}H_\Lambda\tau)\Big] \qquad \text{(B.12)} \\ G^-_\Lambda(\tau) &\simeq (\tfrac{3}{2}H_\Lambda\tau)^{2/3}\left[1+0.37\,(\tau/\tau_{\rm crunch})^{2.18}\right]^{-1}\left[1-(\tau/\tau_{\rm crunch})^2\right]^{-1}\,, \qquad \text{(B.13)} \end{aligned}$$

for the cases $\Lambda > 0$ and $\Lambda < 0$, respectively, where the latter fitting formula is valid for both branches.

We are now prepared to set the calculation of δ_c. Since the universe in Eq. (B.2)

can be viewed as a "perturbation" over a flat universe with $\delta\kappa = \kappa$, the time evolution of the overdensity is described in general by

$$\delta(\tau) = \frac{3}{5}\kappa\, G_\Lambda(\tau)\,. \tag{B.14}$$

The quantity $(3/5)\kappa\, a$ quantifies the size of the initial inhomogeneity.

In order to find the time at which the spherical overdensity collapses, it is convenient to determine the time of turnaround $\tau_{\rm turn}$, corresponding to when $H = 0$. The time of collapse is then given by $2\,\tau_{\rm turn}$. The turnaround time is obtained by integrating Eq. (B.2), choosing $B = 1$:

$$H_\Lambda \tau_{\rm turn}(\kappa) = \int_0^{a_{\rm turn}(\kappa)} \frac{\sqrt{a}\, da}{\sqrt{{\rm sign}(\Lambda)\, a^3 - \kappa\, a + 1}}\,, \tag{B.15}$$

where the scale factor at turnaround $a_{\rm turn}$ corresponds to the smallest positive solution of

$${\rm sign}(\Lambda)\, a_{\rm turn}^3 - \kappa\, a_{\rm turn} + 1 = 0\,. \tag{B.16}$$

For positive Λ, the universe will collapse only if $\kappa > \kappa_{\rm min} \equiv 3/2^{2/3}$; for negative Λ, perturbations that collapse before the universe has crunched have $\kappa > 0$.

The numerical evaluation of the integral in Eq. (B.15) allows one the extract the function $\tau_{\rm turn}(\kappa)$, which can be inverted to give $\kappa_{\rm turn}(\tau)$, expressing the value of κ that leads to turnaround at time τ. Finally, the collapse density threshold as a function of the time of collapse is read from Eq. (B.14):

$$\delta_c(\tau) = \frac{3}{5}\kappa_{\rm turn}(\tau/2)\, G_\Lambda(\tau)\,. \tag{B.17}$$

In the limits of small and large collapse times the above procedure can be carried out analytically to find the limiting values of δ_c. Let us consider first the large-time regime, corresponding to small κ. In the case $\Lambda > 0$, the smallest κ allowed is $\kappa_{\rm min}$; therefore

$$\delta_c^+(\infty) = \frac{3}{5}\kappa_{\rm min}\, G_\Lambda^+(\infty) \simeq 1.629\,, \tag{B.18}$$

where $G_\Lambda^+(\infty) = G^+(\infty) = 5\Gamma(2/3)\Gamma(5/6)/(3\sqrt{\pi}) \simeq 1.437$. The case $\Lambda < 0$ is a little more complicated. The collapse time cannot exceed $\tau_{\rm crunch} = 2\pi/3H_\Lambda$, corresponding to $\kappa = 0$. At small κ, the integral in Eq. (B.15) is expanded to give

$$H_\Lambda \tau_{\rm turn}(\kappa) \simeq \frac{1}{2} H_\Lambda \tau_{\rm crunch} - \frac{2}{5}\frac{\sqrt{\pi}\Gamma\left(\frac{11}{6}\right)}{\Gamma\left(\frac{1}{3}\right)}\,\kappa\,. \tag{B.19}$$

On the other hand, the growth function $G^-(\tau)$ in the neighborhood of $\tau_{\rm crunch}$ behaves

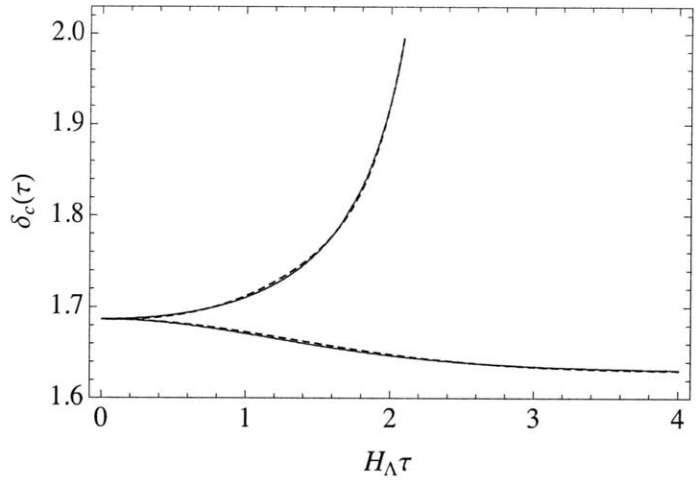

Figure B-1: The collapse density thresholds δ_c^+ (for $\Lambda > 0$) and δ_c^- (for $\Lambda < 0$), as functions of time. The solid curves represent numerical evaluations of $\delta_c^\pm$, while the dashed curves correspond to the fitting functions in Eq. (B.23). Note that δ_c^+ decreases with time, while δ_c^- increases with time.

as

$$G_\Lambda^-(\tau \approx \tau_{\rm crunch}) \simeq \frac{10}{3} \frac{\Gamma\left(\frac{5}{6}\right)}{\sqrt{\pi}\Gamma\left(\frac{1}{3}\right)} \frac{1}{(1-\tau/\tau_{\rm crunch})}\,. \tag{B.20}$$

After using Eqs. (B.19) and (B.20) in the general formula (B.17), we simply get

$$\delta_c^-(\tau_{\rm crunch}) = 2\,. \tag{B.21}$$

In the opposite regime $H_\Lambda \tau \ll 1$, corresponding to large κ, the growth functions are $G_\Lambda^\pm(\tau) \simeq a(\tau) \simeq (3H_\Lambda \tau/2)^{2/3}$. The integral (B.15) can be analytically solved in this limit: $H_\Lambda \tau_{\rm turn}(\kappa) = \pi/(2\kappa^{3/2})$. Combining these results leads to

$$\delta_c^\pm(0) \;=\; \frac{3}{5}\left(\frac{3\pi}{2}\right)^{2/3} \simeq 1.686\,, \tag{B.22}$$

which is also the constant value of δ_c in a $\Lambda = 0$ universe.

The time dependence of δ_c is displayed in Fig. B-1, for both positive and negative values of Λ. We also display the following simple fitting functions,

$$\begin{aligned}
\delta_c^+(\tau) &= 1.629 + 0.057\, e^{-0.28 H_\Lambda^2 \tau^2} \\
\delta_c^-(\tau) &= 1.686 + 0.165\left(\frac{\tau}{\tau_{\rm crunch}}\right)^{2.5} + 0.149\left(\frac{\tau}{\tau_{\rm crunch}}\right)^{11}
\end{aligned} \tag{B.23}$$

which are accurate to better than 0.2%. Although we choose to include the effect of

the time evolution of δ_c, our results are not significantly changed by treating δ_c as a constant. This is easy to understand. First of all, δ_c^+ varies by only about 3%. The evolution of δ_c^- is more significant, about 15%, and most of this happens at very late times. But our anthropic weight in Eq. (3.3) never samples δ_c^- within a time $\Delta\tau$ of $\tau_{\rm crunch}$.

Finally, we point out that the appearance of $G_\Lambda(\tau)$ in this discussion is not needed for the calculation, and appears here primarily to make contact with other work. From Eq. (3.7) one sees that the collapse fraction depends only on the ratio of $\delta_c(\tau)/\sigma(M_G,\tau)$, which from Eqs. (3.8) and (B.17) can be seen to equal (3/5) $\kappa_{\rm turn}(\tau/2)/\bar{\sigma}(M_G)$. Expressed in this way, Eq. (3.7) becomes fairly transparent. Since κ is a measure of the amplitude of an initial perturbation, Eq. (3.7) is saying that the collapse fraction at time τ depends precisely on the magnitude required for an initial top-hat perturbation to collapse by time τ. In more detail, Eq. (3.7) is predicated on a Gaussian distribution of initial fluctuations, where the complementary error function erfc(x) is the integral of a Gaussian. The collapsed fraction at time τ is given by the probability, in this Gaussian approximation, for the initial fluctuations to exceed the magnitude needed for collapse at time τ. From a practical point of view, the use of $G_\Lambda(\tau)$ in the discussion of the collapse fraction can be a helpful simplification if one uses the approximation that $\delta_c \approx$ const. We have not used this approximation, but as described above, our results would not be much different if we had. We have maintained the discussion in terms of $G_\Lambda(\tau)$ to clarify the relationship between our work and this approximation.

Appendix C

Boltzmann Brains in Schwarzschild–de Sitter Space

As explained in Subsection 5.3.1, Eq. (5.86) for the production rate of Boltzmann brains must be reexamined when the Boltzmann brain radius becomes comparable to the de Sitter radius. In this case we need to describe the Boltzmann brain nucleation as a transition from an initial state of empty de Sitter space with horizon radius H_Λ^{-1} to a final state in which the dS space is altered by the presence of an object with mass M. Assuming that the object can be treated as spherically symmetric, the space outside the object is described by the Schwarzschild–de Sitter (SdS) metric [140]:[1]

$$\begin{aligned} ds^2 &= -\left(1-\frac{2GM}{r}-H_\Lambda^2 r^2\right) dt^2 \\ &\quad +\left(1-\frac{2GM}{r}-H_\Lambda^2 r^2\right)^{-1} dr^2 + r^2\, d\Omega^2 \,. \end{aligned} \tag{C.1}$$

The SdS metric has two horizons, determined by the positive zeros of g_{tt}, where the smaller and larger are called $R_{\rm Sch}$ and $R_{\rm dS}$, respectively. We assume the Boltzmann brain is stable but not a black hole, so its radius satisfies $R_{\rm Sch} < R < R_{\rm dS}$. The radii of the two horizons are given by

$$\begin{aligned} R_{\rm Sch} &= \frac{2}{\sqrt{3}\,H_\Lambda}\cos\left(\frac{\pi+\xi}{3}\right), \\ R_{\rm dS} &= \frac{2}{\sqrt{3}\,H_\Lambda}\cos\left(\frac{\pi-\xi}{3}\right), \end{aligned} \tag{C.2}$$

where

$$\cos\xi = 3\sqrt{3}\,GMH_\Lambda \,. \tag{C.3}$$

[1] We restore $G = 1/8\pi$ in this Appendix for clarity.

This last equation implies that for a given value of H_Λ, there is an upper limit on how much mass can be contained within the de Sitter horizon:

$$M \leq M_{\max} = (3\sqrt{3}GH_\Lambda)^{-1} . \tag{C.4}$$

Eqs. (C.2) and (C.3) can be inverted to express M and H_Λ in terms of the horizon radii:

$$\frac{1}{H_\Lambda^2} = R_{\rm Sch}^2 + R_{\rm dS}^2 + R_{\rm Sch}R_{\rm dS} \tag{C.5}$$

$$M = \frac{R_{\rm dS}}{2G}\left(1 - H_\Lambda^2 R_{\rm dS}^2\right) \tag{C.6}$$

$$= \frac{R_{\rm Sch}}{2G}\left(1 - H_\Lambda^2 R_{\rm Sch}^2\right) . \tag{C.7}$$

We relate the Boltzmann brain nucleation rate to the decrease in total entropy ΔS caused by the the nucleation process,

$$\Gamma_{\rm BB} \sim e^{-\Delta S} , \tag{C.8}$$

where the final entropy is the sum of the entropies of the Boltzmann brain and the de Sitter horizon. For a Boltzmann brain with entropy $S_{\rm BB}$, the change in entropy is given by

$$\Delta S = \frac{\pi}{G}H_\Lambda^{-2} - \left(\frac{\pi}{G}R_{\rm dS}^2 + S_{\rm BB}\right) . \tag{C.9}$$

Note that for small M one can expand ΔS to find

$$\Delta S = \frac{2\pi M}{H_\Lambda} - S_{\rm BB} + \mathcal{O}(GM^2) , \tag{C.10}$$

giving a nucleation rate in agreement with Eq. (5.86).

To find a bound on the nucleation rate, we need an upper bound on the entropy that can be attained for a given size and mass. In flat space the entropy is believed to be bounded by Bekenstein's formula, Eq. (5.93), a bound which should also be applicable whenever $R \ll R_{\rm dS}$. More general bounds in de Sitter space have been discussed by Bousso [103], who considers bounds for systems that are allowed to fill the de Sitter space out to the horizon $R = R_{\rm dS}$ of an observer located at the origin. For small mass M, Bousso argues that the tightest known bound on S is the D-bound, which states that

$$S \leq S_{\rm D} \equiv \frac{\pi}{G}\left(\frac{1}{H_\Lambda^2} - R_{\rm dS}^2\right) = \frac{\pi}{G}\left(R_{\rm Sch}^2 + R_{\rm Sch}R_{\rm dS}\right) , \tag{C.11}$$

where the equality of the two expressions follows from Eq. (C.5). This bound can be obtained from the principle that the total entropy cannot increase when an object disappears through the de Sitter horizon. For larger values of M, the tightest bound

(for $R = R_{\rm dS}$) is the holographic bound, which states that

$$S \leq S_{\rm H} \equiv \frac{\pi}{G} R_{\rm dS}^2 \,. \tag{C.12}$$

Bousso suggests the possibility that these bounds have a common origin, in which case one would expect that there exists a valid bound that interpolates smoothly between the two. Specifically, he points out that the function

$$S_{\rm m} \equiv \frac{\pi}{G} R_{\rm Sch} R_{\rm dS} \tag{C.13}$$

is a candidate for such a function. Fig. (C-1) shows a graph of the holographic bound, the D-bound, and the m-bound (Eq. (C.13)) as a function of $M/M_{\rm max}$. While there is no reason to assume that $S_{\rm m}$ is a rigorous bound, it is known to be valid in the extreme cases where it reduces to the D– and holographic bounds. In between it might be valid, but in any case it can be expected to be valid up to a correction of order one. In fact, Fig. (C-1) and the associated equations show that the worst possible violation of the m-bound is at the point where the holographic and D–bounds cross, at $M/M_{\rm max} = 3\sqrt{6}/8 = 0.9186$, where the entropy can be no more than $(1+\sqrt{5})/2 = 1.6180$ times as large as $S_{\rm m}$.

Here we wish to carry the notion of interpolation one step further, because we would like to discuss in the same formalism systems for which $R \ll R_{\rm dS}$, where the Bekenstein bound should apply. Hence we will explore the consequences of the bound

$$S \leq S_{\rm I} \equiv \frac{\pi}{G} R_{\rm Sch} R \,, \tag{C.14}$$

which we will call the interpolating bound. This bound agrees exactly with the m-bound when the object is allowed to fill de Sitter space, with $R = R_{\rm dS}$. Again we have no grounds to assume that the bound is rigorously true, but we do know that it is true in the three limiting cases where it reduces to the Bekenstein bound, the D-bound, and the holographic bound. The limiting cases are generally the most interesting for us in any case, since we wish to explore the limiting cases for Boltzmann brain nucleation. For parameters in between the limiting cases, it again seems reasonable to assume that the bound is at least a valid estimate, presumably accurate up to a factor of order one. We know of no rigorous entropy bounds for de Sitter space with R comparable to $R_{\rm dS}$ but not equal to it, so we don't see any way at this time to do better than the interpolating bound.

Proceeding with the I-bound of Eq. (C.14), we can use Eq. (5.92) to rewrite Eq. (C.9) as

$$\Delta S = \frac{\pi}{G} \left(H_\Lambda^{-2} - R_{\rm dS}^2 \right) - S_{\rm BB,max} + I_{\rm BB} \,, \tag{C.15}$$

which can be combined with $S_{\rm BB,max} \leq S_I$ to give

$$\Delta S \geq \frac{\pi}{G} \left(H_\Lambda^{-2} - R_{\rm dS}^2 - R_{\rm Sch}\, R \right) + I_{\rm BB} \,, \tag{C.16}$$

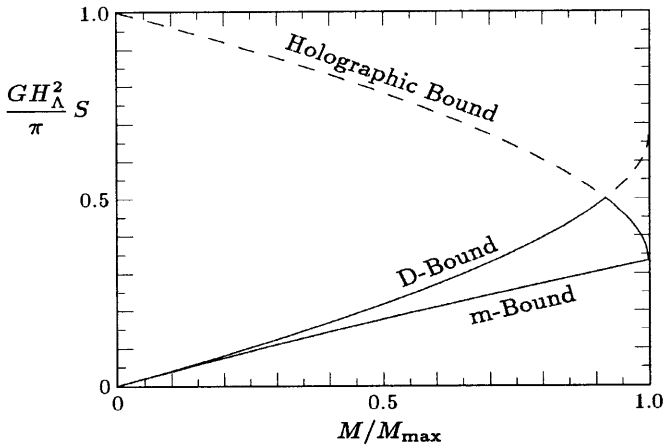

Figure C-1: Graph shows the holographic bound, the D-bound, and the m-bound for the entropy of an object that fills de Sitter space out to the horizon. The holographic and D– bounds are each shown as broken lines in the region where they are superseded by the other. Although the m-bound looks very much like a straight line, it is not.

which can then be simplified using Eq. (C.5) to give

$$\Delta S \geq \frac{\pi}{G} R_{\rm Sch} \left(R_{\rm Sch} + R_{\rm dS} - R \right) + I_{\rm BB} \,. \tag{C.17}$$

To continue, we have to decide what possibilities to consider for the radius R of the Boltzmann brain, which is related to the question of Boltzmann brain stabilization discussed after Eq. (5.97). If we assume that stabilization is not a problem, because it can be achieved by a domain wall or by some other particle physics mechanism, then ΔS is minimized by taking R at its maximum value, $R = R_{\rm dS}$, so

$$\Delta S \geq \frac{\pi}{G} R_{\rm Sch}^2 + I_{\rm BB} \,. \tag{C.18}$$

ΔS is then minimized by taking the minimum possible value of $R_{\rm Sch}$, which is the value that is just large enough to allow the required entropy, $S_{\rm BB,max} \geq I_{\rm BB}$. Using again the I-bound, one finds that saturation of the bound occurs at

$$\xi_{\rm sat} = 3 \sin^{-1} \left(\frac{\sqrt{1 - 3\tilde{I}}}{2} \right) \,, \tag{C.19}$$

where

$$\tilde{I} \equiv \frac{I_{\rm BB}}{S_{\rm dS}} = \frac{G H_\Lambda^2}{\pi} I_{\rm BB} \tag{C.20}$$

is the ratio of the Boltzmann brain information to the entropy of the unperturbed de Sitter space. Note that $\tilde{I}$ varies from zero to a maximum value of $1/3$, which occurs in the limiting case for which $R_{\rm Sch} = R_{\rm dS}$. The saturating value of the mass and the

corresponding values of the Schwarzschild radius and de Sitter radius are given by

$$M_{\rm sat} = \frac{\tilde{I}\sqrt{1+\tilde{I}}}{2GH_\Lambda}\,, \tag{C.21}$$

$$R_{\rm Sch,sat} = \frac{\sqrt{1+\tilde{I}}-\sqrt{1-3\tilde{I}}}{2H_\Lambda}\,, \tag{C.22}$$

$$R_{\rm dS,sat} = \frac{\sqrt{1-3\tilde{I}}+\sqrt{1+\tilde{I}}}{2H_\Lambda}\,. \tag{C.23}$$

Combining these results with Eq. (C.18), one has for this case ($R = R_{\rm dS}$) the bound

$$\frac{\Delta S}{I_{\rm BB}} \geq \frac{1+\tilde{I}-\sqrt{1+\tilde{I}}\sqrt{1-3\tilde{I}}}{2\tilde{I}}\,. \tag{C.24}$$

As can be seen in Figure C-2, the bound on $\Delta S/I_{\rm BB}$ for this case varies from 1, in the limit of vanishing $\tilde{I}$ (or equivalently, the limit $H_\Lambda \to 0$), to 2, in the limit $R_{\rm Sch} \to R_{\rm dS}$.

The limiting case of $\tilde{I}_{\rm BB} \to 0$, with a nucleation rate of order $e^{-I_{\rm BB}}$, has some peculiar features that are worth mentioning. The nucleation rate describes the nucleation of a Boltzmann brain with some particular memory state, so there would be an extra factor of $e^{I_{\rm BB}}$ in the sum over all memory states. Thus, a single-state nucleation rate of $e^{-I_{\rm BB}}$ indicates that the total nucleation rate, including all memory states, is not suppressed at all. It may seem strange that the nucleation rate could be unsuppressed, but one must keep in mind that the system will function as a Boltzmann brain only for very special values of the memory state. In the limiting case discussed here, the "Boltzmann brain" takes the form of a minor perturbation of the degrees of freedom associated with the de Sitter entropy $S_{\rm dS} = \pi/(GH_\Lambda^2)$.

As a second possibility for the radius R, we can consider the case of strong gravitational binding, $R \to R_{\rm Sch}$, as discussed following Eq. (5.97). For this case the bound (C.17) becomes

$$\Delta S \geq \frac{\pi}{G} R_{\rm Sch} R_{\rm dS} + I_{\rm BB}\,. \tag{C.25}$$

(Interestingly, if we take $I = 0$ ($S_{\rm BB} = S_{\rm max}$) this formula agrees with the result found in Ref. [141] for black hole nucleation in de Sitter space.) With $R = R_{\rm Sch}$ the saturation of the I-bound occurs at

$$\xi_{\rm sat} = \frac{\pi}{2} - 3\sin^{-1}\left(\frac{\sqrt{3\tilde{I}}}{2}\right)\,. \tag{C.26}$$

The saturating value of the mass and the corresponding values of the Schwarzschild radius and de Sitter radius are given by

$$M_{\rm sat} = \frac{\sqrt{\tilde{I}}\left(1-\tilde{I}\right)}{2GH_\Lambda}\,, \tag{C.27}$$

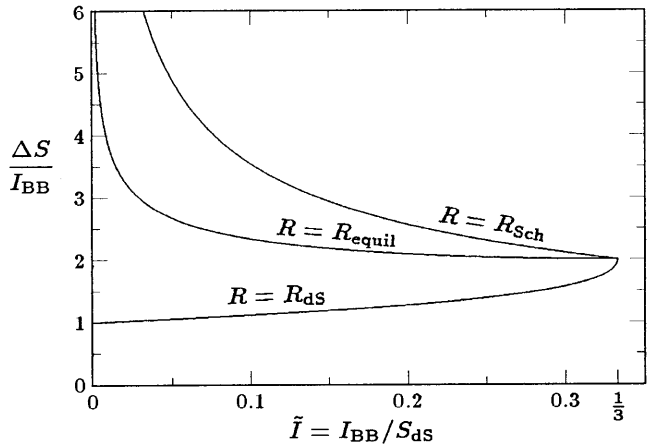

Figure C-2: Graph shows the ratio of ΔS to $I_{\rm BB}$, where the nucleation rate for Boltzmann brains is proportional to $e^{-\Delta S}$. All curves are based on the I-bound, as discussed in the text, but they differ by their assumptions about the size R of the Boltzmann brain.

$$R_{\rm Sch,sat} = \frac{\sqrt{\tilde{I}}}{H_\Lambda}, \tag{C.28}$$

$$R_{\rm dS,sat} = \frac{\sqrt{4-3\tilde{I}}-\sqrt{\tilde{I}}}{2H_\Lambda}. \tag{C.29}$$

Using these relations to evaluate ΔS from Eq. (C.25), one finds

$$\frac{\Delta S}{I_{\rm BB}} = \frac{\sqrt{4-3\tilde{I}}+\sqrt{\tilde{I}}}{2\sqrt{\tilde{I}}}, \tag{C.30}$$

which is also plotted in Figure C-2. In this case ($R = R_{\rm Sch}$) the smallest ratio $\Delta S/I_{\rm BB}$ is 2, occurring at $\tilde{I} = 1/3$, where $R_{\rm Sch} = R_{\rm dS}$. For smaller values of $\tilde{I}$ the ratio becomes larger, blowing up as $1/\sqrt{\tilde{I}}$ for small $\tilde{I}$. Thus, the nucleation rates for this choice of R will be considerably smaller than those for Boltzmann brains with $R \approx R_{\rm dS}$, but this case would still be relevant in cases where Boltzmann brains with $R \approx R_{\rm dS}$ cannot be stabilized.

Another interesting case, which we will consider, is to allow the Boltzmann brain to extend to $R = R_{\rm equil}$, the point of equilibrium between the gravitational attraction of the Boltzmann brain and the outward gravitational pull of the de Sitter expansion. This equilibrium occurs at the stationary point of g_{tt}, which gives

$$R_{\rm equil} = \left(\frac{GM}{H_\Lambda^2}\right)^{1/3}. \tag{C.31}$$

Boltzmann brains within this radius bound would not be pulled by the de Sitter ex-

pansion, so relatively small mechanical forces will be sufficient to hold them together.

Again ΔS will be minimized when the I-bound is saturated, which in this case occurs when

$$\xi_{\rm sat} = \frac{\pi}{2} - 3\sin^{-1}\left[\frac{\sqrt{1-2A(\tilde{I})}}{2}\right], \tag{C.32}$$

where

$$A(\tilde{I}) \equiv \sin\left[\frac{\sin^{-1}\left(1-27\,\tilde{I}^{\,3}\right)}{3}\right]. \tag{C.33}$$

The saturating value of the mass and the Schwarzschild and de Sitter radii are given by

$$M_{\rm sat} = \frac{\sqrt{3}[1+A(\tilde{I})]\sqrt{1-2A(\tilde{I})}}{9GH_\Lambda}, \tag{C.34}$$

$$R_{\rm Sch,sat} = \frac{\sqrt{1-2A(\tilde{I})}}{\sqrt{3}\,H_\Lambda}, \tag{C.35}$$

$$R_{\rm dS,sat} = \frac{\sqrt{3}\left[\sqrt{3\left(3+2A(\tilde{I})\right)}-\sqrt{1-2A(\tilde{I})}\right]}{6H_\Lambda}. \tag{C.36}$$

The equilibrium radius itself is given by

$$R_{\rm equil,sat} = \frac{\left[1-2A(\tilde{I})\right]^{1/6}\left[1+A(\tilde{I})\right]^{1/3}}{\sqrt{3}H_\Lambda}. \tag{C.37}$$

Using these results with Eq. (C.17), ΔS is found to be bounded by

$$\frac{\Delta S}{I_{\rm BB}} = \frac{\sqrt{3\left(1-2A(\tilde{I})\right)\left(3+2A(\tilde{I})\right)}-2A(\tilde{I})+1}{6\tilde{I}}, \tag{C.38}$$

which is also plotted in Figure C-2. As one might expect it is intermediate between the two other cases. Like the $R = R_{\rm Sch}$ case, however, the ratio $\Delta S/I_{\rm BB}$ blows up for small $\tilde{I}$, in this case behaving as $(2/\tilde{I})^{1/4}$.

In summary, we have found that our study of tunneling in Schwarzschild–de Sitter space confirms the qualitative conclusions that were described in Subsection 5.3.1. In particular, we have found that if the entropy bound can be saturated, then the nucleation rate of a Boltzmann brain requiring information content $I_{\rm BB}$ is given approximately by $e^{-aI_{\rm BB}}$, where a is of order a few, as in Eq. (5.97). The coefficient a is always greater than 2 for Boltzmann brains that are small enough to be gravitationally bound. This conclusion applies whether one insists that they be near-black

holes, or whether one merely requires that they be small enough so that their self-gravity overcomes the de Sitter expansion. If, however, one considers Boltzmann brains whose radius is allowed to extend to the de Sitter horizon, then Figure C-2 shows that a can come arbitrarily close to 1. However, one must remember that the $R = R_{\rm dS}$ curve on Figure C-2 can be reached only if several barriers can be overcome. First, these objects are large and diffuse, becoming more and more diffuse as $\tilde{I}$ approaches zero and a approaches 1. There is no known way to saturate the entropy bound for such diffuse systems, and Eq. (5.103) shows that an ideal gas model leads to $a \sim I_{\rm BB}^{1/3} \gg 1$. Furthermore, Boltzmann brains of this size can function only if some particle physics mechanism is available to stabilize them against the de Sitter expansion. A domain wall provides a simple example of such a mechanism, but Eq. (5.100) indicates that the domain wall solution is an option only if a domain wall exists with tension $\sigma \sim I_{\rm BB} H_\Lambda^3$. Thus, it is not clear how close a can come to its limiting value of 1. Finally, we should keep in mind that it is not clear if any of the examples discussed in this appendix can actually be attained, since black holes might be the only objects that saturate the entropy bound for $S \gg 1$.

Bibliography

[1] E. W. Kolb and M. S. Turner, "The Early universe," Front. Phys. **69**, 1 (1990).

[2] A. H. Guth, "The Inflationary Universe: A Possible Solution To The Horizon And Flatness Problems," Phys. Rev. D **23** (1981) 347.

[3] A. D. Linde, "A New Inflationary Universe Scenario: A Possible Solution Of The Horizon, Flatness, Homogeneity, Isotropy And Primordial Monopole Problems," Phys. Lett. B **108**, 389 (1982).

[4] A. Albrecht and P. J. Steinhardt, "Cosmology For Grand Unified Theories With Radiatively Induced Symmetry Breaking," Phys. Rev. Lett. **48**, 1220 (1982).

[5] J. Dunkley et al. [WMAP Collaboration], "Five-Year Wilkinson Microwave Anisotropy Probe (WMAP) Observations: Likelihoods and Parameters from the WMAP data," arXiv:0803.0586 [astro-ph]; E. Komatsu et al. [WMAP Collaboration], "Five-Year Wilkinson Microwave Anisotropy Probe (WMAP) Observations:Cosmological Interpretation," arXiv:0803.0547 [astro-ph].

[6] S. R. Coleman and F. De Luccia, "Gravitational Effects On And Of Vacuum Decay," Phys. Rev. D **21**, 3305 (1980).

[7] A. Linde and V. Mukhanov, "The curvaton web," JCAP **0604**, 009 (2006) [arXiv:astro-ph/0511736].

[8] A. D. Linde, D. A. Linde and A. Mezhlumian, "From the Big Bang theory to the theory of a stationary universe," Phys. Rev. D **49**, 1783 (1994) [arXiv:gr-qc/9306035].

[9] J. Garcia-Bellido, A. D. Linde and D. A. Linde, "Fluctuations Of The Gravitational Constant In The Inflationary Brans-Dicke Cosmology," Phys. Rev. D **50**, 730 (1994) [arXiv:astro-ph/9312039]; J. Garcia-Bellido and A. D. Linde, "Stationarity of inflation and predictions of quantum cosmology," Phys. Rev. D **51**, 429 (1995) [arXiv:hep-th/9408023]; J. Garcia-Bellido and A. D. Linde, "Stationary solutions in Brans-Dicke stochastic inflationary cosmology," Phys. Rev. D **52**, 6730 (1995) [arXiv:gr-qc/9504022].

[10] A. Vilenkin, "Predictions from quantum cosmology," Phys. Rev. Lett. **74**, 846 (1995) [arXiv:gr-qc/9406010].

[11] A. Vilenkin, "Making predictions in eternally inflating universe," Phys. Rev. D **52**, 3365 (1995) [arXiv:gr-qc/9505031].

[12] J. Garriga, T. Tanaka and A. Vilenkin, "The density parameter and the Anthropic Principle," Phys. Rev. D **60**, 023501 (1999) [arXiv:astro-ph/9803268].

[13] A. Vilenkin, "Unambiguous probabilities in an eternally inflating universe," Phys. Rev. Lett. **81**, 5501 (1998) [arXiv:hep-th/9806185]; V. Vanchurin, A. Vilenkin and S. Winitzki, "Predictability crisis in inflationary cosmology and its resolution," Phys. Rev. D **61**, 083507 (2000) [arXiv:gr-qc/9905097].

[14] J. Garriga, D. Schwartz-Perlov, A. Vilenkin and S. Winitzki, "Probabilities in the inflationary multiverse," JCAP **0601**, 017 (2006) [arXiv:hep-th/0509184].

[15] R. Easther, E. A. Lim and M. R. Martin, "Counting pockets with world lines in eternal inflation," JCAP **0603**, 016 (2006) [arXiv:astro-ph/0511233].

[16] R. Bousso, "Holographic probabilities in eternal inflation," Phys. Rev. Lett. **97**, 191302 (2006) [arXiv:hep-th/0605263]; R. Bousso, B. Freivogel and I. S. Yang, "Eternal inflation: The inside story," Phys. Rev. D **74**, 103516 (2006) [arXiv:hep-th/0606114].

[17] L. Susskind, "The Census Taker's Hat," arXiv:0710.1129 [hep-th].

[18] A. Linde, "Sinks in the Landscape, Boltzmann Brains, and the Cosmological Constant Problem," JCAP **0701**, 022 (2007) [arXiv:hep-th/0611043].

[19] A. Linde, "Towards a gauge invariant volume-weighted probability measure for eternal inflation," JCAP **0706**, 017 (2007) [arXiv:0705.1160 [hep-th]].

[20] V. Vanchurin, Phys. Rev. **D75**, 023524 (2007).

[21] S. Winitzki, "A volume-weighted measure for eternal inflation," Phys. Rev. D **78**, 043501 (2008) [arXiv:0803.1300 [gr-qc]].

[22] J. Garriga and A. Vilenkin, "Holographic Multiverse," JCAP **0901**, 021 (2009) [arXiv:0809.4257 [hep-th]].

[23] A. Linde, V. Vanchurin and S. Winitzki, "Stationary Measure in the Multiverse," JCAP **0901**, 031 (2009) [arXiv:0812.0005 [hep-th]].

[24] R. Bousso, "Complementarity in the Multiverse," Phys. Rev. D **79**, 123524 (2009) [arXiv:0901.4806 [hep-th]].

[25] A. D. Linde, D. A. Linde and A. Mezhlumian, "Do we live in the center of the world?," Phys. Lett. B **345**, 203 (1995) [arXiv:hep-th/9411111].

[26] R. Bousso, B. Freivogel and I. S. Yang, "Boltzmann babies in the proper time measure," Phys. Rev. D **77** (2008) 103514 [arXiv:0712.3324 [hep-th]].

[27] B. Feldstein, L. J. Hall and T. Watari, "Density perturbations and the cosmological constant from inflationary landscapes," Phys. Rev. D **72**, 123506 (2005) [arXiv:hep-th/0506235];

[28] J. Garriga and A. Vilenkin, "Anthropic prediction for Lambda and the Q catastrophe," Prog. Theor. Phys. Suppl. **163**, 245 (2006) [arXiv:hep-th/0508005].

[29] M. L. Graesser and M. P. Salem, "The scale of gravity and the cosmological constant within a landscape," Phys. Rev. D **76**, 043506 (2007) [arXiv:astro-ph/0611694].

[30] M. Tegmark and M. J. Rees, "Why is the CMB fluctuation level 10^{-5}?," Astrophys. J. **499**, 526 (1998) [arXiv:astro-ph/9709058].

[31] L. J. Hall, T. Watari and T. T. Yanagida, "Taming the runaway problem of inflationary landscapes," Phys. Rev. D **73**, 103502 (2006) [arXiv:hep-th/0601028].

[32] A. De Simone, A. H. Guth, M. P. Salem and A. Vilenkin, "Predicting the cosmological constant with the scale-factor cutoff measure," Phys. Rev. D **78** (2008) 063520 [arXiv:0805.2173 [hep-th]].

[33] R. Bousso, B. Freivogel and I. S. Yang, "Properties of the scale factor measure," Phys. Rev. D **79**, 063513 (2009) [arXiv:0808.3770 [hep-th]].

[34] A. De Simone, A. H. Guth, A. Linde, M. Noorbala, M. P. Salem and A. Vilenkin, "Boltzmann brains and the scale-factor cutoff measure of the multiverse," arXiv:0808.3778 [hep-th].

[35] M. Rees, Before the Beginning, p.221 (Addison-Wesley, 1997).

[36] A. Albrecht and L. Sorbo, "Can the universe afford inflation?," Phys. Rev. D **70**, 063528 (2004) [arXiv:hep-th/0405270]; see also A. Albrecht, in Science and Ultimate Reality, ed. by J. D. Barrow, P. C. W. Davies, and C. L. Harper (Cambridge University Press, 2003) [arXiv:astro-ph/0210527].

[37] L. Dyson, M. Kleban and L. Susskind, "Disturbing implications of a cosmological constant," JHEP **0210**, 011 (2002) [arXiv:hep-th/0208013].

[38] D. N. Page, "The lifetime of the universe," J. Korean Phys. Soc. **49**, 711 (2006) [arXiv:hep-th/0510003].

[39] D. N. Page, "Susskind's challenge to the Hartle-Hawking no-boundary proposal and possible resolutions," JCAP **0701**, 004 (2007) [arXiv:hep-th/0610199].

[40] D. N. Page, "Is our universe likely to decay within 20 billion years?," Phys. Rev. D **78**, 063535 (2008) [arXiv:hep-th/0610079].

[41] R. Bousso and B. Freivogel, "A paradox in the global description of the multiverse," JHEP **0706**, 018 (2007) [arXiv:hep-th/0610132].

[42] J. Garriga and A. Vilenkin, "Recycling universe," Phys. Rev. D **57**, 2230 (1998) [arXiv:astro-ph/9707292].

[43] D. Schwartz-Perlov and A. Vilenkin, "Probabilities in the Bousso-Polchinski multiverse," JCAP **0606**, 010 (2006) [arXiv:hep-th/0601162]; D. Schwartz-Perlov, "Probabilities in the Arkani-Hamed-Dimopolous-Kachru landscape," J. Phys. A **40**, 7363 (2007) [arXiv:hep-th/0611237].

[44] K. M. Lee and E. J. Weinberg, "Decay of the true vacuum in curved space-time," Phys. Rev. D **36**, 1088 (1987).

[45] J. Garcia-Bellido, A. D. Linde and D. A. Linde, "Fluctuations Of The Gravitational Constant In The Inflationary Brans-Dicke Cosmology," Phys. Rev. D **50**, 730 (1994) [arXiv:astro-ph/9312039]; J. Garcia-Bellido and A. D. Linde, "Stationarity of inflation and predictions of quantum cosmology," Phys. Rev. D **51**, 429 (1995) [arXiv:hep-th/9408023]; J. Garcia-Bellido and A. D. Linde, "Stationary solutions in Brans-Dicke stochastic inflationary cosmology," Phys. Rev. D **52**, 6730 (1995) [arXiv:gr-qc/9504022].

[46] A. Vilenkin and S. Winitzki, "Probability distribution for Omega in open-universe inflation," Phys. Rev. D **55**, 548 (1997) [arXiv:astro-ph/9605191].

[47] R. Bousso, B. Freivogel and I. S. Yang, "Boltzmann babies in the proper time measure," arXiv:0712.3324 [hep-th].

[48] A. D. Linde, D. A. Linde and A. Mezhlumian, "Do we live in the center of the world?," Phys. Lett. B **345**, 203 (1995) [arXiv:hep-th/9411111].

[49] A. H. Guth, Phys. Rept. **333**, 555 (2000); "Eternal inflation and its implications," J. Phys. A **40**, 6811 (2007) [arXiv:hep-th/0702178].

[50] B. Freivogel, M. Kleban, M. Rodriguez Martinez and L. Susskind, "Observational consequences of a landscape," JHEP **0603**, 039 (2006) [arXiv:hep-th/0505232].

[51] A. De Simone and M. P. Salem, "The distribution of Ω_k from the scale-factor cutoff measure," Phys. Rev. D **81**, 083527 (2010) [arXiv:0912.3783 [hep-th]].

[52] S. Weinberg, "Anthropic Bound On The Cosmological Constant," Phys. Rev. Lett. **59**, 2607 (1987).

[53] A. D. Linde, "The Inflationary Universe," Rept. Prog. Phys. **47**, 925 (1984).

[54] A. D. Linde, in *Three hundred years of gravitation*, ed. by S. W. Hawking and W. Israel, Cambridge University Press (1987).

[55] A. Vilenkin, "Predictions from quantum cosmology," Phys. Rev. Lett. **74**, 846 (1995) [arXiv:gr-qc/9406010].

[56] G. Efstathiou, MNRAS **274**, L73 (1995).

[57] H. Martel, P. R. Shapiro and S. Weinberg, "Likely Values of the Cosmological Constant," Astrophys. J. **492**, 29 (1998) [arXiv:astro-ph/9701099].

[58] J. Garriga, M. Livio and A. Vilenkin, "The cosmological constant and the time of its dominance," Phys. Rev. D **61**, 023503 (2000) [arXiv:astro-ph/9906210].

[59] M. Tegmark, A. Aguirre, M. Rees and F. Wilczek, "Dimensionless constants, cosmology and other dark matters," Phys. Rev. D **73**, 023505 (2006) [arXiv:astro-ph/0511774].

[60] L. Pogosian and A. Vilenkin, "Anthropic predictions for vacuum energy and neutrino masses in the light JCAP **0701**, 025 (2007) [arXiv:astro-ph/0611573].

[61] J. A. Peacock, "Testing anthropic predictions for Lambda and the CMB temperature," Mon. Not. Roy. Astron. Soc. **379**, 1067 (2007) [arXiv:0705.0898 [astro-ph]].

[62] R. Bousso, R. Harnik, G. D. Kribs and G. Perez, "Predicting the Cosmological Constant from the Causal Entropic Principle," Phys. Rev. D **76**, 043513 (2007) [arXiv:hep-th/0702115].

[63] K. D. Olum and D. Schwartz-Perlov, "Anthropic prediction in a large toy landscape," JCAP **0710**, 010 (2007) [arXiv:0705.2562 [hep-th]].

[64] T. Clifton, S. Shenker and N. Sivanandam, "Volume Weighted Measures of Eternal Inflation in the Bousso-Polchinski Landscape," JHEP **0709**, 034 (2007) [arXiv:0706.3201 [hep-th]].

[65] W. H. Press and P. Schechter, "Formation of galaxies and clusters of galaxies by selfsimilar gravitational condensation," Astrophys. J. **187** (1974) 425; J. M. Bardeen, J. R. Bond, N. Kaiser and A. S. Szalay, "The Statistics Of Peaks Of Gaussian Random Fields," Astrophys. J. **304**, 15 (1986).

[66] P. B. Lilje, Astrophys. J. **386**, L33–L26 (1992); S. D. M. White, G. Efstathiou and C. S. Frenk, "The Amplitude Of Mass Fluctuations In The Universe," Mon. Not. Roy. Astron. Soc. **262**, 1023 (1993). V. R. Eke, S. Cole and C. S. Frenk, "Using the Evolution of Clusters to Constrain Omega," Mon. Not. Roy. Astron. Soc. **282**, 263 (1996) [arXiv:astro-ph/9601088].

[67] M. Tegmark, A. Vilenkin and L. Pogosian, "Anthropic predictions for neutrino masses," Phys. Rev. D **71**, 103523 (2005) [arXiv:astro-ph/0304536].

[68] A. Jenkins et al., "Mass function of dark matter halos," Mon. Not. Roy. Astron. Soc. **321**, 372 (2001) [arXiv:astro-ph/0005260].

[69] R. K. Sheth and G. Tormen, "Large scale bias and the peak background split," Mon. Not. Roy. Astron. Soc. **308**, 119 (1999) [arXiv:astro-ph/9901122]; R. K. Sheth, H. J. Mo and G. Tormen, "Ellipsoidal collapse and an improved model for the number and spatial distribution of dark matter haloes," Mon. Not. Roy. Astron. Soc. **323**, 1 (2001) [arXiv:astro-ph/9907024].

[70] M. S. Warren, K. Abazajian, D. E. Holz and L. Teodoro, "Precision Determination of the Mass Function of Dark Matter Halos," Astrophys. J. **646**, 881 (2006) [arXiv:astro-ph/0506395].

[71] G. Kauffmann et al. [SDSS Collaboration], "The Dependence of Star Formation History and Internal Structure on Stellar Mass for 80,000 Low-Redshift Galaxies," Mon. Not. Roy. Astron. Soc. **341**, 54 (2003) [arXiv:astro-ph/0205070].

[72] U. Seljak and M. Zaldarriaga, "A Line of Sight Approach to Cosmic Microwave Background Anisotropies," Astrophys. J. **469**, 437 (1996) [arXiv:astro-ph/9603033].

[73] A. Loeb, "An Observational Test for the Anthropic Origin of the Cosmological Constant," JCAP **0605**, 009 (2006) [arXiv:astro-ph/0604242].

[74] S. A. Bludman, "Vacuum energy: If not now, then when?," Nucl. Phys. A **663**, 865 (2000) [arXiv:astro-ph/9907168].

[75] S. R. Coleman and F. De Luccia, "Gravitational Effects On And Of Vacuum Decay," Phys. Rev. D **21**, 3305 (1980).

[76] K. M. Lee and E. J. Weinberg, "Decay of the true vacuum in curved spacetime," Phys. Rev. D **36**, 1088 (1987).

[77] R. Bousso, R. Harnik, G. D. Kribs and G. Perez, "Predicting the Cosmological Constant from the Causal Entropic Principle," Phys. Rev. D **76**, 043513 (2007) [arXiv:hep-th/0702115].

[78] B. Bozek, A. J. Albrecht and D. Phillips, "Curvature Constraints from the Causal Entropic Principle," Phys. Rev. D **80** (2009) 023527 [arXiv:0902.1171 [astro-ph.CO]].

[79] R. Bousso and S. Leichenauer, "Predictions from Star Formation in the Multiverse," arXiv:0907.4917 [hep-th].

[80] T. P. Waterhouse and J. P. Zibin, "The cosmic variance of Omega," arXiv:0804.1771 [astro-ph].

[81] M. Vardanyan, R. Trotta and J. Silk, "How flat can you get? A model comparison perspective on the curvature of the Universe," arXiv:0901.3354 [astro-ph.CO].

[82] M. Tegmark, A. Aguirre, M. Rees and F. Wilczek, "Dimensionless constants, cosmology and other dark matters," Phys. Rev. D **73**, 023505 (2006) [arXiv:astro-ph/0511774].

[83] J. Garriga and A. Vilenkin, "Prediction and explanation in the multiverse," Phys. Rev. D **77**, 043526 (2008) [arXiv:0711.2559 [hep-th]].

[84] D. J. Heath, "The growth of density perturbations in zero pressure Friedmann-Lemaitre universes," Mon. Not. Roy. Astron. Soc. **179**, 351 (1977).

[85] G. W. Gibbons and S. W. Hawking, "Cosmological event horizons, thermodynamics, and particle creation," Phys. Rev. D **15**, 2738 (1977).

[86] L. Susskind, as quoted in Ref. [39]; see also Ref. [37].

[87] For recent reviews of the measure problem, see e.g. S. Winitzki, "Predictions in eternal inflation," Lect. Notes Phys. **738**, 157 (2008) [arXiv:gr-qc/0612164]; A. H. Guth, Phys. Rept. **333**, 555 (2000); "Eternal inflation and its implications," J. Phys. A **40**, 6811 (2007) [arXiv:hep-th/0702178]; A. Linde, "Inflationary Cosmology," Lect. Notes Phys. **738**, 1 (2008) [arXiv:0705.0164 [hep-th]]; A. Vilenkin, "A measure of the multiverse," J. Phys. A **40**, 6777 (2007) [arXiv:hep-th/0609193];

[88] A. D. Linde, "Eternally existing self-reproducing chaotic inflationary universe," Phys. Lett. B **175**, 395 (1986).

[89] A. Linde, "Sinks in the Landscape, Boltzmann Brains, and the Cosmological Constant Problem," JCAP **0701**, 022 (2007) [arXiv:hep-th/0611043].

[90] A. Linde, "Inflationary Cosmology," Lect. Notes Phys. **738**, 1 (2008) [arXiv:0705.0164 [hep-th]].

[91] A. D. Linde, V. Vanchurin and S. Winitzki, "Stationary Measure in the Multiverse," JCAP **0901**, 031 (2009) [arXiv:0812.0005 [hep-th]].

[92] M. Tegmark, "What does inflation really predict?," JCAP **0504**, 001 (2005) [arXiv:astro-ph/0410281]; see also Ref. [26].

[93] J. Garcia-Bellido and A. D. Linde, "Stationarity of inflation and predictions of quantum cosmology," Phys. Rev. D **51**, 429 (1995) [arXiv:hep-th/9408023].

[94] A. Linde and V. Mukhanov, "The curvaton web," JCAP **0604**, 009 (2006) [arXiv:astro-ph/0511736].

[95] A. A. Starobinsky, "Stochastic De Sitter (Inflationary) Stage In The Early Universe," in: Current Topics in Field Theory, Quantum Gravity and Strings, Lecture Notes in Physics, eds. H.J. de Vega and N. Sanchez (Springer, Heidelberg 1986) **206**, p. 107.

[96] T. Clifton, A. Linde and N. Sivanandam, "Islands in the landscape," JHEP **0702**, 024 (2007) [arXiv:hep-th/0701083].

[97] D. N. Page, "Return of the Boltzmann brains," Phys. Rev. D **78**, 063536 (2008) [arXiv:hep-th/0611158].

[98] A. Vilenkin, "Freak observers and the measure of the multiverse," JHEP **0701**, 092 (2007) [arXiv:hep-th/0611271].

[99] A. Aguirre, S. Gratton and M. C. Johnson, "Measures on transitions for cosmology from eternal inflation," Phys. Rev. Lett. **98**, 131301 (2007) [arXiv:hep-th/0612195].

[100] E. V. Koonin, "The cosmological model of eternal inflation and the transition from chance to biological evolution in the history of life," Biology Direct 2007, 2:15 (2007).

[101] See e.g. R. Bousso and J. Polchinski, "The String Theory Landscape," Sci. Am. **291**, 60 (2004).

[102] S. Lloyd, "Ultimate physical limits to computation," Nature **406**, 1047 (2000).

[103] R. Bousso, "Bekenstein bounds in de Sitter and flat space," JHEP **0104**, 035 (2001) [arXiv:hep-th/0012052].

[104] B. Freivogel and M. Lippert, "Evidence for a bound on the lifetime of de Sitter space," JHEP **0812**, 096 (2008) [arXiv:0807.1104 [hep-th]].

[105] J. D. Bekenstein, "Entropy Content And Information Flow In Systems With Limited Energy," Phys. Rev. D **30**, 1669 (1984).

[106] G. Dvali and G. R. Farrar, "Strong CP Problem with 10^{32} Standard Model Copies," Phys. Rev. Lett. **101**, 011801 (2008) [arXiv:0712.3170 [hep-th]].

[107] B. Pakkenberg et al., "Aging and the human neocortex," Experimental Gerontology **38**, 95 (2003).

[108] T. K. Landauer, "How much do people remember? Some estimates of the quantity of learned information in long-term memory," Cognitive Science **10** 477 (1986).

[109] T. K. Landauer, "An estimate of how much people remember, not of underlying cognitive capacities," Cognitive Science **12** 293 (1988).

[110] P. Dayan and L.F. Abbott, Theoretical Neuroscience: Computational and Mathematical Modeling of Neural Systems (MIT Press, Cambridge, Massachusetts, 2001), p. 4.

[111] S. Kachru, R. Kallosh, A. Linde and S. P. Trivedi, "De Sitter vacua in string theory," Phys. Rev. D **68**, 046005 (2003) [arXiv:hep-th/0301240].

[112] A. Ceresole, G. Dall'Agata, A. Giryavets, R. Kallosh and A. Linde, "Domain walls, near-BPS bubbles, and probabilities in the landscape," Phys. Rev. D **74**, 086010 (2006) [arXiv:hep-th/0605266].

[113] J. D. Brown and C. Teitelboim, "Dynamical neutralization of the cosmological constant," Phys. Lett. B **195**, 177 (1987).

[114] J. D. Brown and C. Teitelboim, "Neutralization of the Cosmological Constant by Membrane Creation," Nucl. Phys. B **297**, 787 (1988).

[115] R. Bousso and J. Polchinski, "Quantization of four-form fluxes and dynamical neutralization of the cosmological constant," JHEP **0006**, 006 (2000) [arXiv:hep-th/0004134].

[116] S. Kachru, J. Pearson and H. L. Verlinde, "Brane/flux annihilation and the string dual of a non-supersymmetric field theory," JHEP **0206**, 021 (2002) [arXiv:hep-th/0112197].

[117] A. R. Frey, M. Lippert and B. Williams, "The fall of stringy de Sitter," Phys. Rev. D **68**, 046008 (2003) [arXiv:hep-th/0305018].

[118] M. C. Johnson and M. Larfors, "Field dynamics and tunneling in a flux landscape," Phys. Rev. D **78**, 083534 (2008) [arXiv:0805.3705 [hep-th]].

[119] J. J. Blanco-Pillado, D. Schwartz-Perlov and A. Vilenkin, "Quantum Tunneling in Flux Compactifications," JCAP **0912**, 006 (2009) [arXiv:0904.3106 [hep-th]].

[120] A. D. Linde and M. I. Zelnikov, "Inflationary Universe with Fluctuating Dimension," Phys. Lett. B **215**, 59 (1988).

[121] S. M. Carroll, M. C. Johnson and L. Randall, "Dynamical compactification from de Sitter space," JHEP **0911**, 094 (2009) [arXiv:0904.3115 [hep-th]].

[122] J. J. Blanco-Pillado, D. Schwartz-Perlov and A. Vilenkin, "Transdimensional Tunneling in the Multiverse," arXiv:0912.4082 [hep-th].

[123] M. Cvetic and H. H. Soleng, "Supergravity domain walls," Phys. Rept. **282**, 159 (1997) [arXiv:hep-th/9604090]; M. Cvetic, S. Griffies and S. J. Rey, "Nonperturbative stability of supergravity and superstring vacua," Nucl. Phys. B **389**, 3 (1993) [arXiv:hep-th/9206004]; M. Cvetic, S. Griffies and S. J. Rey, "Static domain walls in N=1 supergravity," Nucl. Phys. B **381**, 301 (1992) [arXiv:hep-th/9201007]; M. Cvetic, S. Griffies and H. H. Soleng, "Local and global gravitational aspects of domain wall space-times," Phys. Rev. D **48**, 2613 (1993) [arXiv:gr-qc/9306005].

[124] A. Ceresole, G. Dall'Agata, R. Kallosh and A. Van Proeyen, "Hypermultiplets, domain walls and supersymmetric attractors," Phys. Rev. D **64**, 104006 (2001) [arXiv:hep-th/0104056].

[125] K. Behrndt, G. Lopes Cardoso and D. Lüst, "Curved BPS domain wall solutions in four-dimensional N = 2 supergravity," Nucl. Phys. B **607**, 391 (2001) [arXiv:hep-th/0102128]; G. Lopes Cardoso, G. Dall'Agata and D. Lüst, "Curved BPS domain wall solutions in five-dimensional gauged supergravity," JHEP **0107** (2001) 026 [arXiv:hep-th/0104156]; G. Lopes Cardoso, G. Dall'Agata and D. Lüst, "Curved BPS domain walls and RG flow in five dimensions," JHEP **0203** (2002) 044 [arXiv:hep-th/0201270]; K. Behrndt and M. Cvetic, "Bent BPS domain walls of D = 5 N = 2 gauged supergravity coupled to hypermultiplets," Phys. Rev. D **65**, 126007 (2002) [arXiv:hep-th/0201272].

[126] J. Louis and S. Vaula, "N=1 domain wall solutions of massive type II supergravity as generalized geometries," JHEP **0608**, 058 (2006) [arXiv:hep-th/0605063].

[127] S. Deser and C. Teitelboim, "Supergravity has positive energy," Phys. Rev. Lett. **39**, 249 (1977).

[128] C. M. Hull, "The positivity of gravitational energy and global supersymmetry," Commun. Math. Phys. **90**, 545 (1983).

[129] E. Witten, "A simple proof of the positive energy theorem," Commun. Math. Phys. **80**, 381 (1981).

[130] S. Weinberg, "Does gravitation resolve the ambiguity among supersymmetry vacua?," Phys. Rev. Lett. **48**, 1776 (1982).

[131] M. Dine, G. Festuccia, A. Morisse and K. van den Broek, "Metastable domains of the landscape," arXiv:0712.1397 [hep-th].

[132] M. Ibe, Y. Nakayama and T. T. Yanagida, "Conformal gauge mediation and light gravitino of mass $m_{3/2}$," Phys. Lett. B **671**, 378 (2009) [arXiv:0804.0636 [hep-ph]].

[133] R. Kallosh and A. Linde, "Landscape, the scale of SUSY breaking, and inflation," JHEP **0412**, 004 (2004) [arXiv:hep-th/0411011].

[134] J. P. Conlon, R. Kallosh, A. Linde and F. Quevedo, "Volume Modulus Inflation and the Gravitino Mass Problem," JCAP **0809**, 011 (2008) [arXiv:0806.0809 [hep-th]].

[135] L. Susskind, The Cosmic Landscape (Little, Brown, and Company, New York, 2005).

[136] C. P. Burgess, R. Kallosh and F. Quevedo, "De Sitter string vacua from supersymmetric D-terms," JHEP **0310**, 056 (2003) [arXiv:hep-th/0309187].

[137] E. Silverstein, "Simple de Sitter solutions," Phys. Rev. D **77**, 106006 (2008) [arXiv:0712.1196 [hep-th]].

[138] A. Vilenkin, "Quantum Creation Of Universes," Phys. Rev. D **30**, 509 (1984); A. Vilenkin, "Boundary Conditions In Quantum Cosmology," Phys. Rev. D **33**, 3560 (1986); A. D. Linde, "Quantum Creation Of The Inflationary Universe," Lett. Nuovo Cim. **39**, 401 (1984); V. A. Rubakov, "Quantum Mechanics In The Tunneling Universe," Phys. Lett. B **148** (1984) 280.

[139] J. B. Hartle and S. W. Hawking, "Wave Function Of The Universe," Phys. Rev. D **28**, 2960 (1983).

[140] For a discussion of the Schwarzschild–de Sitter metric, see e.g. Z. Stuchlik and J. Kovar, "Pseudo-Newtonian gravitational potential for Schwarzschild-de Sitter spacetimes," Int. J. Mod. Phys. D **17**, 2089 (2008) [arXiv:0803.3641 [gr-qc]].

[141] R. Bousso and S. W. Hawking, "Lorentzian condition in quantum gravity," Phys. Rev. D **59**, 103501 (1999) [Erratum-ibid. D **60**, 109903 (1999)] [arXiv:hep-th/9807148].